DOKUZ EYLÜL UNIVERSITY
GRADUATE SCHOOL OF NATURAL AND APPLIED SCIENCES

DEGRADATION OF OLIVE MILL EFFLUENT BY PHOTOOXIDATION ON NANOSILICA-ZnO

by
Çağlar ULUSOY

February, 2016
İZMİR

DEGRADATION OF OLIVE MILL EFFLUENT BY PHOTOOXIDATION ON NANOSILICA-ZnO

A Thesis Submitted to the
Graduate School of Natural and Applied Sciences of Dokuz Eylül University
In Partial Fulfillment of the Requirements for the Degree of Master of Science in Environmental Engineering Program

by

Çağlar ULUSOY

February, 2016
İZMİR

M. Sc THESIS EXAMINATION RESULT FORM

We have read the thesis entitled **"DEGRADATION OF OLIVE MILL EFFLUENT BY PHOTOOXIDATION ON NANOSILICA-ZnO"** completed by **ÇAĞLAR ULUSOY** under supervision of **PROF. DR. DELIA TERESA SPONZA** and we certify that in our opinion it is fully adequate, in scope and in quality, as a thesis for the degree of Master of Science.

Prof.Dr. Delya T. SPONZA

Yönetici

Prof. Dr. Nur OKUR

Jüri Üyesi

Prof. Dr. Ayşegül AKA

Jüri Üyesi

Prof.Dr. Ayşe OKUR

Müdür

Fen Bilimleri Enstitüsü

ACKNOWLEDGMENTS

I would like to express my appreciation to my advisor Prof. Dr. Delia Teresa SPONZA for her advice, guidance and encouragement during my Master Degree studies.

And also, I would like to express appreciation for the support of the sponsors; (TUBITAK PROJECT NUMBER: TOV 113O558).

I wish to thank Cansu DOĞAN, Pelin ALİCANOĞLU, Nefise ERDİNÇMER, Zeynep ALTAN, Merve BALABAN and Selin AKTAŞ for their contribution, guidance, friendship and support.

Finally, my deepest gratitude to my lovely and precious family for their patience, support and contribution, Halil İbrahim ULUSOY, Ayşe Hanım ULUSOY and Efe Şükrü ULUSOY.

Çağlar ULUSOY

DEGRADATION OF OLIVE MILL EFFLUENT BY PHOTOOXIDATION ON NANO SILICA-ZnO

ABSTRACT

High load of organic matter and polyphenols in olive mill wastewater (OMW) may have adverse impacts on soil, surface water and groundwater, and their disposal still represents an unsolved environmental problem. The aim of this study is to remove of COD, total phenol, total solid (TS), total nitrogen, total phosphorus and three polyphenols (gallic acid, para coumaric acid, t-para coumaric acid) in the OMW by nano-ZnO-SiO_2 composite with adsorption and photocatalytic treatment (UV and sunlight). Additionally, optimum treatment conditions were determined to remove the pollutans. The maximum removal efficiencies were obtained with UV treatment. The maximum yields of COD (78%), total phenol (86%), TS (77%) and total nitrogen (100%) were obtained with 1 g/L nano-ZnO-SiO_2 composite excluding total phosphorous (5 g/L). The maximum yields of COD, total phenol, TS and total nitrogen were obtained after 15 min excluding total phenol (90 min) and total nitrogen (60 min). The maximum removal efficiencies of COD, total phenol and TS were obtained at original pH of OMW (4.01) excluding total nitrogen (pH 7), total phosphorous (pH 10). The treatment of OMW with sunlight 3 g/L nano-ZnO-SiO_2 composite is required for maximum yields of COD (77%), total phenol (73%), TS (64%) and total nitrogen (96%) excluding total phosphorous (5 g/L). The maximum yields of COD, total phenol and TS were obtained at original pH of OMW (4.01). The maximum yields of total nitrogen and total phophorous (80%) were obtained at pH 7 and 10, respectively. The last of investigations containing the reusability of the nano-ZnO-SiO_2 composite showed that the old nano-composite can be used again six times for treatment of OMW throughout photocatalytic treatment with UV. 500 TL was spent for 20 UV lamps, while the chemical cost, electricity consumption and nanocomposite cost were only 0.75 TL for 1 liter OMW.

Keywords: Adsorption, nano- ZnO-SiO_2, photocatalytic treatment, UV and sunlight irradiation

ZEYTİN KARASUYUNUN NANO SİLİKA-ZnO İLE FOTOOKSİDASYONLA BOZUNUMU

ÖZ

Yüksek organik yükleme ve zeytin karasuyunun içerdiği polifenoller toprağa, yüzey sularına ve yeraltı sularına oluşturduğu etki hala çözülememiş çevre problemi olarak bilinmektedir. Bu yüzden bu çalışmanın amacı COD, toplam fenol, toplam katı madde (TKM), toplam azot ve toplam fosfor ve zeytin karasuyundaki üç polifenolü (gallic acid, para coumaric acid and t-para coumaric acid) nano-ZnO-SiO_2 kompoziti ile adsorpsiyon ve fotokatalitik arıtmayla (UV ve güneş ışığı) gidermektir. Ek olarak, çalışma sonunda optimum arıtma koşulları belirlenecektir. Maximum giderim verimleri UV ile arıtmayla elde edilmiştir. Fotokatalitik bozunum için (UV), toplam fosfor hariç (5 g/L), KOİ (%78), toplam fenol (%86), TKM (%77) ve toplam azotun (%100) maksimum giderim verimleri 1 g/L nano-ZnO-SiO_2 kompozitiyle elde edilmiştir. Toplam fenol (90 dakika) ve toplam azot (60 dakika) hariç KOİ, toplam fenol, TKM ve toplam azotun maksimum verimleri 15 dakika maruziyet süresi sonrasında elde edilmiştir. Toplam azot (pH 7) ve toplam fosfor (pH 10) hariç KOİ, toplam fenol ve TKM'nin maksimum giderim verimleri zeytin karasuyunun orijinal pH'ında (4.01) elde edilmiştir. Toplam fosfor hariç (5 g/L) zeytin karasuyunun güneş ışığı altında KOİ (%77), toplam fenol (%73), TKM (%64) ve toplam azot (%96) arıtımında 3 g/L nano-ZnO-SiO_2 kompoziti gerekmektedir. KOİ, toplam fenol ve TKM maksimum verimleri zeytin karasuyunun orijinal pH'ında (4.01) elde edilmiştir. Toplam azot ve toplam fosforun (%80) maksimum verimleri sırasıyla pH 7 ve pH 10'da elde edilmiştir. Araştırmalar sonucunda UV ile fotokatalitik arıtmadan nano-ZnO-SiO_2 kompoziti zeytin karasuyu arıtımında 6 kez kullanılabileceğine karar verilmiştir. 1 litre zeytin karasuyu arıtımı için, 500 TL'si 20 adet UV lambası için olmak üzere kimyasal maliyeti, elektrik tüketimi ve nanokompozit tüketimi maliyeti sadece 0.75 TL olarak hesaplanmıştır.

Anahtar kelimeler: Adsorpsiyon, nano-ZnO- SiO_2, fotokatalitik arıtım, UV ve güneş ışığı maruziyeti.

CONTENTS

Page

LIST OF FIGURES

Page

LIST OF TABLES

Page

CHAPTER ONE
INTRODUCTION

1.1 Introduction

Olive and olive oil production generates a black liquid waste called 'olive mill wastewater' (OMW) creating a major environmental problem in Turkey as other Mediterranean countries such as Greece, Spain, Italy. Around 6×10^6 m^3 of OMW is produced yearly worldwide, of which 98% is produced in the Mediterranean basin (Zorpas & Costa, 2010). Figure 1.1 shows the percentage of olive oil production in the world (Devarenne, 2016). There are 41 cities which produce olive and olive oil production in several small plants resulting in about 1.5 million m^3 of olive mill wastewater during the production season (3 months per year) in Turkey.

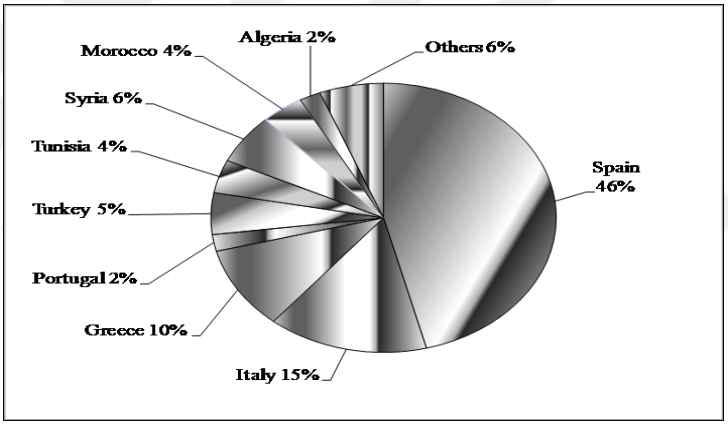

Figure 1.1 World olive oil productions

Due to their high load of organic matter and polyphenols OMW may have adverse impacts on soil, surface water and groundwater, and their disposal still represents an unsolved environmental problem. According to some reports, the chemical oxygen demand and biological oxygen demand (COD and BOD) values of these wastewaters are 200 – 400 times higher than those of typical municipal sewage. The very high levels of organic matter are mainly due to phenols, polyphenols, pectins, colloids, lipids and simple aromatic compounds resulting from olive cell wall degradation during oil extraction (Al Mallah et al., 2000; Centi et al., 2000; Chamkha et al., 2001).

Typically, due to the current absence of appropriate treating technologies for OMW effluents, OMW is discharged directly into sewer systems, valleys, and uncontrolled ponds, despite the fact that such dis-carding methods are forbidden in many Mediterranean countries (Shaheen & Karim, 2007; Brunetti et al., 2007; Boukhoubza et al., 2008; Dhaouadi & Marrot, 2008; Jarboui et al., 2008; Hanifi & El Hadrami, 2009). The inadequate and uncontrolled disposal methods of OMW to the water bodies possess an environmental concern as these effluents contain appreciable amount of COD and BOD concentrations, high amount of microbial growth-inhibiting compounds, such as phenolic compounds and tannins (Hanifi & El Hadrami, 2009; Kallel et al., 2009; Lucas & Peres, 2009). Nonetheless, a number of physical, chemical and biological treatment methods have been reported in literature; including flotation and sedimentation (Achak et al., 2008), sand filtration (Achak et al., 2009a, 2009b), ozonation (Chedeville et al., 2009), membrane filtration (Paraskeva et al., 2007; Dhaouadi & Marrot, 2008; Akdemir & Ozer, 2009), neutralization with addition of acid, advanced chemical oxidation (Fenton reaction) (Gomec et al., 2007; Zorpas & Costa, 2010), adsorption by activated carbon and aerobic and anaerobic digestions (Azbar et al., 2008a, 2008b; Boubaker & Ridha, 2008). These methods, however, are limited because they are too expensive to find a wide application, ineffective in meeting stringent effluent standards, and could result in huge amount of sludge. A summary of OMW treatment technologies and their efficiencies are presented in Table 1.

Table 1.1 Summary of technologies in the treatment of olive mill wastewater (Yalili Kilic & Akal Solmaz, 2013)

Type of treatment	**Results**	**Remarks**
Physicochemical treatment	30-50% COD reduction; 80- 95% COD removal after combination of physicochemical technologies	Technologies include centrifugation, filtration, coagulation flocculation, adsorption
Anaerobic digestion	60-80% COD removal for HRTs 2-5 days; Up to 90% COD removal with long HRTs (25 d) or selected support media	Dilution, alkalinity adjustment and nutrients addition required
Anaerobic digestion after physicochemical pretreatment	50-70% increase in COD reduction, with maximum removal observed 95%. Over 90% phenol reduction	Pretreatment technologies used: filtration, coagulation, GAC adsorption, ozonation
Anaerobic digestion after aerobic pretreatment	COD reduction 40-60% during pretreatment, 60-90% phenol reduction, toxicity reduction	Pretreatment with selected strains of aerobic microorganisms
Aerobic treatment	58-74% COD reduction depending on OLR and HRT; 81-84% for longer HRTs	Technologies include activated sludge and constructed wetlands
Combined biological processes	Up to 90% COD removal and similar percent phenol removal	Combinations of 2 and 3 treatment Stages
Oxidation and advanced oxidation processes (AOPs)	40-60% COD removal under regular oxidation conditions; 70-99% COD removal under excess oxidant concentration, supercritical conditions or after pretreatment	Processes include, ozone/H2O2, UV/H2O2, Wet air oxidation, Fenton oxidation, electrochemical oxidation
Combined processes	80-99% COD removal	Combinations of oxidation/biological processes, membrane processes

Table 1.2 Costs for various combined treatments in OMW, for a three-phase OMW (Yalili Kilic & Akal Solmaz, 2013)

Combined treatment	**Investment cost (€)**	**Total cost (€/m^3)**	**Calculated cost (€/t of olive oil)**
(1)	1.150.000	59	295
(2)	72.600-138.000	2-3.6	~14
(3)	42.200	1.31	1.5
(4)	180.700	3.95	19.7
(5)	250.000	12	60
(6)	500.000-850.000	13.5-22.5	~90

(1): Membranes for polyphenol recovery and composting.
(2): Physico-chemical processing and evaporation.
(3): Forced natural evaporation.
(4): Forced mechanical evaporation and lagooning.
(5): Physicochemical processing-ultrafiltration-reverse osmosis.
(6): Mechanical biological pre-treatment (biogas production)-sludge management (Aerobic stabilization, solar drying)

Adsorption offers some advantages in terms of easy design and operation and its wide applications for removing many types of impurities from water and wastewaters using various types of adsorbents such as activated carbon, clay etc. the adsorbents are mostly used adsorbent in adsorption process for the removal of pollutants compounds because of its high adsorption capacity, large surface area, and micro-porous structure. Nanoparticles or nano composites can be used for adsorption process due to their similar properties. El Hajjouji et al. (2008) searched adsorption of OMW with 1 g/L TiO_2 at room temperature. They obtained 11 % COD and 33 % total phenol decrease after 30 min contact time. Achak et al., (2013) used different adsorbent wheat bran for the treatment of OMW. They obtained 63%, 53% and 63% removal efficiencies for phenolic compounds, COD and color, respectively using 5% wheat bran in OMW after 24 h adsorption time. In addition Achak et al., (2009) studied the adsorption of the pollutants in the OMW using another bio-sorbent namely banana-peel. They obtained 88% removals for phenolic compounds after 3 h contact time with 30 g/L banana peel. Galanakis et al. (2006) used activated carbon with raw and activated Greek lignites for the treatment of OMW with adsorption. In

their study, the adsorption yields in the activated Greek lignites for COD are fivefold higher than that in activated carbon in the OMW.

Nanoparticle technology (i.e., the technology related to the preparation and application of materials at nanoscale, 1–100 nm) has emerged as a fascinating area of interest for removal of various contaminants from wastewater effluents (Nassar, 2012, 2013; Savage & Diallo, 2005; El Saliby et al., 2009; Kaur & Gupta, 2009; Narayan, 2010; Xu et al., 2012). Heterogeneous photocatalysis, involving photoinduced redox reactions at the surface of semiconductor minerals, is a promising technique for the treatment of water contaminated by organic molecules (Hoffmann et al., 1995; Selli et al., 1999). OMW treatment operating with a COD of 1960 mg/l a maximum conversion of 58% with TiO_2 and PAC under sunlight was found by Baransi et al. (Baransi et al., 2012). The corresponding values of COD, TOC, lignin (total phenolic compounds) and total suspended solids (TSSs) removal values for UV/TiO_2 were 68.8%, 67.3%, 40.19% and 48.9%, respectively, after 80 min irradiation time reported by Badawy et al., 2009. Ruzmonava et al., (2013) investigated olive mill wastewater treatment with 1.5 g/L $Fe_3O_4/SiO_2/TiO_2$ and obtained % 50 organic degradation. On the other hand they emphasized that the composite nanoparticles were easily recovered by their magnetic core and re-used without significant reduction of efficiency.

Zinc oxide (ZnO) has gained immense research interest as an effective wastewater purification method because of its efficacy in decomposing and mineralizing the hazardous organic pollutants as well as the opportunity of utilizing the solar UV and visible spectrum. Recently, much effort has been devoted to study the ZnO as a very promising photocatalyst for photocatalytic degradation of water pollutants, due to low cost and environmentally friendly feature (Hariharan, 2006; Lee et al., 2006).The shell increases the reactivity of surface and improves the stability and dispersive ability of the core material (Zhai et al., 2010). In general, the synthesis of core/shell structured material has the goal of obtaining a new composite material having synergetic or complementary behaviors between the core and shell materials. Many studies on the synthesis of composites, i.e. TiO_2 (Zhang et al., 2006), $CaCO_3$ (Bala et al., 2007), γ-Fe_2O_3 (Maurice et al., 2009) and Ag (Chou & Chen, 2007) coated with SiO_2 shells have

been reported. SiO_2 is a most studied shell candidate due to its relative ease in preparation, good environmental stability and compatibility with other materials, which motivated us to prepare the core/shell structured composite of ZnO and SiO_2 and expected to achieve novel properties resulting from the synergic interaction of these two chemical components.

1.2 The Aim of This Master Thesis

The aim of this study is the removals of COD, total phenol, total suspended solid (TS), total nitrogen, total phosphorus and polyphenols (gallic acid, p-coumaric acid and trans p-coumaric acid) in the OMW by nano-ZnO-SiO_2 composite via adsorption and photocatalytic processes.

The general purpose of the master thesis was;

- to evaluate the performance of the adsorption treatment process of OMW with measuring COD, total phenol, polyphenols, TS, total nitrogen, total phosphorous,
- to evaluate the performance of photocatalytic using nano-ZnO-SiO_2 composite under laboratory conditions under UV and sun light irradiation,
- to obtain optimum treatment conditions for three different treatment processes (adsorption, UV and sunlight) using nano-ZnO-SiO_2 composite,
- to obtain the effects of increasing nano-ZnO-SiO_2 composite concentrations (1, 3, 5 and 10 g/L for adsorption and 0.5, 1, 3, 5, 10, 12 and 20 g/L for UV and sun light processes), irradiation times (15, 30, 60, 90, 180, 240, 360 min for adsorption and 15, 30, 60, 90, 180 and 1440 min for UV process and 8, 16, 24 and to 36 h for sunlight process) and pH (original pH of OMW (4.01), 7 and10) on the adsorption and photocatalytic removals of pollutants in the OMW.
- to compare the yields of adsorption, UV irradiation and sunlight irradiation according to pollutant removal efficiencies,
- to choose the best treatment mechanism for the treatment of OMW,
- to explain results of removal mechanism according to zero order kinetic, first order kinetic and second order kinetic

- to make a cost analysis for three removal process and
- to investigate the recovery of the catalyst and to minimize the concentrations of pollutant parameters by reusing of nano-ZnO- SiO_2 composite

The specific objectives of this study are to determine the optimum Nano-ZnO-SiO_2 composite concentration for maximum removals of COD, total phenol, TS, total nitrogen and total phosphorous to evaluate effect of contact timing and pH on the treatment of OMW pollutants, and to determine the kinetic model for the removal of pollutants via adsorption and photocatalytic mechanisms.

1.3 Novelty of this Master Thesis

OMW treatment was widely investigated with classical and inadequate treatment methods**.** Semiconductor photocatalytic process has shown a great potential as a low-cost, environmental friendly and sustainable treatment technology to align with the "zero" waste scheme in the water/wastewater industry. ZnO is a luminescent material which is suitable for use in the photo-catalysis and has a wide direct band gap of about 3.3 eV, enormous surface-to-volume ratio, excellent chemical and thermal stability a very promising photocatalyst for photocatalytic degradation of water pollutants, owing to its high activity, low cost and environmentally. SiO_2 has good activity, chemical stability, commercial availability, high surface area. In addition, SiO_2 can be produced synthetically or bought due to its inexpensiveness and abundant in nature. In this study it is expected that SiO_2 will increase the reactivity of surface and will improve the stability and dispersive ability of the ZnO.

In this work, SiO_2 and ZnO were took advantage of synergetic effect for treatment of OMW for three different treatment methods (adsorption, under UV light and sunlight irradiations). OMW treatment with nano-ZnO-SiO_2 has not been worked yet. Five different pollutant parameters and polyphenol measurements realized detailed under different conditions to get optimum treatment condition. All of these methods were comprised; the optimum dose and optimum retention time and optimum pH for maximum yields were detected. In addition, cost analysis of

treatment methods were investigated to choose treatment mechanism of OMW economically. Reusability of nano-ZnO-SiO_2 composite was investigated; reuse of nanocomposite is eco-friendly approach and decreasing the treatment cost of OMW.

CHAPTER TWO
OLIVE MILL WASTEWATER

Olive oil production has a social and economic importance; particularly in Mediterranean countries. In these countries, the extraction and manufacture of olive oil are carried out in numerous small plants that operate seasonally, which can generate in excess of 30 million t/year of black effluent referred to as olive mill wastewater (OMW) (Niaounakis & Halvadakis, 2006).

Olive oil can be obtained by means of two different processes. The first one is a two-phase procedure, in which oil is separated from the solid mass of olive milling, producing olive oil and a pasty residue very difficult to handle. The second process is a three-phase system, in which water is added to enhance oil separation and recovery. In this way, oil and vegetation waters are separated from the solid phase, then olive oil is separated from olive mill wastewater (OMW) by decantation (Frascari et al., 2016).

OMW is highly polluting due to its high biochemical oxygen demand (BOD_5, typically 50,000–100,000 mg/L) and chemical oxygen demand (COD, typically 80,000–200,000 mg/L) (Khoufi et al., 2006). These values are on average 200–400 times higher than those of typical municipal sewage. Besides its high organic loading: the presence of polyphenols and tannins, high concentration of suspended solids (SS) and its acidity render OMW, highly recalcitrant to conventional wastewater treatment (Dermeche et al., 2013). Until now, several methods have been proposed for the treatment of OMW such as lagooning, evaporation, co-composting (Moraetis et al., 2011), chemical oxidation and coagulation (Yalili Kilic et al., 2013), biological processes including anaerobic, aerobic and fungal treatment (Ntougias et al., 2013) as well as membrane technologies (El-Abbasi et al., 2013). A variety of advanced oxidation processes (Zorpas & Costa, 2010) and (Chatzisymeon et al., 2013) such as catalytic ozonation, Fenton and Photo-Fenton processes as well as heterogeneous TiO_2-mediated photocatalysis have been proposed for OMW treatment. Besides, combined treatments such as advanced oxidation processes and

biodegradation (Lafi et al., 2009) as well as coagulation coupled with advanced oxidation processes (Lafi et al., 2010), (Kestioglu et al., 2005) and (Kiril- Mert et al., 2010) have been examined. However, most of them appeared to be rather inefficient and economically unattractive since it is quite difficult to efficiently treat high-strength, complex wastewater without pre-treatment and in-depth knowledge regarding its properties.

2.1 Treatment of OMW

2.1.1 Literature Review on the Treatment of OMW with Different Treatment Technologies

Conventional wastewater treatment consists of a combination of physical, chemical, and biological processes and operations to remove solids, organic matter and, sometimes, nutrients from wastewater. General terms used to describe different degrees of treatment, in order of increasing treatment level, are preliminary, primary, secondary, and tertiary and/or advanced wastewater treatment (Pescod, 1992).

Simple physical processes such as dilution, evaporation, sedimentation, filtration and centrifugation have been employed to treat OMW. None of these processes alone is able to reduce the organic load and toxicity of OMW to acceptable limits. Dilution is very often used prior to biological treatment to reduce toxicity to the micro-organisms responsible for organic matter decomposition. Evaporation and sedimentation can concentrate OMW to the extent of 70–75%, this being mainly attributable to phase separation/dehydration and not as much too subsequent organic matter degradation (Paraskeva & Diamadopoulos, 2006).

Thermal treatment methods such as combustion, co-combustion and pyrolysis have also been tried as a means of recovering energy for cofuelling the olive oil extraction plant. Combustion and pyrolysis have the advantages of reducing the volume of waste and providing the possibility of energy recovery, but they require expensive facilities and entail possible emission into the atmosphere of toxic

substances. Some degree of pre-concentration of OMW as well as mixing with other wastes is also required (Niaounakis & Halvadakis, 2004; Caputo et al., 2003).

Centrifugation and filtration increase the pH and conductivity of the effluents and remove organic matter through phase separation and exclusion respectively. Usually a combination of physical processes or often a combination of physical processes coupled with coagulation/flocculation or adsorption technologies leads to more efficient organic matter removal. Application of sedimentation followed by centrifugation and then filtration (Al-Malah et al., 2000) showed that, after centrifugation, COD was reduced by 21% and BOD by 15%. Additional filtration did not remove any COD, but a further 16% reduction in BOD was observed. Adsorption of the OMW onto activated clay reduced the COD by a further 71% and the phenol content by a maximum of 81%. Adsorption/desorption equilibrium needs special care, as organic matter and phenols start to desorb after a certain contact time. The combination of four treatment steps, namely settling, centrifugation, filtration and activated carbon adsorption (Azzam et al., 2000), achieved a maximum phenol removal of 94% and a maximum organic matter removal of 83%. A study of the effect of lime treatment on various OMW after a classic coagulation/ flocculation/sedimentation/filtration process (Aktas et al., 2001), using a range of lime doses from 10 to 40 g/L, revealed that lime dosing corresponding to a pH increase to 12 gave the optimal performance, resulting in 62–73% phenol removal depending on the process used for olive oil extraction. More than 40% COD removal and about 95% oil and grease removal were also observed.

The use of direct flocculation with polyelectrolytes for the treatment of OMW (Sarika et al., 2005) showed that two polyelectrolytes, one anionic and one cationic, failed to yield separation, whereas for three others a minimum dose of 2.3–3g/L was required. Nearly complete reduction of solids was observed in subsequent analysis, while COD and BOD reductions were up to 55 and 23% respectively. The sludge generated was about 20% of the initial volume and in some samples the biodegradability of the effluent increased, making aerobic post-treatment appealing. The use of typical coagulants such as alum and ferric chloride has also been

examined (Sarika et al., 2005; Kestioglu et al., 2005). Ferric chloride treatment after acid cracking resulted in 95% COD removal and 90% phenol removal at a dose of 3 g/L. Alum achieved similar reductions (94 and 91% for COD and phenols respectively) at a dose of 6 g/L. Sludge generation was 500–700 ml/L influent.

Adsorption on granular activated carbon (GAC) after coagulation/flocculation/sedimentation showed about 30% COD reduction and a requirement of 50 kg carbon m^{-3} effluent (Kestioglu et al., 2005).

Electrocoagulation is a method that has attracted attention recently for the treatment of olive mill and other industrial effluents. In an electrocoagulation cell the coagulant is generated in the solution from a sacrificial electrode, namely aluminium or iron. Respective metal hydroxides are formed in situ and remove pollutants (Inan et al., 2003). In such a system an aluminium anode achieved 52% COD reduction in 30 min reaction time and an iron anode achieved 42% COD reduction in the same time at an optimal pH of 6. An increase in current density increased COD removal, and colour was almost eliminated (96% removal). Other studies (Adhoum & Monser, 2004) found 76% COD reduction, 91% phenol reduction and 95% colour reduction after 25 min of treatment. The optimal pH range was 4–6, which is a typical pH range for OMW, and the optimal (economical) current density was 75 mA cm^{-2}. An additional advantage of electrocoagulation is the generation of a lower volume of sludge compared with the classic coagulation technology.

Biological processes for the treatment of wastewaters have seen worldwide applications. They are considered environmentally friendly, reliable and, in most cases, cost-effective. Biological treatment is able to remove organic matter and inorganic nutrients. Care needs to be taken in the selection of the micro-organisms employed and in their adaptation to treating olive mill wastewater, as phenolic substances are inhibitory to micro-organisms (Niaounakis & Halvadakis, 2004; Caputo et al., 2003; Mantzavinos & Kalogerakis, 2005).

In recent studies with laboratory-scale upflow anaerobic sludge bed (UASB) reactors (Ubay & Ozturk, 1997; Zouari & Ellouz, 1996). COD reductions of 70–80% were achieved for an initial COD range of 22.6–97 g L^{-1}. Organic loading rates (OLRs) varied considerably from 0.83 to 21.9 kg COD m^{-3}/day, with an average of 5 kg COD m^{-3}/day. Hydraulic retention times (HRTs) were from 2 to 5 days. Dilution of the initial effluent was required, especially in the initial operating period, and nutrient addition and alkalinity adjustment were necessary. With increasing HRT up to 25 days, COD reduction reached 87.9%. Methane production was found to correlate with COD removal at a ratio of 0.30–0.35 m^3 CH_4 kg^{-1} COD removed, except in one study (Zouari & Ellouz, 1996), where it was found that biogas production was insufficient for the UASB systems used. Application of an anaerobic sequencing batch reactor (Ammary, 2005) showed COD reductions of up to 80% with an HRT of 3 days and an average OLR of 5.3 kg COD m^{-3}/day. No nutrients were added, but the influent was diluted to 16 g/L COD from an initial 97 g/L COD.

Aerobic treatment is a commonly used technology in wastewater treatment. For OMW an acclimatization period for the micro-organisms is required. Studies on activated sludge treatment listed in Rozzi & Malpei, (1996) report COD removal rates of 80–85% and HRTs in the range 20–25 days. More recent studies (Benitez et al., (1997) and Benitez et al., (1999)) examined the aerobic degradation of OMW in a completely mixed batch activated sludge reactor after micro-organism adaptation. COD removals in the range 58–68% were observed for corresponding initial CODs of 65–98 g/L, and reductions between 81 and 84% for an initial COD of 22 g/L. Phenol removal was 90% in all experiments.

Three-stage aerobic/anaerobic/aerobic treatment employing *A. niger*/anaerobic filter/activated sludge (Hamdi et al., 1992) was able to remove a total of more than 90% COD, with partial removals of 58, 60 and 45% respectively. Despite the three-step treatment and the high removal percentage, the effluent still had a substantial COD content and dark colour.

Complete treatment of OMW was achieved by the combined anaerobic/aerobic treatment of OMW diluted with primary municipal wastewater (Gizgis et al., 2005). The anaerobic reactor was a high-rate UASB reactor and the OMW was diluted with primary municipal wastewater at dilutions between 1:17 and 1:33. The effluent of the anaerobic reactor was treated in a bench scale activated sludge system. Although the influent COD varied greatly from 1800 to 4800 mg/L, the effluent COD was always between 400 and 600 mg/L, with a range of removal of 70–90%. Biogas production was 0.3 m^3/kg COD removed. Aerobic treatment resulted in final COD values between 85 and 175 mg/L, and BOD was always below 20 mg/L.

2.1.2 OMW Treatment with Advanced Process

The use of a strong oxidizing agent can result in a high degree of wastewater treatment, including the breakdown of recalcitrant and toxic compounds. In theory, depending on the oxidation potential of the agent and the contact time, complete mineralization can occur. In recent years there has been growing interest in oxidation and advanced oxidation processes for the treatment of industrial effluents and therefore for the treatment of olive mill wastewater as well. Ozone is a powerful oxidizing agent that selectively attacks compounds containing aromatic rings and double bonds (Paraskeva & Diamadopoulos, 2006). Small COD reductions of 18–20% observed after 2 h of ozonation of OMW with an initial COD of 10 g/L can be attributed to the breakdown of larger organic substances into smaller ones (Benitez et al., 1999). On the other hand, 76% reduction of aromaticity and almost complete phenol removal for the same ozonation time verify the selectivity of ozone. Depending on the contact time and ozone dose, ozonation removed up to 90% of phenols and colour when applied to a weathered (in evaporation ponds) OMW (Karageorgos et al., 2006). COD removal varied from 4 to 60% and toxicity was reduced independently of ozonation conditions.

Advanced oxidation processes (AOPs) involve the creation and action of hydroxyl radicals, which are unstable and reactive species created by an oxygen source and an energy source. The oxygen source is usually ozone (O_3) or hydrogen

peroxide (H_2O_2) and the energy source is UV or solar energy. Comparison of two AOPs for the treatment of OMW (Aktas et al., 2001) namely O_3/UV and H_2O_2/UV operating at optimal pH values of 7 and 2 respectively, resulted in 99% COD and phenol removal for an H_2O_2 dose between 750 and 1000 mg/L and an optimal ozonation time of 5 h at 0.3 g/h ozone generation (535 mg/L applied dose). Costs of power, pH adjustment and maintenance have to be co-evaluated when scaling up. Wet air oxidation with or without the use of catalysts can improve the biodegradability of OMW or lead to almost complete mineralisation (Rivas et al., 2001). For OWM diluted 1:10 with synthetic municipal wastewater at 180 ◦C temperature and 7 MPa pressure, 30% COD reduction was observed and 80% reduction in phenolic substances under mild acidic conditions. Under neutral conditions, COD removals of up to 52% were observed for the same oxidation time without affecting the phenol removal. Use of heterogeneous catalysts of copper oxide and platinum increased COD removal by 10–17%. Under supercritical conditions and with addition of radical promoters, COD removal can be as high as 99%.

An oxidation process that combines chemical oxidation and coagulation by means of hydrogen peroxide and ferrous sulphate addition (Fenton oxidation) is another promising technology. Parameters such as ferric or ferrous concentration, peroxide concentration, pH and reaction time are of paramount importance in this process. Fenton reactions can treat recalcitrant organics and remove up to 65% of COD (Rivas et al., 2001) when the Fe concentration is 0.5 mol/L and the reaction time is longer than 4 h. Complete removal of phenols and COD reductions in the range 40–60% were also found in other studies Vlyssides et al., 2003; Vlyssides et al., 2004 with a 2 h reaction time at a dose of 2–3 g/L ferrous sulphate ($FeSO_4 \cdot 7H_2O$) and 3 mL of peroxide (60% w/w). For lower Fe (II) and peroxide concentrations (0.03 and 0.25 mol/L respectively), COD removals were 40% after 2 h of treatment and remained unchanged there after 2 h (Ahmadi et al., 2005).

An enhanced Fenton process with UV or solar light (photo-Fenton) showed a marked ability to reduce the phenolic content present in olive mill and other agroindustrial wastes (Gernjak et al., 2003). Experiments in a falling film

photoreactor after pre-treatment with flocculation/separation resulted in 85% COD removal and complete phenol removal from an OMW (Gernjak et al., 2004) whereas photocatalysis with titanium dioxide alone was not successful and had a limited effect on organic matter removal only after peroxydisulfate addition. Electrochemical oxidation with a Ti/Ta/Pt/Ir anode (Gotsi et al., 2005) has also been used to study the effect of electrochemical oxidation on OMW. It was found that the process was able to remove almost entirely the content of phenols and the appearance of colour but did not achieve a high degree of mineralisation, as COD removals were up to 40%. Increasing voltage and salinity improved the performance of the cell. Toxicity according to the Daphnia magna test increased with oxidation. For an optimal salinity of 3% (w/v) NaCl, electrochemical oxidation with a Ti/Ta/Pt/Ir anode resulted in 70.8% COD reduction after 8 h of electrolysis. Turbidity, colour and odour were eliminated and toxicity remained unchanged (Giannes et al., 2003).

Drouiche et al. (2004) have examined the removal capacity of ultrafiltration coupled with UV/H_2O_2. Ultrafiltration alone using a tubular polysulfone module of 20 000 Da MW cut-off reduced the COD by 94% when operating at 0.15 MPa pressure. Further treatment by UV/ H_2O_2 for 35 min reduced the COD to 52 mg L−1 and completely removed colour. A centrifugation step before ultrafiltration can be used to reduce membrane fouling (Turano et al., 2002) and lead to COD reductions of up to 90%.

2.1.3 Treatment of OMW with Nano-ZnO-SiO_2 Composite

We investigated effect of concentration of nano- nano-ZnO-SiO_2 composite, contact time for adsorption, irradiation time for UV and sunlight irradiation and pH of OMW in this study.

Six different increasing concentrations of nano-ZnO-SiO_2 composite 1, 3, 5, 10, 12 and 20 g/L were chosen to determine the optimum nano-ZnO-SiO_2 composite concentration on the adsorption of pollutants in the OMW to nanocomposite. All experiments were realized after 180 min adsorption time (since the results of

preliminary studies 180 min was the optimum contact time for effect of concentration of nano-ZnO-SiO_2 composite) at 20 ^{0}C and at original pH of OMW. For maximum adsorptions of pollutants the optimum nano-ZnO-SiO_2 composite concentration was determined at the end of those experiments. Effect of contact time on the removals of COD, total solids, phenol, total nitrogen and total phosphorous in the OMW for the nano-ZnO-SiO_2 composite concentration of 1 g/L, at original pH of OMW and 20 ^{0}C were illustrated in figures. Contact times were selected as 15, 30, 60, 90, 180, 240, 360 min. The pH of OMW is a major effect on adsorption capacity of nano particles that's why original pH of OMW (4.01), 7 and 10 were investigated for optimum treatment pH.

The recent literature survey showed that the photocatalytic removal of the OMW with nano-ZnO-SiO_2 composite has not studied yet. On the other hand photocatalytic activity of nano-ZnO-SiO_2 composite has studied by some researchers. Mohamed et al., (2013) has studied photocatalytic property of nano-ZnO-SiO_2 composite on degredation of Methylen Blue (MB). The effect of the reaction time on the photodegradation efficiency of MB and the surface area was conducted by changing the reaction time from 30 to 120 min. The results according to their study reveal that the photodegradation efficiency of MB was increased from 92 to 95% by increasing the reaction time from 30 to 60 min. A further increase in the reaction time from 90 min to 120 min slightly increased photodegradation efficiency of MB to 95.50% and to 95.55%. In another study, the surface area increased very slowly from 472 to 473 m^2/g, which meant that the hydrolysis and condensation reactions were completed within the first 60 min, and the growth of the particles was stopped (Ismail et al. 2003). Therefore in their study the best reaction time was accepted as 60 min.

Zhai et al., (2010) studied the photocatalytic efficiency of nano-ZnO-SiO_2 composite with Rhodamine B. They obtained that the zeta potential of ZnO (9.8) changed when ZnO combined with SiO_2. This showed that the detection of pH in the treated solution is important for photocatalytic reactions. They found that the nano-ZnO-SiO_2 nanoparticles exhibited a better photocatalytic activity at lower pH values like of 4.5.

CHAPTER THREE
ADSORPTION MECHANISM

Adsorption is a process in which a substance (adsorbate), in gas or liquid phase, accumulates on a solid surface. It is based on the capability of porous materials with large surfaces to selectively retain compounds on the surface of the solid (adsorbent). Adsorption is defined as the increase in concentration of a particular component at the surface or interface between two phases (Faust & Aly, 1998). In this case, the interaction of H^+ and metal ions between the solid peat and the surrounding aqueous solution is the main focus. There are two types of adsorption; physical and chemical adsorptions. Physical adsorption is achieved by Van der Waals forces, dipole interactions, and hydrogen binding. There is no electron exchange between adsorbent and adsorbate. Chemical adsorption results from the chemical link between adsorbent and adsorbate molecule, therefore it is specific as well as irreversible and chemical as well as electronic properties of adsorbent are changed (Mohamed, 2011).

The adsorption process of the adsorbate molecules from the bulk liquid phase into the adsorbent surface is presumed to involve the following stages (Figure 3.1):

1. Mass transfer of the adsorbate molecules across the external boundary layer towards the solid particle.
2. Adsorbate molecules transport from the particle surface into the active sites by diffusion within the pore–filled liquid and migrate along the solid surface of the pore.
3. Solute molecules adsorption on the active sites on the interior surfaces of the pores.
4. Once the molecule adsorbed, it may migrate on the pore surface trough surface diffusion.

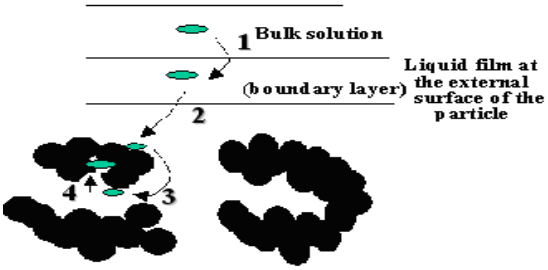

Figure 3.1 Mechanism of molecule adsorption using microporous adsorbent (Tchobanoglous et al., 2003).

The most important property of adsorbent, which determines its usage, is the pore structure and the specific surface area. The total number of pores, their shape and size determine the adsorption capacity and even the dynamic adsorption rate of the adsorbent (Wu, 2004). The specific surface area is another important property that determines adsorbent usage and its capacity. The micropores usually provide the largest proportion of the internal surface of the adsorbent and contribute to most of the total pore volume (Wu, 2004).

The removal of ions from aqueous solutions involves concentration of the solute on the solid surface. As the adsorption proceeds, solutes are simultaneously adsorbed and desorbed. Eventually the rates of adsorption and desorption will attain an equilibrium state, called the adsorption equilibrium (Faust & Aly, 1987). At equilibrium, no change can be observed in the concentration of the solute on the solid surface or in the bulk solution. The position of equilibrium is characteristic of the entire system and is dependent on the solute, adsorbent, solvent, temperature and pH, among others (Faust & Aly, 1987).

Generally Langmuir and Freundlich adsorption models represent adsorption isotherm. These methods are performed to investigate the coverage or adsorption of molecules on a solid surface at a fixed temperature. It also provides some information about how fast the species are adsorbed on the adsorbent surfaces. This is important in designing and modeling of the adsorption process.

CHAPTER FOUR
PHOTOCATALYTIC MECHANISM

Photocatalytic oxidation is an advanced oxidation process for removal of trace contaminants and microbial pathogens. It is a useful pretreatment for hazardous and non-biodegradable contaminants to enhance their biodegradability. Photocatalysis can also be used as a polishing step to treat recalcitrant organic compounds. The major barrier for its wide application is the slow kinetics due to limited light fluence and photocatalytic activity (Qu et al., 2013).

The UV spectrum is arbitrarily divided into three bands: UV-A (315 to 400 nm), UV-B (280 to 315nm) and UV-C (100 to 280 nm). UV-A and UV-C are generally used in environmental applications. UV-A radiations are referred to as long wavelength radiations or black light and UV-C are referred to as short wave radiations (Mohamed, 2011).

Heterogeneous photocatalysis means that the reactants and the photocatalyst are present in two or more phases. The basis of photocatalysis is the photoexcitation of a semiconductor solid as a result of the absorption of radiation, often but not exclusively in the near ultraviolet spectrum (Herrmann et al., 2007). Under near UV irradiation, a suitable semiconductor material may be excited by high energy photons producing conduction band electrons and valence band holes. These charge carriers are able to induce reduction or oxidation, respectively, and react with both water and organic compounds (Detlef, 2004). The holes are extremely oxidants and should thus be able to oxidize almost all chemicals, as well as water, resulting in the formation of hydroxyl radicals (Malato et al., 2002; Mills & McFarlane, 2007; Allen et al., 2008; Gaya & Abdullah, 2008).

The band gap energy is the main factor that defines the kind of substances; conductor, semi-conductor or insulator. The surface containing electrons and holes generates ·OH radicals and other radicals formed by the oxidation of oxygen, water, or hydroxide ions (Ibhadon & Fitzpatrick, 2013). Direct oxidation of the pollutant

may be possible by photo induced holes. Several UV/semiconductor systems have been used for the photocatalytic degradation of organic pollutants. Most of these semiconductor particles have photocatalytic properties (Bessa et al., 2001; Salem, 2003; Byrappa et al., 2006; Colon et al., 2007) such as the metal oxides, TiO_2, WO_3, ZnO, and Fe_2O_3. Table 4.1 summarizes the most common semiconductors employed as photocatalysts, their band gap energies (Ebg) and respective wavelength sensitivity. The bang gap energy and the wavelength (λ) of the SiO_2 were 3.25 Ev and 587 nm, respectively (Polyanskiy, 2015).

Table 4.1 Band gap energy and wavelength sensitivity of semiconductors (Stumm, 1992)

Semiconductor	**Ebg (eV)**	**λ (nm)**
Fe_2O_3	2.3	539
TiO_2 (rutile)	3.0	413
TiO_2 (anatase)	3.2	388
WO_3	2.8	443
ZnO	3.2	388

As for classical heterogeneous catalysis, the overall process can be decomposed into five independent steps (Herrmann, 1999):

1. Transfer of the reactants from the fluid phase to the surface
2. Adsorption on the nano particle surface
3. Reaction of the adsorbed molecules
4. Desorption of the reaction products
5. Transfer of the products from the interface region to the solution

The mass transfer steps (1) and (5) depend on reactant/product concentration as well as photocatalyst loading and particle size. Steps (2), (3), and (4) depend on the chemical compatibility of reactant and product molecules with the active sites. One of these steps will control the overall reaction rate. It is essential to understand which is controlling so that the photocatalyst or operating conditions can be varied to obtain optimum performance.

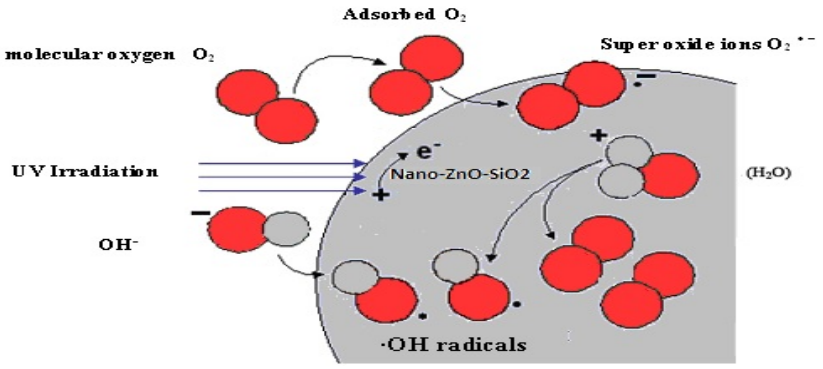

Figure 4.1 Formation of hydroxyl radicals and superoxide ions on the surface of nano- ZnO-SiO_2 composite surface

The photocatalytic reaction occurs in the step (3); upon absorption of a photon, the nano composite acts as photocatalyst forming a hole and an electron which produce reactive radicals (mainly ·OH radicals) (Figure 4.1). The hole reacts with water to generate the hydroxyl radical and the electron can reduce molecular oxygen, hydrogen peroxide or some other oxidizing agent in the solution or over the nano composite surface. This creates the reactive radicals responsible for the removal of hazardous components and may totally mineralize them. Firstly, the light energy (hv), greater than the band gap energy (Eg), strikes the surface of the catalyst and excites an electron from the valence band to the conduction band. A valence-band hole, VB h^+, is created, which migrates to the surface and initiates a reduction reaction. The valence-band hole and conduction-band electron can recombine in the bulk material and on the surface (Mohamed, 2011).

The efficiency of this processes is based on the production of reactive species, such as electron pair (2 e^-) that reduce protons to produce H_2 and also, produce holes (h^+), hydroxyl radicals ($^{\cdot}OH$), and superoxide anions ($O_2^{\cdot -}$) which are able to oxidize and mineralize almost all organic pollutants yielding CO_2 and inorganic ions as final products according to the following equations (Figure 4.2):

$$ZnO/SiO_2 + hv \rightarrow e^-_{cb} + h^+_{vb} \quad (4.1)$$

$$O_2 + e^-_{cb} \rightarrow O_2^{\bullet -} \quad (4.2)$$

$$O_2^{\bullet -} + H_2O \rightarrow O^{\bullet} + OH^- + O_2 + HO_2^- \quad (4.3)$$

$$H_2O + h^+_{vb} \rightarrow HO^{\bullet} + H^+ \quad (4.4)$$

The high concentration of $HO^{\bullet}$ and $O_2^{\bullet-}$ absorbed in the particle surface, organic compounds could be broken down through oxidative decomposition as indicated in (4.5):

$$\text{Organic composite} + O_2^{\bullet-} + HO^{\bullet} \rightarrow CO_2 + H_2O + \text{sub composite} \quad (4.5)$$

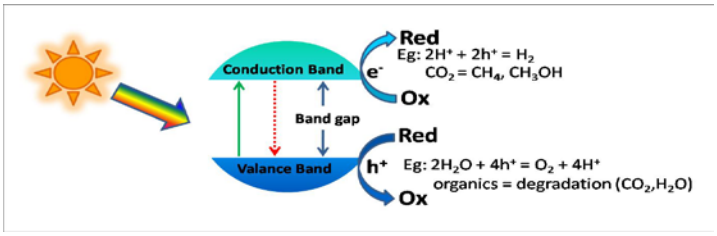

Figure 4.2 Photo-catalysis reactions (Kamat, 2002)

4.1 ZnO Nanoparticles

The metal oxide nanoparticles stand out as one of the most versatile materials, due to their diverse properties and functionalities (Figure 4.3). ZnO is an attractive material for short-wavelength optoelectronic applications owing to its wide band gap 3.37 eV, large bond strength, and large exciton binding energy (60 meV) at room temperature. As a wide band gap material, ZnO is used in solid state blue to ultraviolet (UV) optoelectronics, including laser developments. In addition, due to its non-centrosymmetric crystallographic phase, ZnO shows the piezoelectric property, which is highly useful for the fabrication of devices, such as electromagnetic coupled sensors and actuators (Minne et al., 1995).

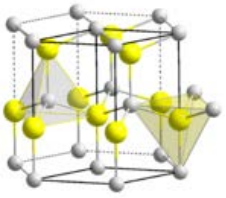

Figure 4.3 Chemical structure of ZnO (State, 2008)

ZnO is abundant in nature, nontoxic nature and environmental friendly photocatalyst (Jin et al., 2008). It can absorb wider range of spectrum of radiation

which also makes it more applicable for dye sensitized solar cells and solar photovoltaic applications (Zhang et al., 2009). The nanosized ZnO oxides are most efficient functional materials for photocatalytic applications which are available at low cost, exhibit mild reaction conditions and high photochemical reactivity, while affording the use of sunlight (Yang et al., 2004). It is extensively used to treat wastewater, such as dairy and food wastewater, drugs and pesticides wastewater, textile wastewater, etc. (Chakrabarti & Dutta, 2004; Mathur et al., 2007; Daneshvar et al., 2007). Zinc oxide is a photoactive semiconducting material oxide and able to activate itself by taking energy for the photocatalytic reaction from photons. Therefore ZnO photocatalyst must have to simultaneously adsorb reasonable amount of O_2 and reducing species (i.e., the organic pollutant molecules). A good photocatalyst like zinc oxide is considered to provide adsorption sites for the organic pollutants, which means that an open porous structure with high specific surface area is needed (Hao et al., 2000).

4.2 SiO_2 Nanoparticles

Silicon dioxide nanoparticles, also known as silica nanoparticles or nanosilica, are the basis for a great deal of biomedical, environmental engineering, electronic engineering, chemical industry research due to their stability, low toxicity and ability to be functionalized with a range of molecules and polymers (Figure 4.4). SiO_2 can be produced synthetically or bought due to its inexpensiveness. SiO_2 has high surface area (over 800 m^2/g) and it provides absorbing the pollutants from wastewater.

In addition to the already mentioned properties of SiO_2, the grafting of metal oxides onto its surface highly increases the matrix reusability, stability and adsorption capacity for metal ions in a wide pH range. Furthermore, such materials possess strong chemical activity due to the abundance of Lewis and Brønsted acid/base binding sites that enable high retention of cationic and anionic metal species (Liu & Liang, 2008).

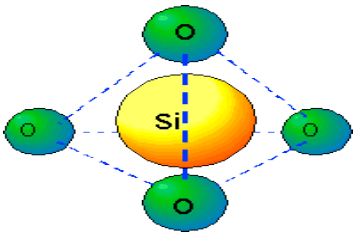

Figure 4.4 Chemical structure of SiO_2 (Dobkin, 2003)

4.3 Nano-ZnO-SiO_2 Composite

In recent years, the development of core/shell structured materials on a nanometer scale has been receiving extensive attention (Lee et al, 2001). The shell can alter the charge, functionality, and reactivity of surface, or improve the stability and dispersive ability of the core material. Furthermore, catalytic, optical, or magnetic functions can be imparted to the core particles by the shell material. In general, the synthesis of core/shell structured material has the goal of obtaining a new composite material having synergetic or complementary behaviors between the core and shell materials (Zhai et al., 2010).

Among the various semiconductors recently studied, zinc oxide (ZnO) stands out for use in decomposition of organic pollutants because of its high photosensitivity, excellent mechanical characteristics, low cost and environmentally safe nature (Singhal et al. 2008). The use of ZnO for photocatalytic degradation of organic pollutants has been studied extensively. Examples of such studies may include degradation of 2-chlorophenol (Abdel Aal et al. 2008), Rhodamine dyes (Yu et al. 2004), azo-reactive dyes (Fouad et al. 2006) and Methylene Blue (MB) (Chu et al. 2010).

Silicon dioxide (SiO_2) has been coupled with semiconductor photocatalysts to enhance the photocatalytic process. SiO_2 has high thermal stability, excellent mechanical strength and helps to create new catalytic active sites due to the interaction between semiconductor photocatalysts and SiO_2. Additionally, SiO_2 helps to obtain a large surface area as well as a suitable porous structure (Abd Aziz & Sopyan 2009).

The photocatalyst nano-ZnO-SiO_2 was used in the photocatalytic degradation of methylene blue (Mohamed et al., 2013; Ali et al., 2014) and Rhodamine B (Zhai et al., 2010).

CHAPTER FIVE
MATERIALS AND METHODS

5.1 Wastewater Origin

Raw OMW was taken from the olive mill industry located in Aydın and used without any pre-treatment, in November 2013.

5.2 Reagents and Chemicals

Nano-ZnO and SiO_2 were bought externally. Nano-SiO_2 was provided Ege Nanotek Kimya Sanayi Ltd. Şti. Nano-ZnO was purchased from Synergy Laboratory Products Ltd., Turkey. Demineralized water was used for preparation of reagents solutions. 0.1 M HCl and 0.1 M NaOH are used to adjust pH vales of olive mill wastewater.

5.3 Experimental Procedures

5.3.1 Batch Reactors for Adsorption Process

The investigations were carried out in batches in different conditions of pH, nano-ZnO-SiO_2 composite concentrations, and time to get the optimum operational conditions for maximum adsorption yields in the treatment of OMW. The adsorption experiments were carried out isothermally in static mode at room temperature. The experiments were conducted by adding nano-ZnO- SiO_2 composite concentrations increasing from 1 g/L, 3 g/L, 5 g/L, 10 g/L, 12 g/L and 20 g/L (each concentration for 1 liter OMW) of OMW in conical glass reactors coated with teflone with a volume of 250 mL (0.25, 0.75, 1.25, 2.5, 3 and 5 g for 250 mL OMW). These reactors were placed on a rotating shaker and tested at 50 rpm, 150 rpm and 300 rpm shaking rates. The studies were performed at Original pH of OMW and also the pH of OMW were adjusted to 7 and 10 during the contact periods of 15, 30, 60, 90, 180, 240 and 360 min. Samples were withdrawn at suitable intervals and were separated

from the nano-ZnO-SiO_2 composite by centrifugation at 9000 rpm for 15 min. The analyses were carried out in supernatant samples and duplicated analysis for performed for every for every run.

The amount of maximum adsorption capacity of nano-ZnO- SiO_2 composite for the pollutant parameters was calculated according to Eq. (5.1):

$$qe = \frac{(Co - Ce).V}{W} \quad (5.1)$$

where; qe is the capacity of adsorbent (mg/g), C_0 and Ce are the initial and equilibrium liquid concentrations (mg/L), respectively; V is the volume of solution (L); and W is the weight of adsorbent (g).

5.3.2 Quartz Glass Reactors for Photocatalytic Processes

Photocatalytic degradation experiments were carried out in self-designed quartz glass reactors. The dimensions of the reactors were 38 and 3.5 cm and the total power of the UV lamps was 15 W x 20 = 300 Watt. The experiments were performed at room temperature and the pH of the reaction mixture was adjusted from 4 to7 and 10 using 1 mol/L of H_2SO_4 and NaOH solution. Photocatalytic experiments were carried out with a known quantity of nano-ZnO-SiO_2 composite concentration (0.5, 1, 3, 5 and 10 g/L). The glass quartz reactors were filled with 100 mL OMW and 0.05 g, 0.1 g, 0.3 g, 0.5 g and 1 g nano-ZnO-SiO_2 composite were added to the quartz glass reactors. Then, they were irradiated in a closed isolated device with UV lamps with a power of 300 Watt.

Figure 5.1 UV reactor for photocatalytic treatment

And also, photocatalytic degradation experiments were carried out under sunlight in same quartz glass reactors which have the same proportions. Experiments were carried out at different retention times of the day and the reactors were placed at an angle of 90 degrees to the sun. The pH of the reaction mixture was adjusted from 4 to 7 and 10 using 1 mol/L of H_2SO_4 and NaOH solution. Experiments were carried out with nano-ZnO-SiO_2 composite concentrations varying between 0.5 g/L, 1 g/L, 3 g/L, 5 g/L and 10 g/L. During the experimentation, the samples were taken out from the reactors after a definite time interval, were centrifuged for 15 min and the supernatants were analyzed.

5.4 Synthesis of Nano-ZnO-SiO_2 Composite

Nano-ZnO and nano-SiO_2 were bought externally. Nano-ZnO–SiO_2 composites were prepared by physical synthesis by mixing fixed amount of ZnO and SiO_2 at 120 ^{0}C in an incubator during its preparation stage and stirred for 3 h at that temperature. The ratio of nano-ZnO to nano-SiO_2 used in the synthesis of the composite was 1:1. No chemical is used for synthesis of nano-ZnO–SiO_2 composite.

5.5 Analytical Methods

5.5.1 Chemical Oxygen Demand (COD) Measurements

COD was determined with Close Reflux Method following the Standard Methods 5220-D (APHA-AWWA-WEF, 2005) using an Aqua mate thermo electron corporation UV visible spectrophotometer. First, the samples were centrifuged for 10 min at 9000 rpm. Secondly, 2.50 ml volume wastewater samples were treated with 1.50 ml 10216 mg/L $K_2Cr_2O_7$ with 33.30 g/L $HgSO_4$ and 3.50 H_2SO_4 which contains 0.55% (w/w) Ag_2SO_4. Thirdly, the closed sample tubes were stored in a 148 ^{0}C heater (thermo reactor, CR 4200 WTW, 2008) for 2 h. Finally, after cooling, the samples were measured at 610 nm with an Aqua mate thermo electron corporation UV visible spectrophotometer. The Close Reflux Method COD was used to measure the COD in synthetic wastewater before and after anaerobic/aerobic sequential treatments.

5.5.1.1 COD Calibration Curves

KPH was used to prepare the standard solution 17 gKPH/L, which is equivalent to 20 g COD/L (Table 5.1 and Figure 5.2).

Table 5.1 Absorbance data for COD calibration.

Concentration of COD (mg/L)	Absorbance (Wavelength 610 nm)
100,0000	0,111
300,0000	0,148
500,0000	0,234
700,0000	0,274
900,0000	0,326

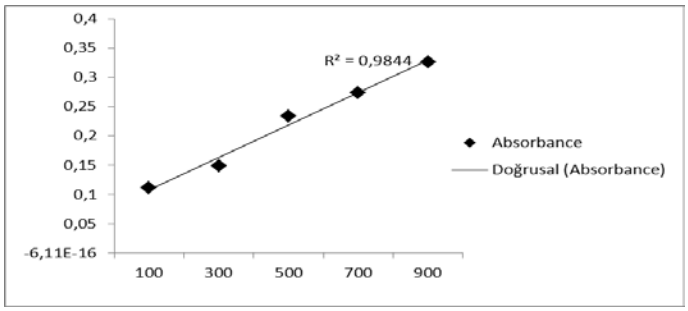

Figure 5.2 Calibration curve of the COD

5.5.1.2 COD Subcategories

The total inert COD and soluble inert COD were measured following the methods proposed by Ekama et al., (1986). The soluble inert COD was measured using the glucose comparison method. This method involves running three batch reactors, two with the wastewater to be studied and the third with glucose. One of the wastewater reactors has the total COD; the second has the total soluble COD, whereas the initial COD in the glucose reactor is adjusted to equal COD value. The experimental studies are performed until all the biodegradable COD is depleted, where the COD profiles reach a plateau and stay unchanged. The difference between glucose COD and wastewater COD gives the inert COD.

5.5.2 Phenol Measurements

The total phenol was determined by using analytical kits (Specturoquant N 1.14551.0001, Merck Chemical Company, Germany) and a NOVA-60 spectrophotometer (Merck).

5.5.3 Polyphenol Measurements

HPLC Equipment Specifications: A HPLC Degasser (Agilent 1100), a HPLC Pump (Agilent 1100), a HPLC Auto-Sampler (Agilent 1100), a HPLC Column Oven (Agilent 1100) and a HPLC Diode-Array-Detector (DAD) (Agilent 1100) were used.

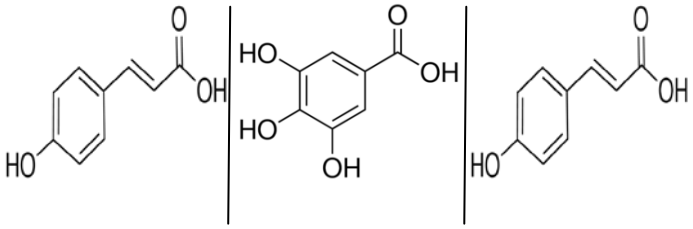

Figure 5.3 The structures of 3 phenolic acids (p-coumaric acid, gallic acid and trans p-coumaric acid, respectively)

Standard Solutions and Calibration Curves: For quantitation, an external standard method was utilized. Peak areas from the HPLC chromatogram were plotted against the known concentrations of stock solutions at varying concentrations. Equations generated by linear regression were used to establish concentrations for OMW and standard solutions.

About 10 mg of a standard of phenolic acid weighed accurately was dissolved into a 10 mL volumetric flask in 1:1 MeOH/water to obtain stock solutions. For calibration curves, the stock solution was diluted with 1:4 MeOH/water to obtain the concentration sequence. The linear range and the equations of linear regression were obtained through such a sequence of 50, 20, 10, 5 and 1 mg/L. Mean areas generated from the standard solutions were plotted against concentration to establish calibration equations

5.5.3.1 Gallic Acid, P-coumaric Acid and Trans p-coumaric Acid

Reagent and Materials: Gallic acid was purchased from Dr. Ehrenstorfer GmbH (Augsburg, Germany). p-coumaric acid and trans p-coumaric acid were purchased from Fluka (Buchs, Switzerland). Trifluoroacetic acid (TFA), purchased from Merck (Hohenbrunn, Germany), was of analytical grade. Methanol of HPLC grade was purchased from Fisher (Fairlawn, NJ). Deionized water (10^{-18}ohm) was purified by using an Aquapro purification system (Aquapro, Chongqing, China).

HPLC Analysis: Agela XBP-C18 (5 mm, 4.6 mm 150 mm, Agela, Newark, DE) was utilized for succeeding optimization. The flow rate of the mobile phase was kept

at 0.5 mL/min. Mobile phase A was water containing 0.02% TFA, and phase B was methanol containing 0.02% TFA. The gradient conditions were as follows: 0-5min, 25% B; 5-10 min, 25-30% B; 10-16 min, 30-45% B; 16-18 min, 45% B; 18-25 min, 45-80% B; 25-30 min, 80% B; 30-40 min, 80-25% B. The temperature of column was controlled at 25 °C. Injection volume was 10 µL. The detection wavelengths of DAD were set at: 254 nm. Prior to each run, the HPLC-DAD system was allowed to warm, and the baseline was monitored until it was stable before sample analysis.

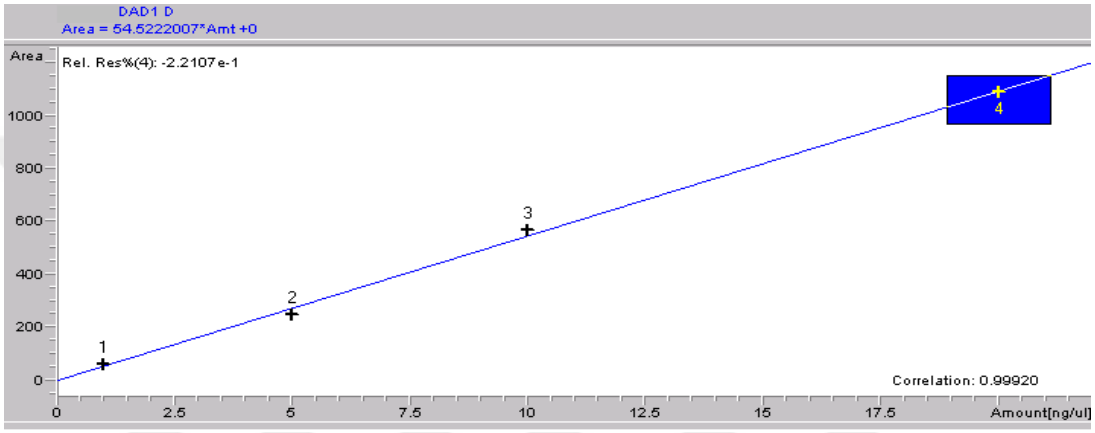

Figure 5.4 Calibration graph of gallic acid

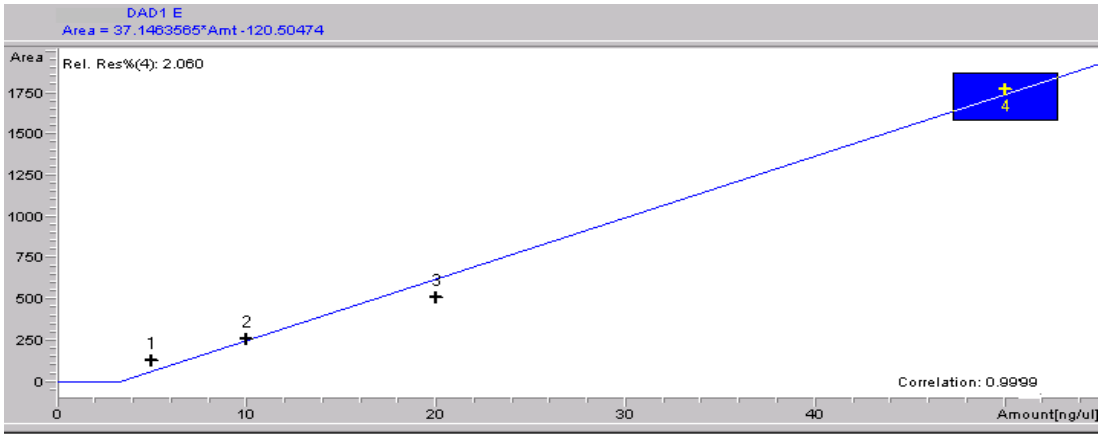

Figure 5.5 Calibration graph of p-coumaric acid

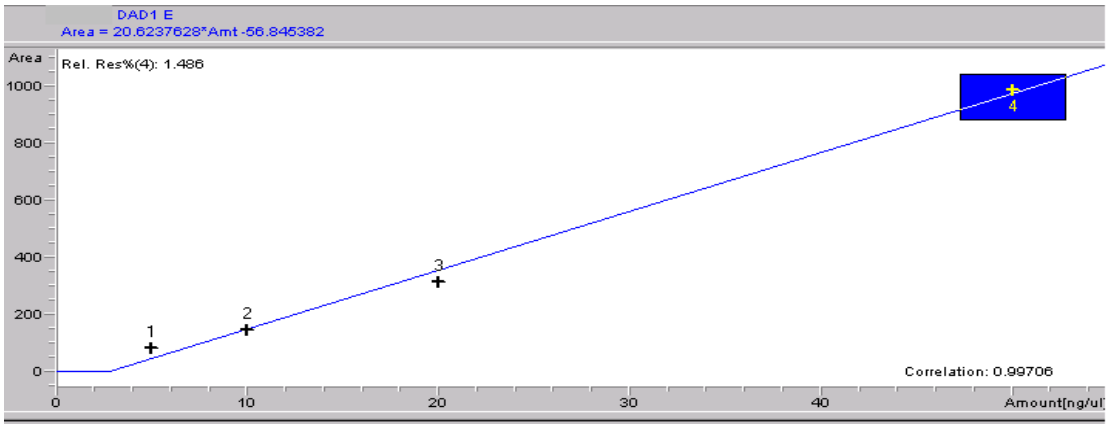

Figure 5.6 Calibration graph of trans p-coumaric acid

5.5.4 Total Solid Measurements

‘‘Total solids’’ is the term applied to the material residue left in the vessel after evaporation of a sample and its subsequent drying in an oven at a defined temperature. TS was determined with following the Standard Methods 2540-B (APHA-AWWA-WEF, 2005) using an oven brand of Stuart Scientific Oven 251. A well-mixed sample is evaporated in a weighed dish and dried to constant weight (g/L) in an oven at 103 to 105°C. The differences in weight over that of the empty dish represent the total solids.

5.5.5 Total Nitrogen and Total Phosphorous Measurements

The total nitrogen and total phosphorous were determined by using analytical kits (Specturoquant N 1.14537.0001 and Specturoquant PO_4-P1.14729.0001, Merck Chemical Company, Germany) and a NOVA-60 spectrophotometer (Merck).

5.6 Instrumental Characterization

5.6.1 X-ray diffraction (XRD)

XRD measurements were carried out with the D/max-2200 PC (Rigaku, Japan), using Cu-Ka radiation.

5.6.2 Fourier transform infrared (FT-IR)

FT- IR is a technique which is used to obtain an infrared spectrum of absorption, emission, photoconductivity or Raman scattering of a solid, liquid or gas. FT- IR spectra were measured with the Perkin Elmer FTIR System Spectrum BX with the KBr method.

5.6.3 Scanning Electron Microscope (SEM)

The morphological and structural observation was made on a scanning electron microscope VegaII/LMU (Tescan, Czech Republic).

5.7 Kinetic Studies

Absorption is the process through which a substance, originally present in one phase, is removed from that phase by dissolution in another (typically a liquid), as opposed to the accumulation at the interface as in the case of adsorption. Since, during adsorption, the pollutant is removed by accumulation at the interface between the nano-ZnO-SiO_2 composite (absorbent) and the OMW (liquid phase) the adsorbing capacity of nano-ZnO-SiO_2 composite is always associated with very high surface area per unit volume. Upon contacting an amount of nano-ZnO-SiO_2 composite with OMW containing an adsorbable substance adsorption will take place. Adsorption will continue until equilibrium will be established between the substance in solution and the same substance in the adsorbed state. Different adsorbates-adsorbents exhibit different types of equilibrium relationships (i.e., the function q = f(C) may take different mathematical forms). It has been found that for most of the cases of importance in wastewater treatment the function q = f(C) takes the form of one of the following isotherms: Langmuir isotherm, Brauner-Emmet-Teller (BET) isotherm, Freundlich isotherm. In this study, Langmuir, Freundlich kinetic models were used to fit the equilibrium data on nano ZnO-SiO_2 composite.

5.7.1 Langmuir Isotherm

The assumptions made in the derivation of the Langmuir model are , adsorption is a reversible process, the adsorbed layer is made up of a single layer of molecules , the adsorbed molecules do not move on the surface of the adsorbent. However, they can be lost back to the solution; the enthalpy of adsorption is the same for all molecules independently of how many have been adsorbed.

The Langmuir adsorption isotherm is often expressed as equation Eq.(5.2);

$$qe = \frac{qm.KL.Ce}{1 + KL.Ce} \tag{5.2}$$

The Langmuir constants, K_L and q_m were calculated by the linearization of Eq.(5.2): This gives the Eq.(5.3)

$$\frac{Ce}{qe} = \frac{1}{qm.KL} + \frac{1}{qm}.Ce \tag{5.3}$$

where qe is the capacity of adsorbent (mg/g), Ce is the initial and equilibrium liquid concentrations (mg/L), q_m is the maximum capacity of adsorbent, respectively; K_L is the Langmuir isotherm constant (function of enthalpy of adsorption and temperature).

5.7.2 Freundlich Isotherm

The Freundlich isotherm represents an empirical model. The Freundlich equation can be mathematically represented by in Eq.(5.4) and linearization of Eq. (5.4) can be shown as Eq.(5.5);

$$qe = Kf.Ce^{\frac{1}{n}} \tag{5.4}$$

$$lnq_e = lnK_f + \frac{1}{n} lnC_e \tag{5.5}$$

where is K_F = constant (function of energy of adsorption and temperature), n=constant, Ce is the initial and equilibrium liquid concentrations (mg/L), qe is the concentrations of the pollutants compound on the sorbent (mg/g).

5.8 Recovery of Nano-ZnO-SiO_2 composite

After first use the nano-ZnO-SiO_2 composite were filtered after photocatalytic degradation by UV, washed three times by water and ethanol and dried at 75 ^{0}C.

Six sequential treatment steps were investigated in order to detect the effect of reuse of nano-ZnO-SiO_2 composite based on significant removal yields of COD, phenol and TS under UV irradiation.

5.9 Analysis of Variance

Analysis of variance (ANOVA) is a collection of statistical models used to analyze the differences among group means and their associated procedures (such as "variation" among and between groups). This method is often used in scientific experiments when treatments, processes, materials or products are being compared. (Scheffé, 1959). In this study, the ANOVA test is used all of the experiments. α (Alpha) value of ANOVA is taken as 0.05.

CHAPTER SIX
RESULTS AND DISCUSSIONS

6.1 Characterization of OMW

The average COD, total solids, phenol, total nitrogen and total phosphorous contents of the raw olive mill effluent were 117000 mg/L, 84250 mg/L, 660 mg/L, 330 mg/L and 890 mg/L, respectively, while its average pH value was 3.5 - 4.5 (Table 6.1). The samples were stored at room temperature and shaken well before all the experiments.

Table 6.1 Characterization of OMW

Parameters	**Initial Value (mean ±SD)**
COD	117000 mg/L± 1000 mg/L
Total Phenol	660 mg/L±100 mg/L
Total Solids	84250 mg/L±1000 mg/L
Total Nitrogen	330 mg/L±50 mg/L
Total Phosphorous	890 mg/L±50 mg/L
Inert COD	13000 mg/L±100 mg/L
pH	3.5-4.01

6.2 Physicochemical Properties of Nano-ZnO-SiO_2

6.2.1 X-Ray Diffraction (XRD) Analysis Results

X-ray Diffraction is a tool used for identifying the structures of bare ZnO nanoparticles, bare SiO_2 nanoparticles, raw nano-ZnO-SiO_2 composite and aged nano-ZnO-SiO_2 composite after OMW treatment under UV with crystal shapes of bare ZnO nanoparticles and raw nano-ZnO-SiO_2 composite or amorphous shapes of bare SiO_2 and aged nano-ZnO-SiO_2 composite. The XRD spectra of bare ZnO nanoparticles, bare SiO_2 nanoparticles, and raw nano-ZnO-SiO_2 composite and aged nano-ZnO-SiO_2 composite after OMW treatment under UV nanoparticles are shown in Figure 6.1, 6.2, 6.3, 6.4.

Series of characteristic peaks at the ranges of 2θ=30-32^0, 34-36^0, 36-38^0, 46-48^0, 56-58^0, 62-64^0, 66-68^0 and 68-70^0 versus intensities were observed, and they are in accordance with the zincite phase of ZnO nanoparticles (Figure 6.1). These ranges of ZnO nanoparticles XRD pattern are similar as in the studies of Zhai et al., (2010), Li et al., (2009) and Ntwaeaborwa et al., (2009) which their 2θ value ranges were between 30-32^0, 34-36^0, 36-38^0, 46-48^0, 56-58^0, 62-64^0, 66-68^0 and 68-70^0.

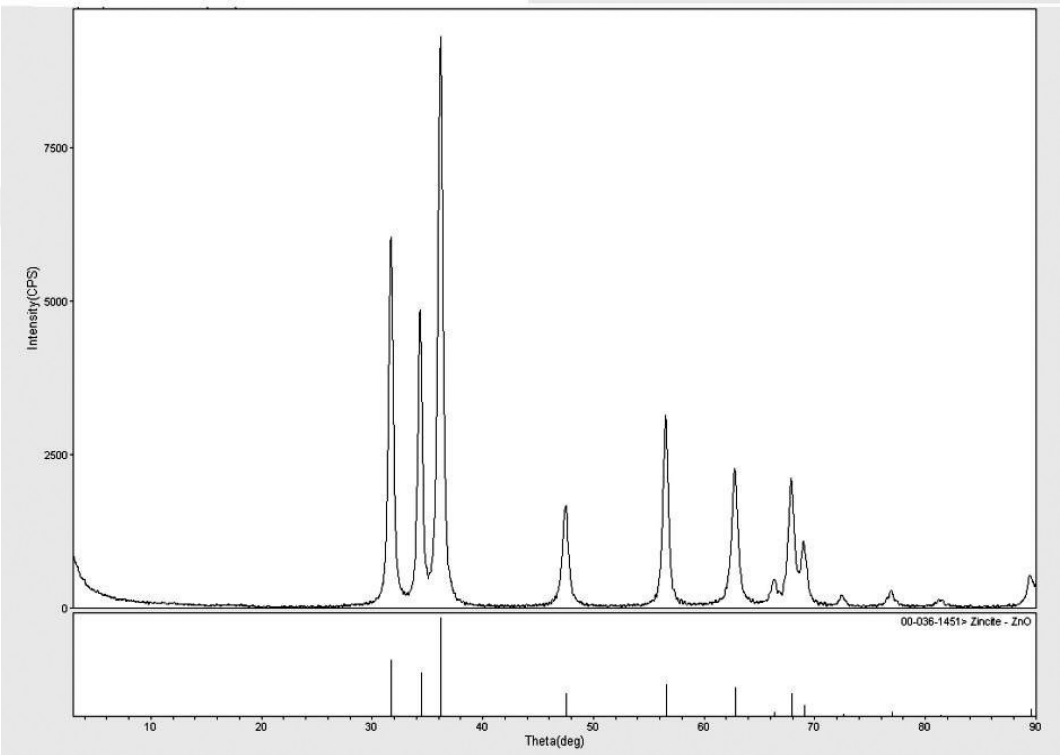

Figure 6.1 XRD patterns of bare ZnO nanoparticles buying commercially

XRD pattern of bare SiO_2 nanoparticles can be seen from Figure 6.2. A familiar broad band of bare SiO_2 nanoparticles is at range of 2θ=22-26° versus 1900 intensity spectrum and it is clear that SiO_2 nanoparticles remained amorphous. This range of bare SiO_2 nanoparticles is similar to studies of Li et al., (2010). Ntwaeaborwa et al., (2009) found XRD pattern of SiO_2 as 2θ=25.

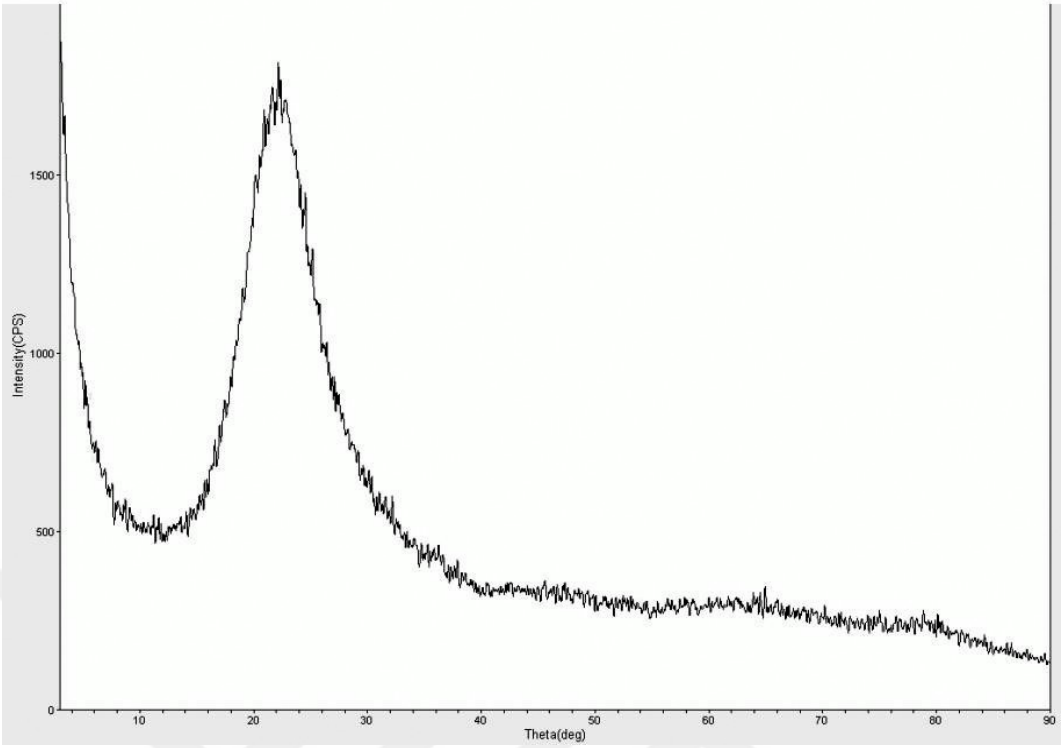

Figure 6.2 XRD pattern of bare SiO_2 nanoparticles buying commercially

After modifying with SiO_2 nanoparticles, the characteristic peaks of samples are still in accordance with the zincite phase of ZnO (Figure 6.3), indicating that the SiO_2 nanoparticles does not influence the crystalline structure of nano-ZnO-SiO_2 composite. As a results of small amount of SiO_2 nanoparticles, the diffraction peaks of amorphous SiO_2 nanoparticles were obviously detected at the range of 2θ=22-26°. Similar report on nano-ZnO-SiO_2 core–shell nanoparticles of Li et al., (2009) also showed peaks of SiO_2 nanoparticles shell in the same XRD spectra (2θ=22-25°). The peak intensities of nano-ZnO-SiO_2 nanocomposites are a little weaker than that of bare ZnO nanoparticles, which is possibly the result of the presence of SiO_2 nanoparticles in an amorphous state around the ZnO nanoparticles. Finally XRD pattern of raw nano-ZnO-SiO_2 composite shows that SiO_2 nanoparticles are coated on ZnO nanoparticles successfully**.** The molar ratio of 1:1 (ZnO: SiO_2) is optimum ratio for synthesis of nano-ZnO-SiO_2 composite.

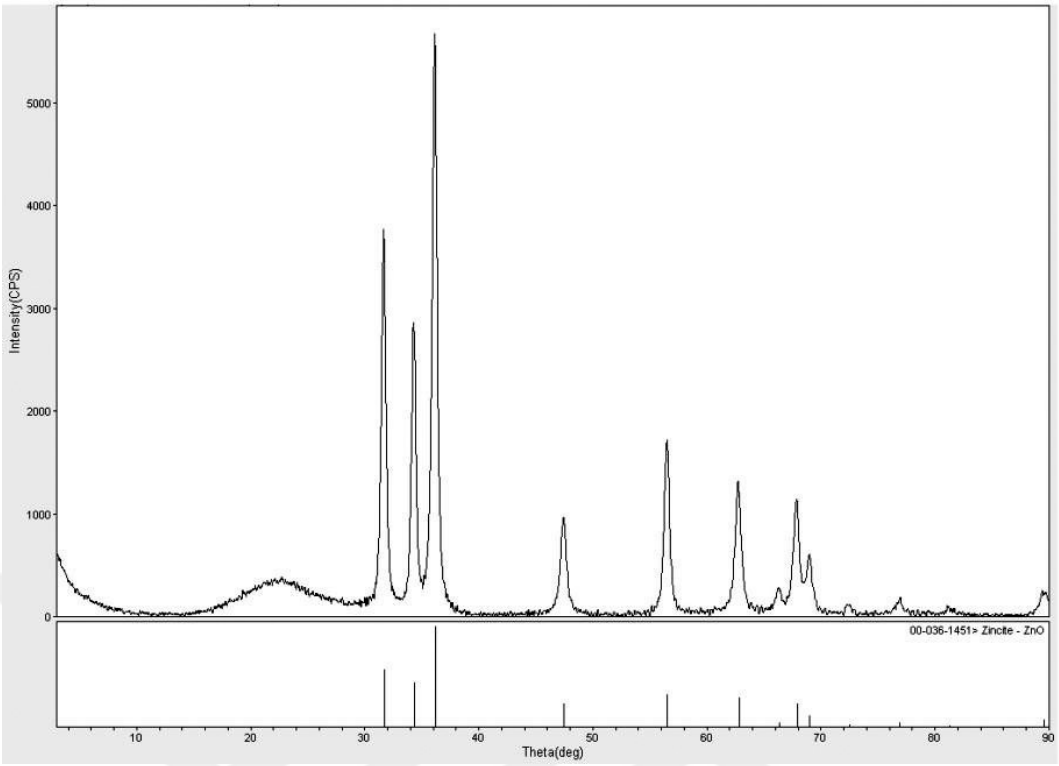

Figure 6.3 XRD pattern of raw nano-ZnO-SiO_2 composite (molar ratio 1:1)

XRD pattern of nano-ZnO-SiO_2 composite investigated after using for the treatment of OMW under UV irradiation in Figure 6.4. Maximum peak was obtained at 2θ=22 and this range can be interpreted as peak of SiO_2 nanoparticles according to this figure. The structure of nano-ZnO-SiO_2 composite turned to amorphous. This situation can be explained as follows; after contacting with OMW, pollutants may cover the surface of nano-ZnO-SiO_2 composite. On the other hand, after UV irradiation structure of nano-ZnO-SiO_2 composite can be changed by UV lights.

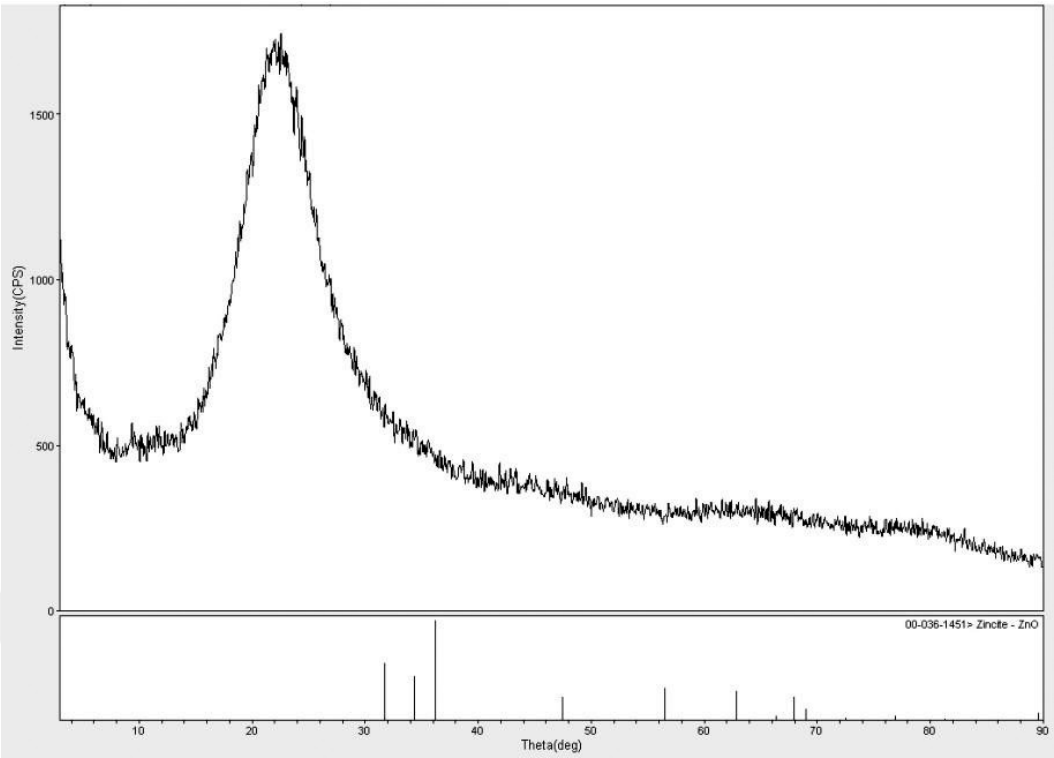

Figure 6.4 XRD pattern of nano-ZnO-SiO_2 composite after OMW treatment under UV (T: room temperature, irradiation time: 15 min, concentration of nano-ZnO-SiO_2 composite: 1 g/L, 300 Watt UV light)

6.2.2 Fourier Transform Infrared (FTIR) Analyses Results

FT-IR analysis is a useful way to study chemical structure of the surface of nano-ZnO/SiO_2 composites. Figure 6.5, 6.6, 6.7 and 6.8 show the FT-IR spectra of bare ZnO nanoparticles, bare SiO_2 nanoparticles, raw nano-ZnO-SiO_2 composites and aged nano-ZnO-SiO_2 composite after OMW treatment under UV, respectively.

Figure 6.5 shows the peaks of bare ZnO in plotted between wave number $(cm)^{-1}$ and percent transmittance (%). Metal oxides generally give absorption bands in finger print region i.e. below 1000 cm^{-1} arising from inter-atomic vibrations (Kumar & Rani, 2013). In our study the peaks at 857.30 cm^{-1} and 700.56 cm^{-1} exhibited the absorption bands in finger print region as mentioned by Kumar & Rani, 2013.

The peak is shown in Figure 6.5, at 3371 cm^{-1} indicating the O-H stretching vibrations. The absorption peak at 3400–3500 cm^{-1} can be attributed to the stretching

vibrations of structural hydroxyl groups (Li et al., 2009). Kumar & Rani, (2013), found O-H stretching vibrations at 3452.30 cm^{-1} in FT-IR spectra of bare ZnO nanoparticles in their studies. Zhai et al, (2010) found a peak at 3380 cm^{-1} and interpreted that the peak of absorption of ZnO nanoparticles in water. Kumar & Rani, (2013) also observed a peak at 1634.00 cm^{-1} corresponding to Zn-O stretching. In our study, similar peak was obtained at 1598.03 cm^{-1}.

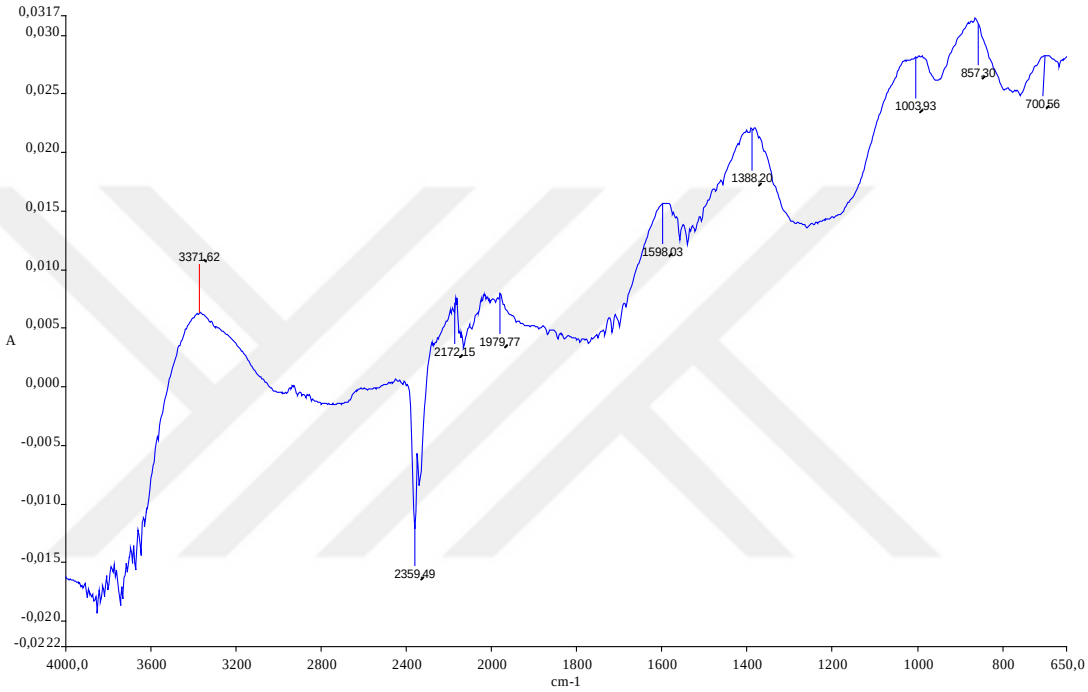

Figure 6.5 FT-IR analysis of bare ZnO nanoparticles

Figure 6.6 illustrates the FT-IR spectrum of bare SiO_2. 980–1200 cm^{-1} could be ascribed to the characteristic of Si–O–Si asymmetric stretching vibration (Liden et al., 1991). In our sample the strong and broad irradiation at 1059.55 cm^{-1} indicates the Si-O-Si asymmetric stretching vibrations. There was an absorption peak of bending vibration of Si–OH at 960 cm^{-1}. This result is similar to the study of Li et al., (2009). They obtained Si-OH peak at 956 cm^{-1}. The irradiation band at 3326.58 cm^{-1} could be assigned to the stretching vibrations of characteristic of Si-OH groups in the amorphous SiO_2. The irradiation band at 1623.31 cm^{-1} is due to the bending vibration of H_2O molecules. The irradiation band at the range of 800- 900 cm^{-1} can be assigned to Si-O-Si symmetric stretching vibrations, whereas the irradiation band at 798.00 cm^{-1} is due to O-Si-0 bending vibrations.

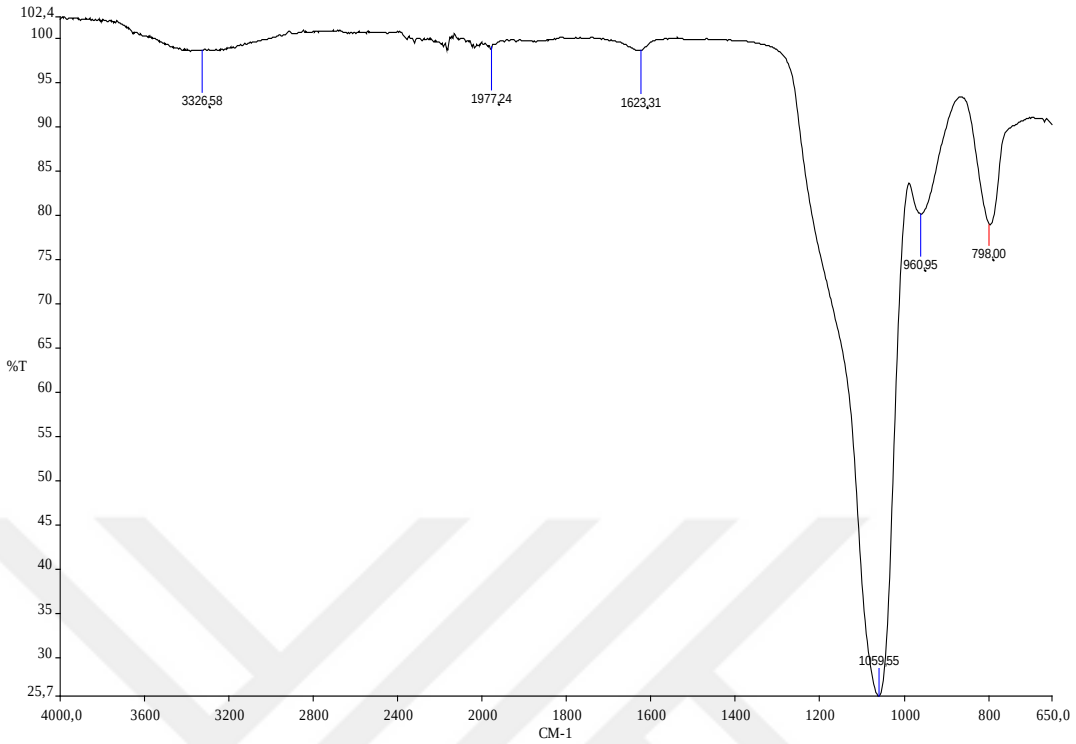

Figure 6.6 FT-IR analysis of bare SiO_2 nanoparticles

In Figure 6.7, it was also found that the nano-ZnO-SiO_2 composite exhibit absorption at 3341.77 cm^{-1}, 1608.14 cm^{-1}, 1074.71 cm^{-1} 960.95 cm^{-1} and 796.62 cm^{-1} which could be ascribed to the characteristic Si-O-Si asymmetric stretching vibration as reported by Zhai et al, (2010). Thus we can speculated that the SiO_2 shells originated from the condensation of physical synthesis since in the preparation of nano-ZnO-SiO_2 composite under laboratory conditions the addition of equal molar ratio of nano-SiO_2 to nano-ZnO (1:1) at a temperature of 120 ^{0} were performed. As a result, SiO_2 were successfully coated onto the ZnO surface.

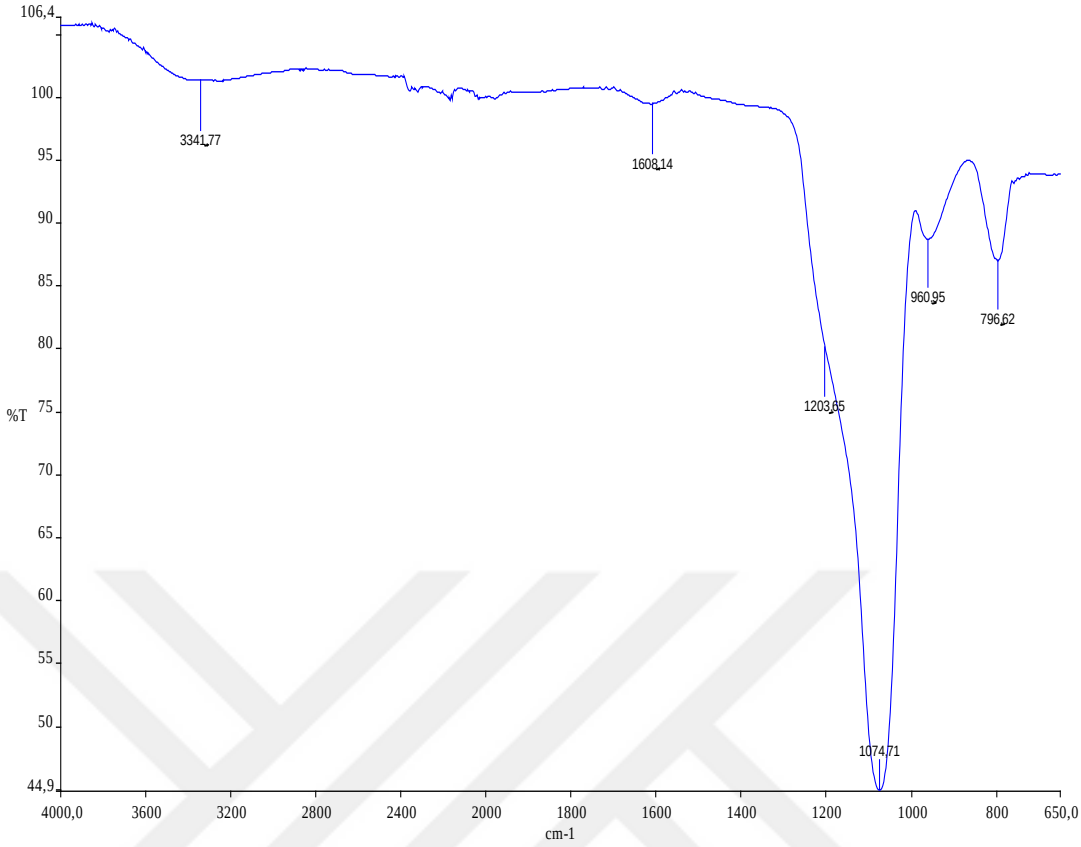

Figure 6.7 FT-IR analysis of raw nano-ZnO-SiO_2 composite (the molar ratio of ZnO:SiO_2 1:1)

Figure 6.8 shows the FTIR analysis of nano-ZnO-SiO_2 composite after UV treatment for OMW. The maximum peaks obtained in this figure are similar to the nano composite before UV treatment. Condensation of nano-ZnO-SiO_2 composite remained constant after UV treatment in the OMW with nano-ZnO-SiO_2 composite. Condensation of nano-ZnO-SiO_2 composite decreases slightly from 3341.77 cm^{-1} to 3321,51 cm^{-1}, from 1608.14 cm^{-1} to 1598.03 cm^{-1}, from 1074.71 cm^{-1} to 1057 cm^{-1}. (Figure 6.8). The peak for nano-ZnO-SiO_2 composite observed at 960.95 cm^{-1} increased to 966.01 cm^{-1}. 796.62 cm^{-1}, which could be ascribed to the characteristic Si-O-Si asymmetric stretching vibration, remained same after utilized in the treatment of OMW under UV irradiation. This shows that nano-ZnO-SiO_2 composite can be recovered without any change and can be used again for OMW treatment with UV in many sequential.

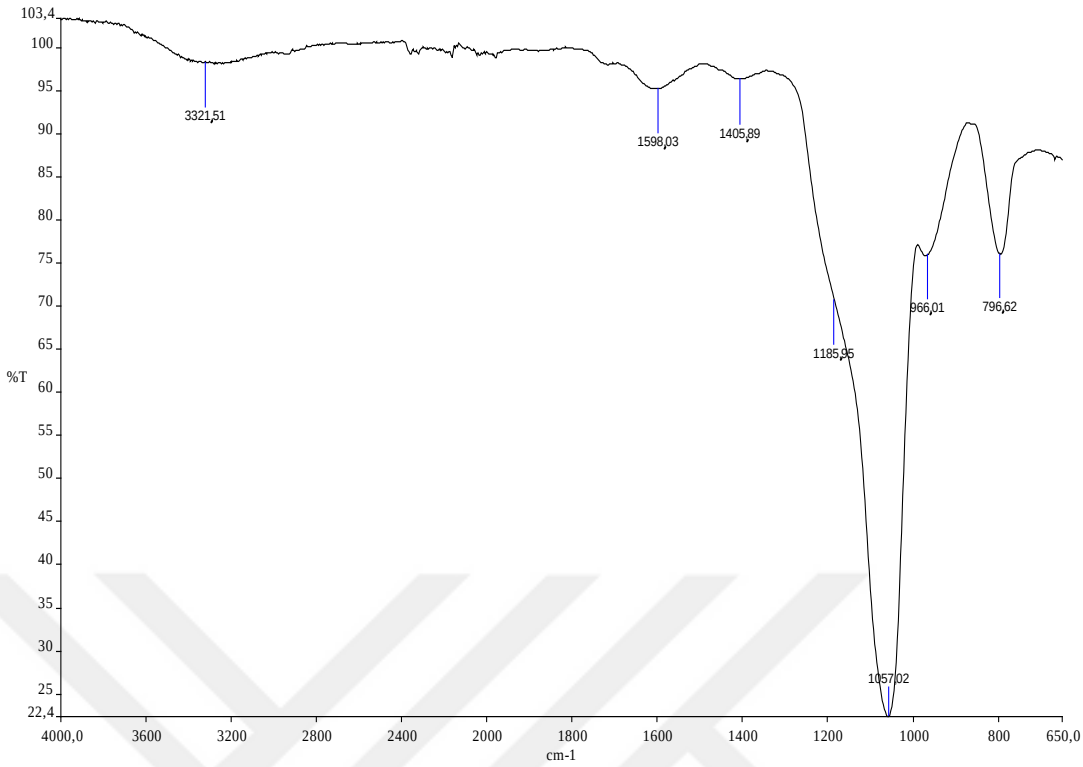

Figure 6.8 FT-IR analysis of aged nano-ZnO-SiO_2 composite (the molar ratio of ZnO: SiO_2 1:1) (T: room temperature, irradiation time: 15 min, concentration of nano-ZnO-SiO_2 composite: 1 g/L, 300 Watt UV light)

6.2.3 Scanning Electron Microscope (SEM) Analysis Results

The SEM images of raw nano-ZnO-SiO_2 composite and aged nano-ZnO-SiO_2 composite after OMW treatment under UV are shown in Figure 6.9 and Figure 6.10, respectively.

Color of nano-ZnO-SiO_2 composite turns to black/grey after treatment of OMW under UV and surface of composite fills with pollutants in OMW as illustrated in Figure 6.9. Crystalline structure of nano-ZnO-SiO_2 composite turns to amorphous form due to filling of pollutants on to surface of nano-ZnO-SiO_2 composite found in the OMW.

The average particle size was were measured about 500 nm and 200 µm for nano-ZnO-SiO_2 composite and aged nano-ZnO-SiO_2 composite, respectively, after UV treatment as illustrated in Figures 6.9 and 6.10. With the addition of nano-ZnO-SiO_2

composite to 1 liter OMW the thickness of nano-ZnO-SiO_2 composite reached from 500 nm to 200 µm as shown in Figure 6.10.

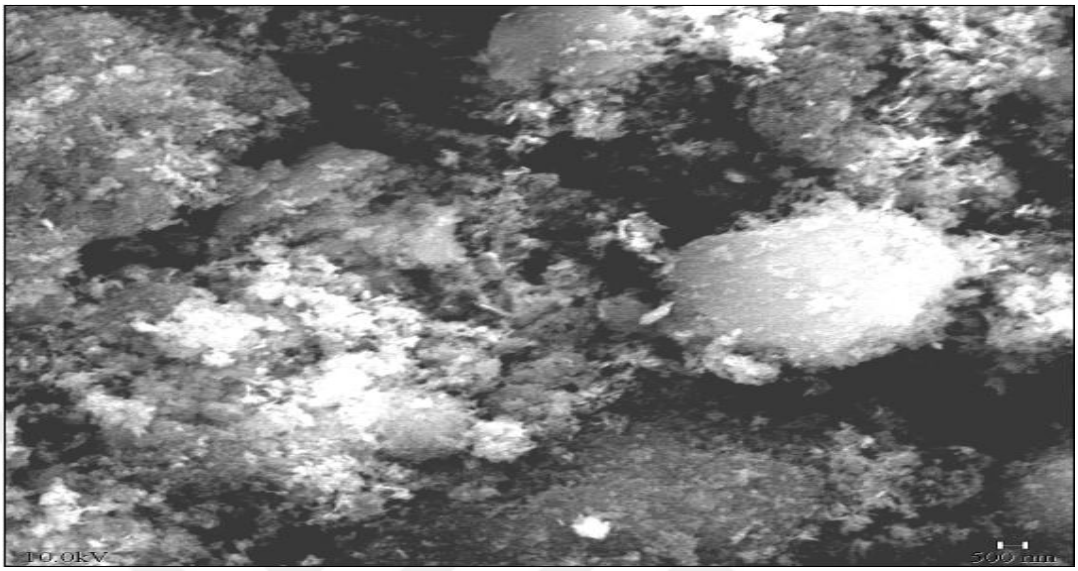

Figure 6.9 SEM image of raw nano-ZnO-SiO_2 composite (the molar ratio of ZnO:SiO_2 1:1)

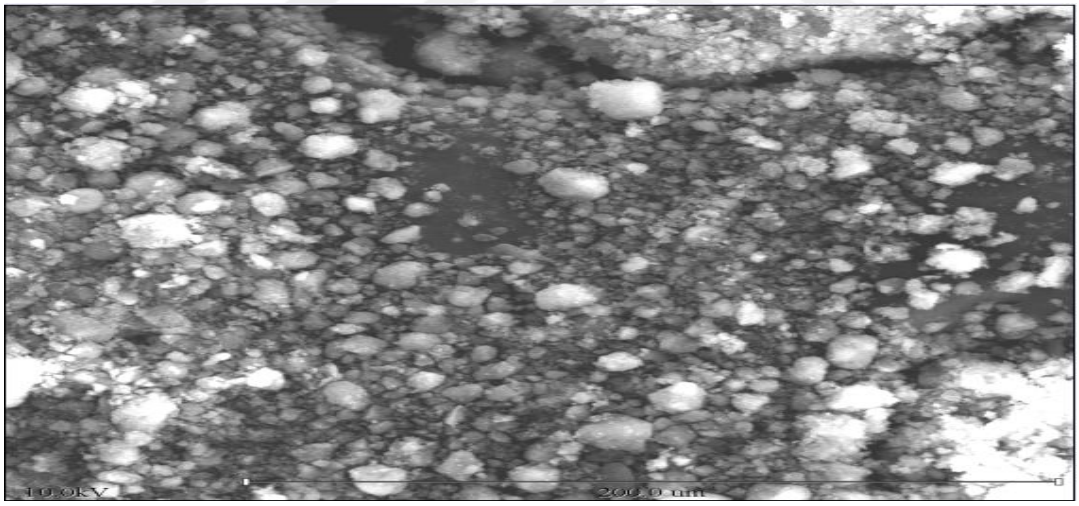

Figure 6.10 SEM image of aged nano-ZnO-SiO_2 composite after OMW treatment under UV (the molar ratio of ZnO: SiO_2 1:1) (T: room temperature, irradiation time: 15 min, concentration of nano-ZnO-SiO_2 composite: 1 g/L, 300 Watt UV light)

6.3 Batch Adsorption Studies

6.3.1 Effects of Concentration of Nano-ZnO-SiO_2 Composite on the Treatment of OMW with Adsorption

Adsorption of OMW with nano-ZnO-SiO_2 composite has not been studied yet. On the other hand, the other types of nanoparticles such as γ- Fe_2O_3, TiO_2 were investigated for the removal of some pollutants (such as total phenols, COD etc.) by adsorption mechanism.

Nano particles concentration is an important parameter for the treatment of OMW with using nanotechnology. Six different increasing concentrations of nano-ZnO-SiO_2 composite 1, 3, 5, 10, 12 and 20 g/L were chosen to determine the optimum nano-ZnO-SiO_2 composite concentration on the adsorption of pollutants in the OMW to nanocomposite. All experiments were realized after 180 min adsorption time (since the results of preliminary studies 180 min was the optimum contact time for effect of concentration of nano-ZnO-SiO_2 composite) at 20^0C and at original pH of OMW. For maximum adsorptions of pollutants the optimum nano-ZnO-SiO_2 composite concentration was determined at the end of those experiments.

With increasing concentrations of nano-ZnO-SiO_2 composite from 1 up to 20 g/L, COD removal efficiencies were obtained as 25 %, 28 %, 27 %, 25 %, 23 % and 23 % after 180 min adsorption time at 20 ^{0}C and at original pH of OMW (Figure 6.11). The maximum COD removal efficiency was obtained as 28 % at 3 g/L of nano-ZnO-SiO_2 composite. Increasing the concentration of nano-ZnO-SiO_2 composite from 1 g to 3 g did not increase the COD yields effectively. Increasing the concentration of nano-ZnO-SiO_2 composite from 3 g to 20 g did not change significantly the percentage of removal efficiency. As it is seen from Figure 6.11, as the amount of adsorbent increased the adsorption of COD decreased slightly. When the concentrations of nano-ZnO-SiO_2 composite are slightly high all the holes in the surface of nano-ZnO-SiO_2 composite are not covered by the pollutants such as COD.

In other words certain amount of nano-ZnO-SiO_2 composite is capable of adsorbing a certain amount of COD and reaches a maximum value.

A linear relationship between nano-ZnO-SiO_2 composite concentration, influent COD concentration in OMW and COD adsorption efficiencies was not obtained (R =0.49) and this regression is not significant (ANOVA $p=0.3 > \alpha=0.05$ and F=1.31).

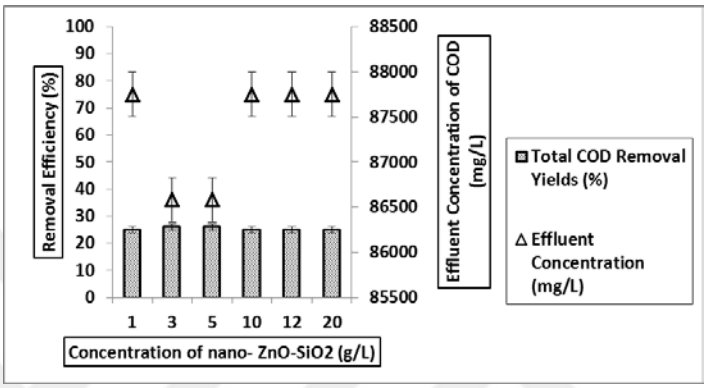

Figure 6.11 The effect of concentration of nano-ZnO-SiO_2 composite on the COD yield (T: 20 °C, original pH of OMW, adsorption time: 180 min, influent concentration of COD: 117000 mg/L)

The total phenol removal yields were obtained as 34 %, 34 %, 35 %, 35 %, 39 % and 39 % at 1, 3, 5, 10, 12 and 20 g/L nano-ZnO-SiO_2 composite, respectively, after 180 min adsorption time at 20 ^{0}C and at original pH of OMW (Figure 6.12). The maximum yield 39 % obtained at 12 g nano-ZnO-SiO_2 composite. Increasing the concentration of L nano-ZnO-SiO_2 composite from 1 g nano-ZnO-SiO_2 composite to 5 g L nano-ZnO-SiO_2 composite did not change the yields effectively that means active sites on nano-ZnO-SiO_2 composite at 1, 3 and 5 g nano-ZnO-SiO_2 composite are inadequate for total phenol removal. At a fixed olive mill wastewater volume (1 liter), it can easily be inferred that the percent removal of total phenol increases from 35 % to 39 % with increasing of the nano-ZnO-SiO_2 composite concentrations from 10 to 12 g as shown from Figure 6.12. This is due to the greater availability of the exchangeable sites or surface area at higher concentration of the nano-ZnO-SiO_2 composite. When concentration of nano-ZnO-SiO_2 composite was chosen as 20 g, the removal efficiency did not change and it remained as is in the 12 g nano-ZnO-SiO_2 composite (%39). The increasing of nanocomposite concentrations did not affect the

phenol yields. This seems to be due to the binding of almost molecules of phenolic compounds to the sorbent and the establishment of equilibrium between the molecules bounded to the sorbent and unabsorbed molecules in the solution (Achak et al., 2009).

A linear relationship between nano-ZnO-SiO_2 composite concentration, influent total phenol concentration in OMW and total phenol adsorption efficiencies was obtained (R = 0.90) and this regression is not significant (ANOVA p=0.51> α = 0.05 and F = 6.41)

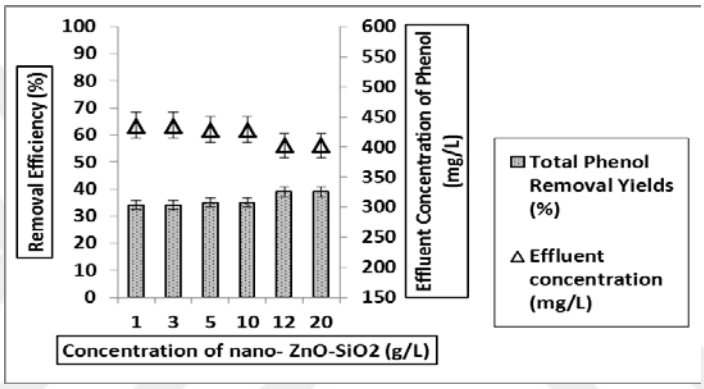

Figure 6.12 The effect of concentration of nano-ZnO-SiO_2 composite on the phenol yield (T: 20 °C, original pH of OMW, adsorption time: 180 min, influent total phenol concentration: 660 mg/L)

The TS removal yields were obtained as 30 %, 33 %, 33 %, 32 %, 30 % and 29 % at 1, 3, 5, 10, 12 and 20 g/L nano-ZnO-SiO_2 composite concentrations under this conditions (T:20 °C, original pH of OMW, adsorption time: 180 min) , respectively (Figure 6.13). The maximum removal efficiency was obtained as 33 % at 3 g nano-ZnO-SiO_2 composite. When the increasing the concentration from 1 to 5 g nano-ZnO-SiO_2 composite yields increased from 30 % to 33%. On the other increasing the concentration from 5 to 20 g nano-ZnO-SiO_2 composite decreased the yields of COD, slightly. TS removal mechanism is similar to COD removal. When the concentrations of nano-ZnO-SiO_2 composite are slightly high all the holes in the surface of nano-ZnO-SiO_2 composite are not covered by the pollutants such as total solids. In other words certain amount of nano-ZnO-SiO_2 composite is capable of adsorbing a certain amount of total solids and reaches a maximum value.

A linear relationship between nano-ZnO-SiO_2 composite concentration, influent TS concentration in OMW and TS adsorption efficiencies was not obtained (R =0.67) and this regression is not significant (ANOVA p=0.48 > α=0.05 and F=1.26).

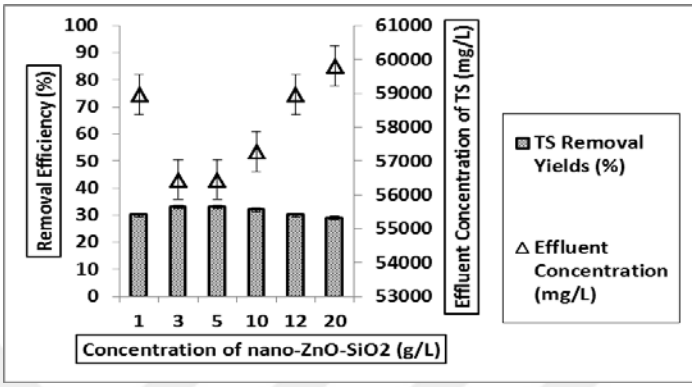

Figure 6.13 The effect of concentration of nano-ZnO-SiO_2 composite on the TS yield (T: 20 °C, original pH of OMW, adsorption time: 180 min, influent TS concentration: 84250 mg/L)

The total nitrogen removal yields were obtained as 12 %, 14 %, 16 %, 13 %, 12 % and 12 % at 1, 3, 5, 10, 12 and 20 g/L nano-ZnO-SiO_2 composite after 180 min adsorption time at 20 ^{0}C and at original pH of OMW, respectively (Figure 6.14). The maximum removal efficiency was obtained as 16 % at 5 g nano-ZnO-SiO_2 composite. It was observed that the percentage removal of the total nitrogen slightly increases with increasing the nano-ZnO-SiO_2 composite concentration from 1 g to 5 g and further increase of the nano-ZnO-SiO_2 composite concentration did not provide more increment in the percentage of the total nitrogen removed. The slightly increase in the percentage of the total nitrogen removal with increase in nano-ZnO-SiO_2 composite concentration is due to the greater availability of the exchangeable sites in the surface area of 5 g nano-ZnO-SiO_2 composite leading to adsorption to pollutants in the OMW under adsorptive conditions. Non-significant increase in total nitrogen yields was observed when the nano-ZnO-SiO_2 composite concentration were increased from 5 g to 20 g, suggests that after a certain concentration of nano-ZnO-SiO_2 composite the maximum adsorption is attained. The adsorbed amount of total nitrogen remains constant even with further addition of nano-ZnO-SiO_2 composite as reported by Abdel-Ghani et al. (2006), Alok Mittal (2006) and Teker et al. (1999).

A linear relationship between nano-ZnO-SiO_2 composite concentration, influent total nitrogen concentration in OMW and total nitrogen adsorption efficiencies was not obtained (R=0.50) and this regression is not significant (ANOVA p=0.54 > α=0.05 and F=0.51)

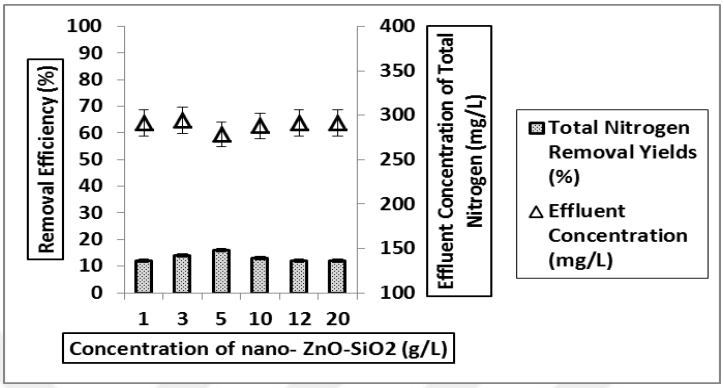

Figure 6.14 The effect of concentration of nano-ZnO-SiO_2 composite on the total nitrogen yield (T:20 °C, original pH of OMW, adsorption time: 180 min, influent total nitrogen concentration:330 mg/L)

The total phosphorous removal yields were obtained as 20 %, 20 %, 21 %, 19 %, 20 % and 20 % at 1, 3, 5, 10, 12 and 20 g/L nano-ZnO-SiO_2 composite after 180 min adsorption time at 20 ^{0}C and at original pH of OMW, (Figure 6.15). The increasing of the concentration of nano-ZnO-SiO_2 composite from 1 g to 5 g, increased slightly the removal efficiency of total phosphorous from 20 % to 21 %. On the other hand, increasing the concentration of nano-ZnO-SiO_2 composite from 5 g to 20 g decreased slightly the removal efficiency from 21 % to 20 %. The maximum yield (21 %) was obtained at 5 g nano-ZnO-SiO_2 composite. Increasing the concentration of nano composite did not significantly change the removal efficiency of total phosphorous. When the concentrations of nano-ZnO-SiO_2 composite are high all the holes in the surface of nano-ZnO-SiO_2 composite are not covered by total phosphorous. Certain amount of nano-ZnO-SiO_2 composite is capable of adsorbing a certain amount of total phosphorous and reaches a maximum value at 5 g.

A linear relationship between nano-ZnO-SiO_2 composite concentration, influent total phosphorous concentration in OMW and total phosphorous adsorption

efficiencies was not obtained (R=0.25) and this regression is not significant (ANOVA p=0.85 > α=0.05 and F=0.10).

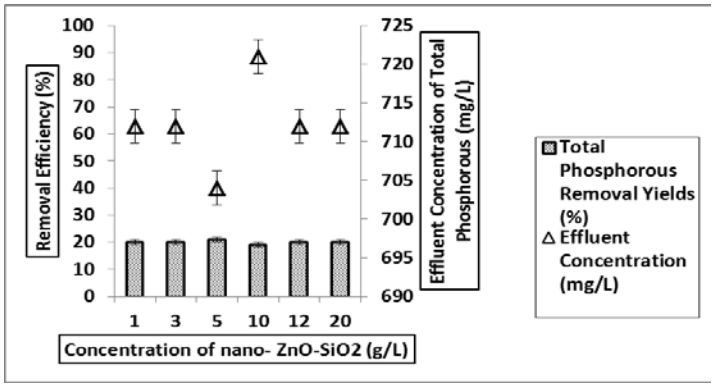

Figure 6.15 The effect of concentration of nano-ZnO-SiO_2 composite on the total phosphorous yield (T:20 °C, original pH of OMW, adsorption time: 180 min, influent total phosphorous concentration: 890 mg/L)

6.3.2 Effects of Adsorption Time on the Treatment of OMW with Adsorption

Effect of contact time on the removals of COD, total solids, phenol, total nitrogen and total phosphorous in the OMW for the nano-ZnO-SiO_2 composite concentration of 1 g/L, at original pH of OMW and 20 ^{0}C were illustrated in Figures 6.16, 6.17, 6.18, 6.19 and 6.20.

Contact times were selected as 15, 30, 60, 90, 180, 240, 360 min for COD removal and removal efficiencies were obtained as 17 %, 18%, 19%, 20 %, 28%, 28% and 28 %, respectively (Figure 6.16). Among those contact times it was found that maximum COD yields were 28 % after 180 min contact time for 3 g nano-ZnO-SiO_2 composite at 20 ^{0}C, original pH of OMW. As seen Figure 6.16, adsorption was quite fast, as adsorption equilibrium was reached within 180 min for COD. When the classical adsorbents such as activated carbon and activated alumina were used the equilibrium time for adsorption could take days (Crittenden, 2005). This short adsorption time suggests that, owing to good degree of treatment with nanoparticles. Adsorption is only affected by two mechanisms; first, rapid adsorption due to electrostatic attraction followed by slow gradual adsorption of pollutants onto nanoparticle surface by complexation (Nassar & Ringsred, 2012; Franco et al.,

2014a; Nassar, 2012a). Increasing the contact time from 180 min to 360 min did not change the adsorption efficiency of COD and remained constant as %28. This shows that the adsorption way is not physical adsorption. Since the physical adsorption occurs when attractive forces are weak (Van Der Waals forces) resulting in reversible adsorption. Chemical adsorption occurs when there is a sharing of electrons between the pollutants and the nano-ZnO-SiO_2 composite surface (Sanghi & Verma, 2013). Other forces controlling adsorption processes are hydrophobicity, hydrogen bonds and $\pi - \pi$ interactions (Lakshmanan, 2013). El Hajjouji et al. (2008) searched adsorption of OMW with 1 g/L TiO_2 at room temperature. They obtained 11 % COD decrease after 30 min In our study, COD yield was 18% at 1 g/L nano-ZnO-SiO_2 after 30 min contact time. Although the adsorption yields were not so high, the adsorption of COD on to nano-ZnO-SiO_2 composite is more successful when compared with TiO_2 due to obtaining higher yields than TiO_2.

A linear relationship between adsorption time, influent COD concentration in OMW and COD adsorption efficiencies was obtained (R=0.90) and this regression is not significant (ANOVA p=0.90 > α=0.05 and F=9.4).

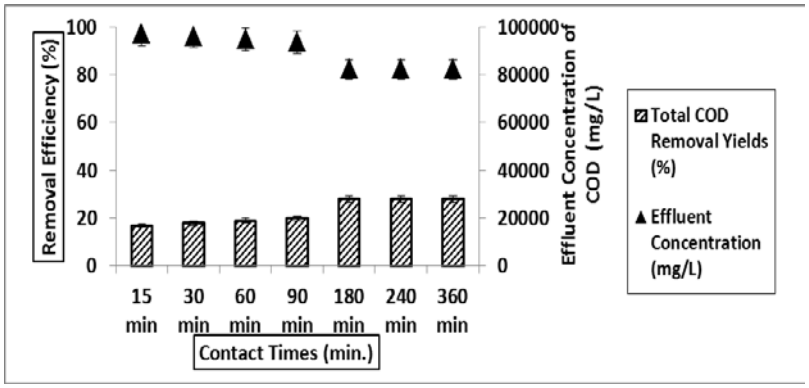

Figure 6.16 The effect of contact time on the COD yield (T: 20 °C, original pH of OMW, concentration of nano-ZnO-SiO_2 composite: 1 g/L, influent COD concentration: 117000 mg/L)

The phenol removal was studied for six different contact times (15, 30, 60, 90, 180 and 240 min). The removal efficiencies were obtained as 17 %, 35 %, 35 %, 35 %, 36 % and 36 %, respectively (Figure 6.17). The maximum removal efficiency was obtained as 36 % at 180 min while the removal efficiency was 35% at 30 min. In

order to save time 30 min adsorption time was chosen as optimum adsorption time. El Hajjouji et al. (2008) investigated the adsorption of OMW with 1 g/L TiO_2 at room temperature. They obtained that the total phenols decreased 33% by adsorption after 30 min in dark conditions. In our study slightly higher adsorption yields (35%) were found than the adsorption yields obtained by El Hajjouji et al. (2008) (their yield was 33%) at 1 g/L nano-ZnO-SiO_2 composite after 30 min contact time. Increasing the contact time from 30 min to 240 min did not change the removal efficiency of total phenol.

A linear relationship between adsorption time, influent total phenol concentration in OMW and total phenol adsorption efficiencies was obtained (R =0.95) and this regression is significant (ANOVA $p=0.019 < \alpha=0.05$ and F=15.07).

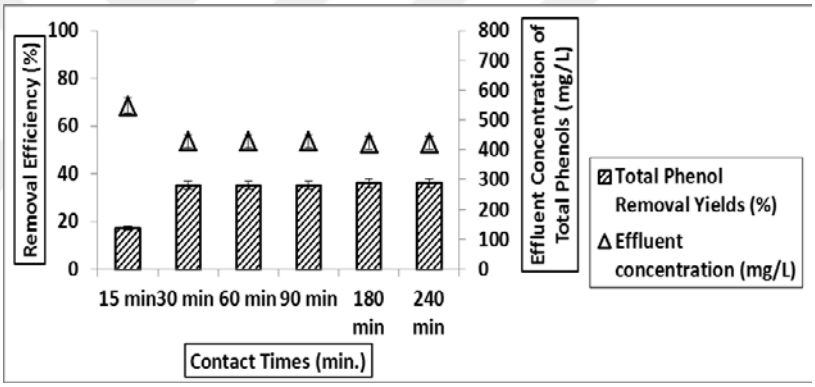

Figure 6.17 The effect of contact time on the total phenol yield (T:20 °C, original pH of OMW, concentration of nano-ZnO-SiO_2 composite: 1 g/L, influent total phenol concentration: 660 mg/L)

The TS removal was studied for six different contact times (15, 30, 60, 90, 180 and 240 min) and adsorption efficiencies were obtained as 20 %, 22 %, 33 %, 35 %, 36 % and 36 %, respectively (Figure 6.18).The maximum adsorption efficiency was obtained as 36% at 90 min. Increasing the contact time from 90 min to 240 min did not change the yield effectively. The removal efficiencies show similarity with other pollutant parameters such as COD and total phenol. The maximum removal efficiency of TS is compatible with COD, total phenol and total phosphorous yields. Increasing the contact time from 180 min to 240 min did not raise the removal

efficiency of TS and remained constant as 36 %. The adsorption of OMW reaches equilibrium after 90 min.

A linear relationship between adsorption time, influent TS concentration in OMW and TS adsorption efficiencies was obtained (R =0.97) and this regression is significant (ANOVA $p=0.018 < \alpha=0.05$ and F=30.54)

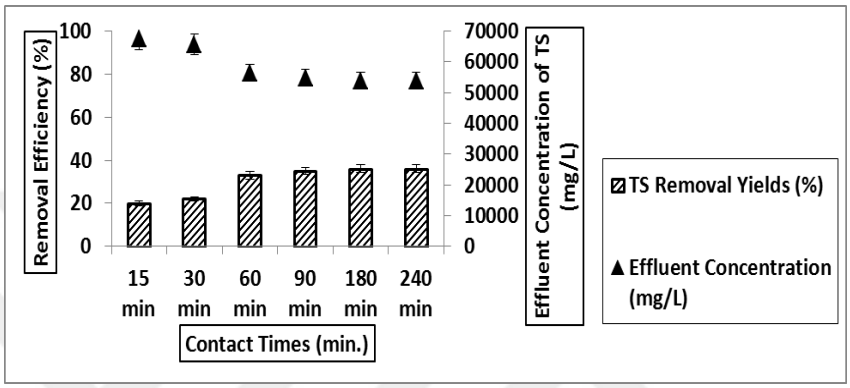

Figure 6.18 The effect of contact time on the TS yield (T: 20 °C, original pH of OMW, concentration of nano-ZnO-SiO_2 composite: 1 g/L, influent TS concentration: 84250 mg/L)

The total nitrogen removal was studied for five different contact times (15, 30, 60, 90 and 180 min) with 1 g/L nano-ZnO-SiO_2 composite at original pH of OMW. The removal efficiencies were obtained as 10 %, 12%, 15 %, 14% and 12% by increasing of contact times from 15 to 180, respectively (Figure 6.19). The maximum adsorption efficiency of total nitrogen was obtained as 15 % at 60 min. The total nitrogen can present in OMW is in the form of ammonium (NH_4^+), nitrate (NO_3^-), nitrite (NO_2^-) and organic nitrogen. The total nitrogen removal by nano-ZnO-SiO_2 composite is usually explained on the basis of the electrostatic interactions between the negative nitrogen ions and the protonated active sites in the nano-ZnO-SiO_2 composite surface. Increasing the contact time from 60 min to 180 min decreased slightly the adsorption yields.

A linear relationship between adsorption time, influent total nitrogen concentration in OMW and total nitrogen adsorption efficiencies was not obtained

(R=0.45) and this regression is not significant (ANOVA p=0.58 > α=0.05 and F=0.25).

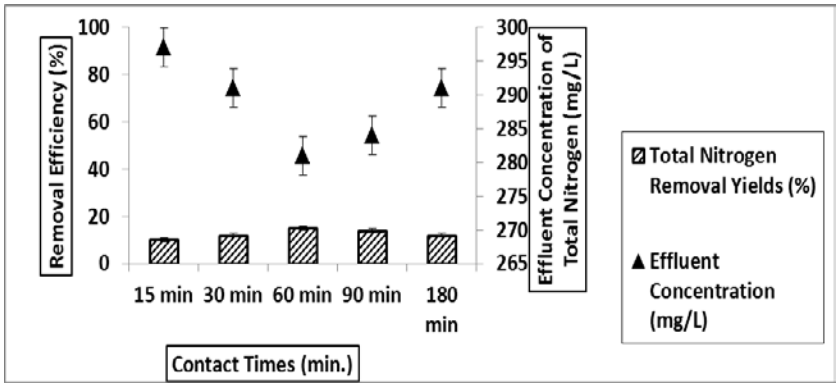

Figure 6.19 The effect of contact time on the total nitrogen yield (T: 20 °C, original pH of OMW, concentration of nano-ZnO-SiO_2 composite: 1 g/L, influent total nitrogen concentration: 330 mg/L)

The common form of phosphorous in wastewater are orthophosphates or reactive phosphorous, polyphosphates (polymeric form of phosphoric acid) and organic bound phosphates. Polyphosphates or orthophosphates mainly occur in dissolved form, while organic phosphorous are found in solid substances (Lakshmanan, 2013). The total phosphorous removal was studied for six different contact times (15, 30, 60, 90 and 180 min) with 1 g/L nano-ZnO-SiO_2 composite at original pH of OMW and adsorption efficiencies were obtained as 7 %, 8 %, 12 %, 20 %, 20 % and 20 %, respectively (Figure 6.20). The adsorbed total phosphorous on nano-ZnO-SiO_2 composite increased as the contact time elevated from 15 min up to 90 min while further increase of contact time did not affect the adsorption yield and remained at 20%. For maximum total phosphorous removal (20 %) the optimum adsorption time was found as 90 min Adsorption experiments show that the adsorption of total nitrogen onto nano-ZnO-SiO_2 composite is comparatively faster than total phosphorous and attains equilibrium at about 60 min while the equilibrium time for phosphorous adsorption is found to be around 90 min Further increase in contact time does not seem to have any impact on the equilibrium concentration of total phosphorous. Similar results were obtained as Sowmya et al. (2013) who studied the adsorption of nitrogen and phosphate by varying the time from 10 to 150 min with

0.1 g amine modified chitosan. As aforementioned in their study increasing the contact time elevated the adsorption capacity.

A linear relationship between adsorption time, influent total phosphorous concentration in OMW and total phosphorous adsorption efficiencies was not obtained (R =0.84) and this regression is not significant (ANOVA p=0.83 > α=0.05 and F=3.7).

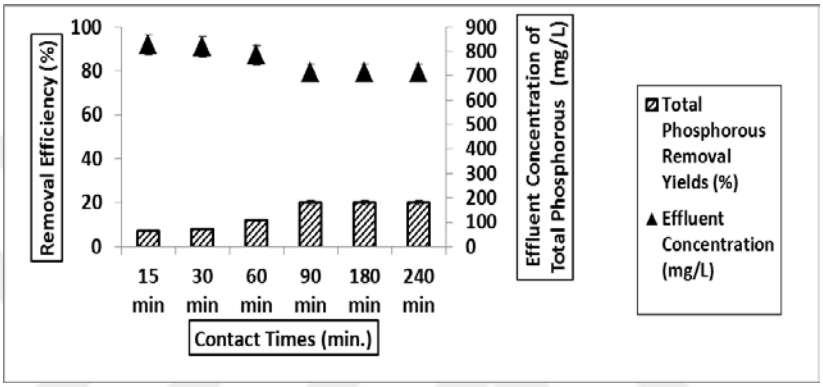

Figure 6.20 The effect of contact time on the total phosphorous yield (T: 20°C, original pH of OMW, concentration nano-ZnO-SiO_2 composite: 1 g/L, influent total phosphorous concentration: 890 mg/L)

6.3.3 Effects of pH of OMW on the Treatment of OMW with Adsorption

The pH of OMW is a major effect on adsorption capacity of nano particles. The pH rose slightly (data not shown) after the addition of the nano-ZnO-SiO_2 composite into the OMW, following adsorption of the organic matter onto nano particles. pH decreased very small (about 0.3 pH unit) throughout the longer adsorption time (data not shown) as reported by El Hajjouji et al. (2008) by formation of acidic functions through oxidation. Acidic, neutral and alkaline pHs of OMW were investigated to determine the optimum pH of OMW to obtain maximum pollutants removal efficiencies. pH 4.01 (original pH of OMW), pH 7 and pH 10 were chosen for the experiments. All experiments were realized at 1 g/L nano-ZnO-SiO_2 composite after 180 min contact time, at 20 °C.

The COD removal yields obtained at pH 4.01, pH 7 and pH 10 were 28 %, 18 % and 9 %, respectively (Figure 6.21). The maximum adsorption efficiency (28%) was obtained at original pH of OMW. Higher pHs of OMW than original pH decreased the removal yields slightly. It is reported that pHzpc (pH at the zero point of charge) of ZnO and SiO_2 are at between 9 and 9.6 and at between 2 and 4, respectively (Lewis 2000; Sverjensky 2005).

An acidic pH value of original pH of OMW has been found to be favorable for the adsorption of COD in the OMW. The reason is that the point of zero charge of SiO_2 is in a pH range of 2 and 4. In other words its surface is positively charged in acidic medium. This helps the adsorption of organic pollutants on the surface of SiO_2 surface since the organic pollutants in the OMW were negatively charged. As a result these conditions facilitate the adsorption of the pollutants. At neutral pH decreasing the COD yields from 28 % to 18 % can be explained by the positively charged surface of the ZnO.

A linear relationship between pH of OMW and COD adsorption efficiencies was obtained (R =0.99) and this regression is significant (ANOVA $p=0.009 < \alpha=0.05$ and F=1083).

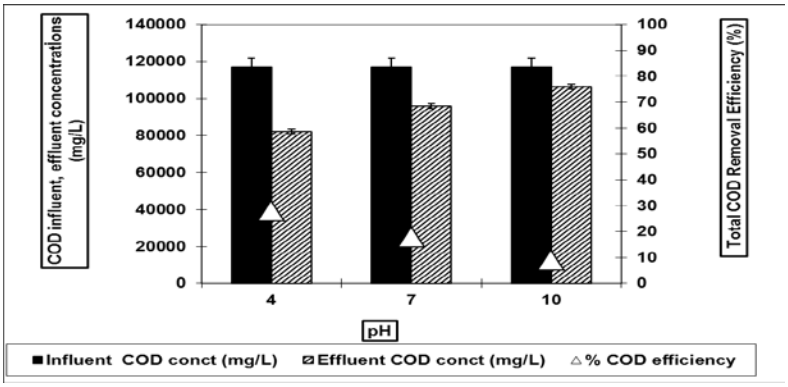

Figure 6.21 The effect of pH of OMW on the COD yield (T: 20 °C, contact time: 180 min, concentration of nano-ZnO-SiO_2 composite: 1 g/L, influent COD concentration: 117000 mg/L)

Removal efficiencies of the phenol were as 36 %, 26 % and 25 % at pH 4, pH 7 and pH 10, respectively (Figure 6.22). Increasing pH from 4.01 to 7 and 10

decreased the removal yields of the phenol. On the other hand, increasing of pH from 7 to 10 did not change the adsorption efficiency of phenol. At pH 4.01, where the nano-ZnO-SiO_2 composite surface was positively charged and the phenolic compounds took proton, higher adsorption capacity can be obtained. For the adsorption of phenolic compounds by nano-ZnO-SiO_2 composite in the OMW did not require a special pH adjustment, since the usual acidic pH of OMW effluents (pH 4-5) contributes to higher adsorption capacity of the phenolic compounds on nano-ZnO-SiO_2 composite. Similar results were found by Baransi et al. (2012): High phenol adsorption yields were found at low pH levels in the OMW with TiO_2-PAC (0.45 -3.00 g/L) and TiO_2 (3 g/L).

Phenol is a water-soluble weak acid. In aqueous solution, the phenol molecule dissociates negative anion as illustrated in reaction Eq.(6.1). As per Eq. (6.1), hydrogen atom leaves the molecule to form H_3O^+ and resulted in a negatively charged phenoxide ion. Hence, at low pH value, acidic media, an electrostatic attraction exists between the positively charged surface of the nanoparticles and the phenoxide molecules (Clifford & Luis, 1979).

$$C_6H_5OH + H_2O \Leftrightarrow C_6H_5O^- + H_3O^+ \quad (6.1)$$

On the other hand, in an alkaline environment, at high values of pH, phenol reacts with NaOH as per reaction Eq. (6.2) to form a positively charged sodium phenoxide, which prefers adsorption onto a negatively charged surface (Clifford and Luis, 1979).

$$C_6H_5OH + NaOH \Leftrightarrow C_6H_5ONa+ + H_2O \quad (6.2)$$

For OMW, as shown in Figure 6.22 the amount adsorbed phenol was independent for pH ranges between 7 and 10. However, adsorption decreased sharply with further increase in solution pH. This could be probably due to the increase of solubility of the pollutant at high pH values (Nassar et al., 2014).

A linear relationship between pH of OMW and total phenol adsorption efficiencies was obtained (R =0.90) and this regression is not significant (ANOVA $p=0.19 > \alpha=0.05$ and F=4.48).

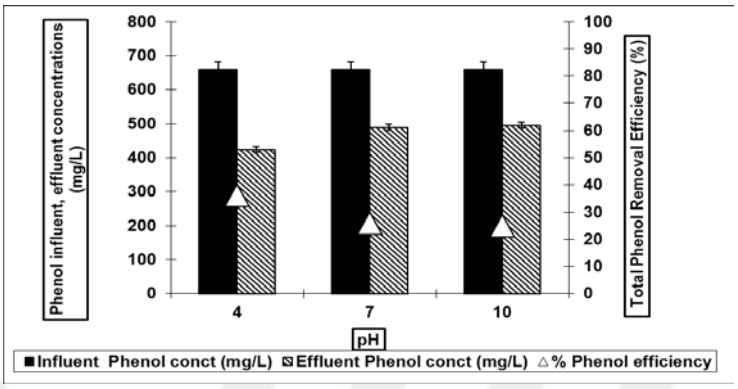

Figure 6.22 The effect of pH of OMW on the total phenol yield (T:20 °C, contact time: 180 min, concentration of nano-ZnO-SiO_2 composite: 1 g/L, influent total phenol concentration: 660 mg/L)

TS removal efficiencies decreased by increasing the pH of OMW from 4.01 to 7 and 10. The removal yields were obtained as 36 %, 25 % and 21 % at pH 4.01, pH 7 and pH 10, respectively (Figure 6.23). The maximum TS yield was found as 36 % at pH 4. This can be explained as follows: at pH 4, where the nano-ZnO-SiO_2 composite surface was positively charged and the total solids scavenge proton, higher adsorption capacity can be obtained.

A linear relationship between pH of OMW and TS adsorption efficiencies was obtained (R =0.96) and this regression is significant (ANOVA $p=0.10 < \alpha=0.05$ and F=13.77).

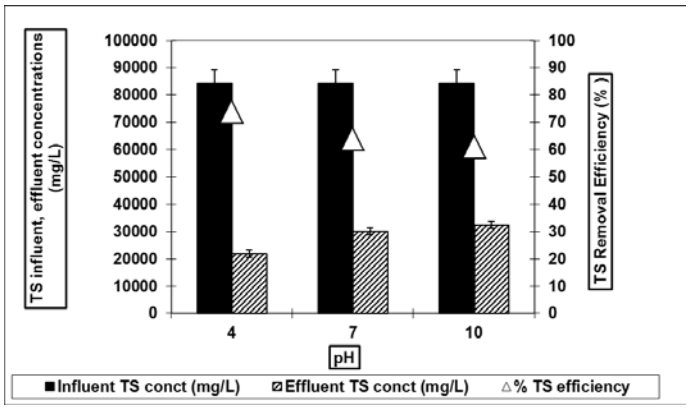

Figure 6.23 The effect of pH of OMW on the TS yield (T:20 °C, contact time: 180 min, concentration of nano-ZnO-SiO_2 composite: 1 g/L, influent TS concentration: 84250 mg/L)

Total nitrogen adsorption efficiencies were different from other pollutant parameters. Increasing the pH from 4 to 7 increased the adsorption yields of total nitrogen from 12 % to 15 %. As the pH was increased from 7 to 10 the yields remained the same (15%). The removal yields were obtained as 12 %, 15 % and 15 % at pH 4.01, pH 7 and pH 10, respectively. The maximum yield of total nitrogen was obtained as 15 % at pH 7 and 10 (Figure 6.24).

A linear relationship between pH of OMW and total nitrogen adsorption efficiencies was not obtained (R=0.86) and this regression is not significant (ANOVA $p=0.45 < \alpha=0.05$ and F=3).

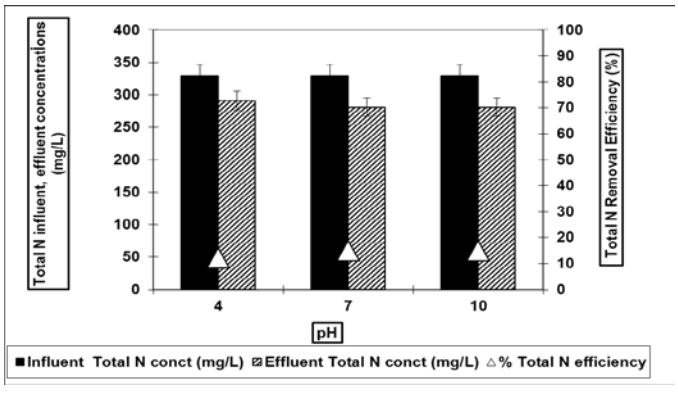

Figure 6.24 The effect of pH of OMW on the total nitrogen yield (T: 20 °C, contact time: 180 min, concentration of nano-ZnO-SiO_2 composite: 1 g/L, influent total nitrogen concentration: 330 mg/L)

The phosphorous adsorption yields were obtained as 20 %, 10 % and 8 % at pH 4.01, 7 and 10, respectively (Figure 6.25). The amount of total phosphorous adsorbed at pH 4.01 was the greatest. This result is similar to Tanada et al. (2002) who studied phosphate removal with aluminum oxide hydroxide. They studied the effects of pH ranges varying between 2 and 11. They found the maximum removal efficiency at pH 4. The amount of total phosphorous adsorbed onto nano-ZnO-SiO_2 composite decreased as increasing of pH. Tanada et al., (2002) found that the mechanism of phosphate adsorption onto aluminum oxide hydroxide was ion exchange. The phosphorous adsorbed as complex to nano-ZnO-SiO_2 composite from OMW solutions. Phosphate mostly deposited on the active sites on aluminum hydroxide at lower pH range (Tanada et al. (2002)). The columbic attraction can readily occur in conjunction with specific chemical adsorption due to an exchange reaction as reported by Tanada et al. (2002). In higher pH range, the concentration of hydroxide groups is too high, competing strongly with phosphate for the active sites (Tanada et al., 2002). In our study at pH higher than pHpzc (pH at the zero point of charge), the nano-ZnO-SiO_2 composite surface is negatively charged, whereas at a lower pH, the surface is positively charged (Tanada et al., 2002). This mechanism can be accepted for the adsorption of both COD and phosphorous adsorptions.

A linear relationship between pH of OMW and total phenol adsorption efficiencies was obtained (R=0.93) and this regression is not significant (ANOVA $p=0.11 < \alpha=0.05$ and F=6.75).

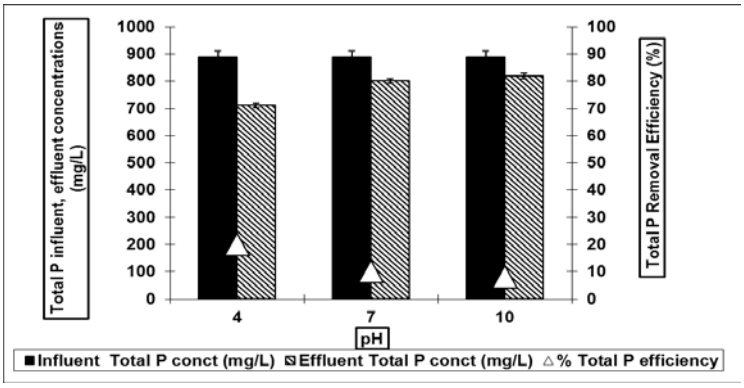

Figure 6.25 The effect of pH of OMW on the total phosphorous yield (T: 20°C, contact time: 180 min, concentration of nano-ZnO-SiO_2 composite: 1 g/L, influent total phosphorous concentration: 890 mg/L)

6.3.4 Adsorption Capacity of Nano-ZnO-SiO_2 composite

The amount of adsorption capacity of nano-ZnO-SiO_2 composite for the COD was calculated according to Eq. (6.3):

$$qe = \frac{(Co - Ce).V}{W} \tag{6.3}$$

where q_e is the capacity of adsorbent (mg/g), C_0 and Ce are the initial and equilibrium liquid concentrations (mg/L), respectively; V is the volume of solution (L); and W is the weight of adsorbent (g).

Table 6.2 Adsorption capacity of nano-ZnO-SiO_2 composite for COD

Nano-ZnO-SiO_2 Composite Conc. (g/L)	1	3	5	10	12	20
Influent COD conc.(mg/L)	117000	117000	117000	117000	117000	117000
Effluent COD conc.(mg/L)	87750	84240	85410	87750	90090	90090
q_e (mg/g)	29250	10916	6318	2925	2242	1345

Table 6.3 Adsorption capacity of nano-ZnO-SiO_2 composite for phenol

Nano-ZnO-SiO_2 Composite Conc. (g/L)	1	3	5	10	12	20
Influent phenol conc.(mg/L)	660	660	660	660	660	660
Effluent phenol conc.(mg/L)	436	436	429	429	403	403
q_e (mg/g)	224	74	46	23	21	12

When the concentration of nano-ZnO-SiO_2 composite increased from 1 g/L to 3 g/L, to 5 g/L, to 10 g/L, to 12 g/L and to 20 g/L, the adsorption capacity of nano-ZnO-SiO_2 composite decreased from 29250 mg/g to 10916 mg/g, to 6318 mg/g, to 2925 mg/g, to 2242 mg/g and to 1345 mg/g for COD, respectively. Similarly, When the concentration of nano-ZnO-SiO_2 composite increased from 1 g/L to 3 g/L, to 5 g/L, to 10 g/L, to 12 g/L and to 20 g/L, the adsorption capacity of nano-ZnO-SiO_2 composite decreased from 224 mg/g to 74 mg/g, to 46 mg/g, to 23 mg/g, to 21 mg/g and to 12 mg/g for phenol, respectively.

6.3.5 Adsorption Isotherms of COD and Total Phenol on Nano-ZnO-SiO_2 Composite

6.3.5.1 Langmuir Isotherms

In the Langmuir model (1918) adsorption is assumed to be a dynamic process. At equilibrium the number of molecules being adsorbed will be equal to the number of molecules leaving the adsorbed state. The Langmuir isotherm assumes reversible adsorption and desorption of the adsorbate molecules. The Langmuir isotherm typically represents well data for single components. The expression for the Langmuir isotherm in Eq. (6.4):

$$qe = \frac{qm \times b \times Ce}{1 + b \times Ce} \tag{6.4}$$

where qe and Ce are the equilibrium concentrations of the phenolic compound on the sorbent (mg/g) and in the solution (mg/L), respectively. q_m and b are the fitted Langmuir parameters, where the former represents the maximum adsorption capacity.

Figure 6.26 represents the Langmuir isotherm slopes for adsorption of COD on nano- ZnO-SiO_2 composite. In Langmuir isotherm the R^2 value of the linear line was 0.93, while b and q_m values were calculated as 18.52 unitless and 0.018 mg/g, respectively.

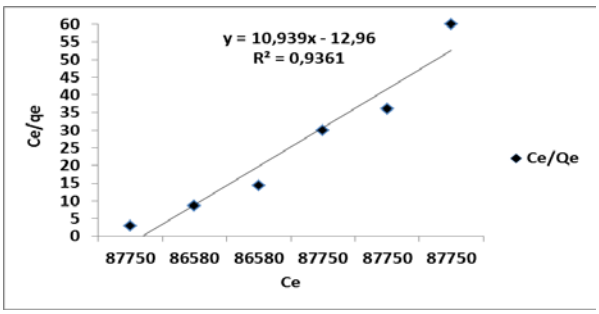

Figure 6.26 Langmuir isotherm for COD adsorption (T: 20 °C, contact time: 180 min, concentration of nano-ZnO-SiO_2 composite: 1 g/L, influent COD concentration: 117000 mg/L)

Figure 6.27 represents the Langmuir isotherm slopes for adsorption of total phenol on nano- $ZnO\text{-}SiO_2$ composite. In Langmuir isotherm the R^2 value of the linear line was 0.94, while b and q_m values were calculated as 0.22 unitless and 1.8 mg/g, respectively.

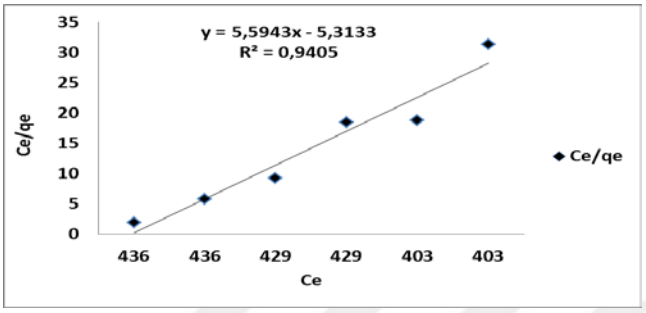

Figure 6.27 Langmuir isotherm for total phenol adsorption (T: 20 °C, contact time: 180 min, concentration of nano-$ZnO\text{-}SiO_2$ composite: 1 g/L, influent total phenol concentration: 660 mg/L)

6.3.5.2 Freundlich Isotherms

The Freundlich isotherm represents an empirical model. No assumption is made for the Freundlich isotherm. The Freundlich isotherm can be used also for mixtures of compounds.

The Freundlich equation can be mathematically represented by in Eq. (6.5):

$$q = Kf \times C^{\frac{1}{n}} \tag{6.5}$$

where:

K_F = constant (function of energy of adsorption and temperature)

n = constant

q and C are the equilibrium concentrations of the phenolic compound on the sorbent (mg/g) and in the solution (mg/L).

Figure 6.28 represents the Freundlich isotherm slopes for adsorption of COD on nano-$ZnO\text{-}SiO_2$ composite. In Freundlich isotherm the R^2 value of the linear line was

0.17, while b and q_m values were calculated as 0.0023 unitless and 0.0072 mg/g, respectively.

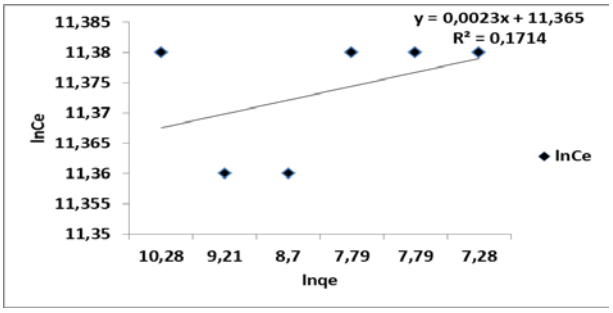

Figure 6.28 Freundlich isotherm for COD adsorption (T: 20 °C, contact time: 180 min, concentration of nano-ZnO-SiO_2 composite: 1 g/L, influent COD concentration: 117000 mg/L)

Figure 6.29 represents the Freundlich isotherm slopes for adsorption of total phenol on nano-ZnO-SiO_2 composite. In Freundlich isotherm the R^2 value of the linear line was 0.76, while b and q_m values were calculated as 0.045 unitless and 0.0058 mg/g, respectively.

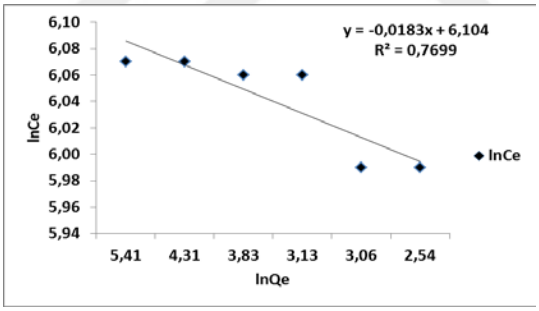

Figure 6.29 Freundlich isotherm for total phenol adsorption (T: 20 °C, contact time: 180 min, concentration of nano-ZnO-SiO_2 composite: 1 g/L, influent total phenol concentration: 660 mg/L)

These isotherms show us the Langmuir isotherm is suitable both for COD and phenol adsorption since R^2 values were 0.93 and 0.94, respectively with suitable kinetic constants.

6.4 Photocatalytic Treatment of OMW under UV

6.4.1 Effects of Concentration of Nano-ZnO-SiO_2 on the Treatment of OMW with UV

The degradation mechanism can be interpreted as the following equations. Firstly, the reaction was initiated by photoexcitation of nano-ZnO-SiO_2 composite followed by the formation of electron–hole pair on the surface of photocatalyst Eq. (6.6). Secondly, the high oxidative potential of the hole (h^+_{VB}) in the catalyst allows the direct oxidation of pollutant compounds to reactive intermediates Eq.(6.7) (Maasumeh & Zahra, 2012). Thirdly, large numbers of $^{\bullet}OH$ were generated by decomposition of water or reaction of the hole with the OH^- (Eqs.(6.8) and (6.9)), and the e_{CB} in the conduction band oxidized molecular oxygen to $^{\bullet}O_2^-$ (Eq.(6.10), which may form organic peroxides in the presence of organic scavengers (Eq. (6.11).Finally the organic were decomposed completely (Eq. (6.12).

$$ZnO\text{-}SiO_2 + hv \longrightarrow ZnO\text{-}SiO_2\,(e_{CB+}\,h^+_{VB}) \quad (6.6)$$

$$h^+_{VB} + \text{pollutant compounds} \longrightarrow \text{oxidation of pollutant compounds} \quad (6.7)$$

$$h^+_{VB} + H_2O \longrightarrow H^+ + {}^{\bullet}OH \quad (6.8)$$

$$h^+_{VB} + OH^- \longrightarrow {}^{\bullet}OH \quad (6.9)$$

$$e_{CB} + O_2 \longrightarrow {}^{\bullet}O_2^- \quad (6.10)$$

$$^{\bullet}O_2^- + \text{pollutant compounds} \longrightarrow \text{pollutant compounds-}OO^{\cdot} \quad (6.11)$$

$$^{\bullet}OH + \text{pollutant compounds} \longrightarrow \text{degradation of pollutant compounds} \quad (6.12)$$

It is beyond question that, h^+_{VB} and e_{CB} occupy an important position in degradation of organic molecules, because they are responsible for the production of hydroxyl radicals and superoxide anion (Xiuwen et. al, 2012). When under the UV light irradiation, these OH^- ions will accept any generated holes and form hydroxyl radicals, which have the potential to oxidize adsorbed organics. As a result, the electron–hole pair recombination problem can be suppressed leading to enhanced photocatalytic activity (Sonny & Walid, 2011).

Nano particles concentration is an important parameter for the treatment of OMW using nanotechnology under UV. Five different increasing concentrations of nano-ZnO-SiO_2 composite (0.5, 1, 3, 5 and 10 g/L) were chosen to determine the optimum nano-ZnO-SiO_2 composite concentration on the photooxidation of pollutants in the OMW via nanocomposite. All experiments were realized after 15 min UV irradiation time (since the results of preliminary studies showed that 15 min was the optimum irradiation time for the photocatalytic effect of concentration of nano-ZnO-SiO_2 composite) at room temperature and at original pH of OMW. For maximum removal of pollutants the optimum nano-ZnO-SiO_2 composite concentration was determined at the end of those experiments.

With increasing concentrations of nano-ZnO-SiO_2 composite from 0.5, 1, 3 5 and 10 g/L, COD removal efficiencies were obtained as 60 %, 78 %, 77 %, 77 % and 77 % after 15 min irradiation time at room temperature and at original pH of OMW under 300 Watt power (Figure 6.30). The maximum COD removal efficiency was obtained as 78 % at 1 g/L of nano-ZnO-SiO_2 composite. As the nano composite concentration was increased from 0.5 g/L to 1 g/L the yield increased from 60 % to 78 % (Figure 6.30). At a low level of nano composite concentration (1g/L), the photocatalytic reaction is mainly governed by active sites which are available for adsorption of light for photooxidation. At this nanocomposite concentration, probably the active sites on the surface are fully filled with COD pollutants (Daskalaki et al., 2009). Increasing the concentration of nano-ZnO-SiO_2 composite from 3 g to 10 g did not increase the COD yields (Figure 6.19). As the amount of nanocomposite concentration was increased from 3 to 10 g/L the photooxidation of COD remained same as 77 %. This indicates that the optimum nanocomposite concentration was found to be 1 g/L for maximum COD removal efficiency of 78%.

When the nano composite concentration is above the optimum level (1 g/L), the solution becomes not turbid and UV light is greatly scattered by the nano-ZnO-SiO_2 composite. The photocatalytic reaction is mainly subject to transmission of UV light. Due to scattering of UV light on the active sites of the nano-ZnO-SiO_2 composite, the

transmission of UV light in suspension is not inhibited the 1 g/L nano-ZnO-SiO_2 composite as reported by Badawy et al., (2011).

The photooxidation mechanism can be explained as follows: the increase in the amount of nano-ZnO-SiO_2 composite particles will increase the number of photons absorbed and consequently the number of the COD molecule adsorbed. This situation was explained by Kashıf and Ouyang, 2009. Further increase of catalyst concentration led to decrease in the degradation as reported earlier (Qamar et al., 2006; Chen et al., 2007). At high nano-ZnO-SiO_2 composite concentrations, decreases in the photodegradation may be due to the aggregation of free nano-ZnO-SiO_2 composite particles that results in a decrease in the number of surface active sites. Further, the excessive opacity and screening effect of excess nano-ZnO-SiO_2 composite act as shield as the increased number of particles in solution, and consequently hinder the light penetration. Therefore, there is loss of available surface area for light-harvesting and as a result reduction of the catalytic activity (Lea & Adesina, 1998). We found high yield (78%) for lower concentration (1 g/L) at low irradiation time (15 min).

A linear relationship between concentration of nano-ZnO-SiO_2 composite, effluent COD and COD removal efficiencies was not obtained (R=0.46) and this regression is not significant (ANOVA $p=0.24 > \alpha=0.05$ and F=0.81).

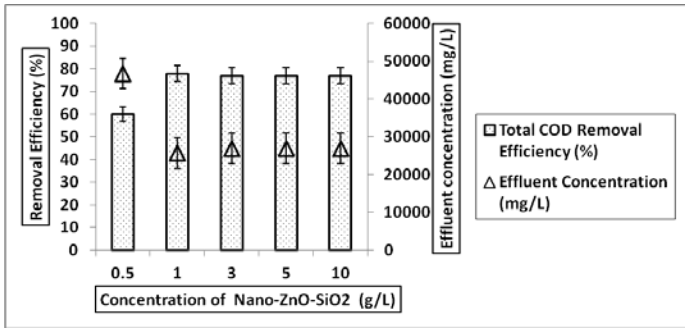

Figure 6.30 The effect of concentration of nano-ZnO-SiO_2 composite on the COD yield (T: room temperature, original pH of OMW, UV irradiation time: 15 min, UV power: 300 Watt, influent COD concentration: 117000 mg/L)

With increasing concentrations of nano-ZnO-SiO_2 composite from 0.5 up to 10 g/L, total phenol removal efficiencies were obtained as 60 %, 86 %, 77 %, 75 % and 74 % after 15 min irradiation time at room temperature and at original pH of OMW under 300 Watt (Figure 6.31). The maximum total phenol removal efficiency was obtained as 86 % at 1 g/L of nano-ZnO-SiO_2 composite. Figure 6.31 shows that the photo-degradation removal efficiencies increases with the increase in concentration of nano-ZnO-SiO_2 composite from 0.5 up to a certain limit (1 g/L) and further increase of catalyst concentration led to decrease in the photo-degradation.

Increasing the concentration of nano-ZnO-SiO_2 composite from 1 to 10 g decreased the removal efficiencies, slightly. Higher concentrations of nano-ZnO-SiO_2 composite cause turbidity and light penetration. Turbidity and light penetration causes loss of available surface area for light-harvesting and as a result the catalytic activity decreased slightly.

A linear relationship between concentration of nano-ZnO-SiO_2 composite, effluent total phenol and total phenol removal efficiencies was not obtained (R=0.13) and this regression is not significant (ANOVA $p=0.89 > \alpha=0.05$ and F=0.017).

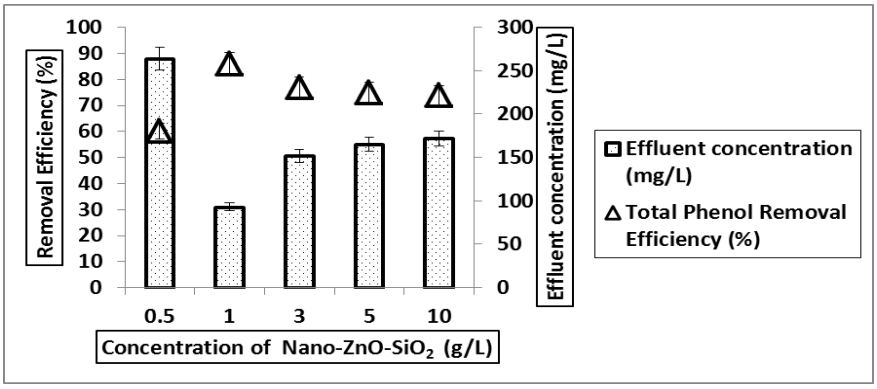

Figure 6.31 The effect of concentration of nano-ZnO-SiO_2 composite on the total phenol yield (T: room temperature, original pH of OMW, UV irradiation time: 15 min, UV power: 300 Watt, influent total phenol concentration: 660 mg/L)

With increasing concentrations of nano-ZnO-SiO_2 composite from 0.5 up to 10 g/L, TS removal efficiencies were obtained as 70 %, 77 %, 76 %, 75 % and 70 % after 15 min irradiation time at room temperature and at original pH of OMW under

300 Watt (Figure 6.32). The maximum TS removal efficiency was obtained as 77 % at 1 g/L of nano-ZnO-SiO_2 composite. Increasing the nano composite concentration from 0.5 to 1 g increased the yield from 70% to 77 % due to increase the number of photons absorbed and consequently the number of the total solids molecule adsorbed. On the other hand when the nano composite concentration increased from 1 to 10 g the removal efficiencies decreased slightly. This result can be explained as follows: higher concentration of nano composite causes turbidity in OMW and UV light could not reach to surface of nano composite effectively. Therefore photocatalytic reaction did not occur to remove the TS effectively.

A linear relationship between concentration of nano-ZnO-SiO_2 composite, effluent total solids and total solids removal efficiencies was not obtained (R=0.84) and this regression is not significant (ANOVA p=0.81 and F=1.29).

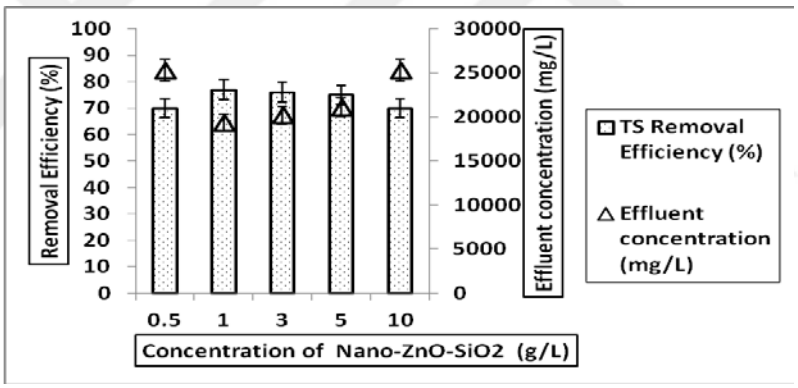

Figure 6.32 The effect of concentration of nano-ZnO-SiO_2 composite on the TS yield (T: room temperature, original pH of OMW, UV irradiation time: 15 min, UV power: 300 Watt, influent TS concentration: 84250 mg/L)

With increasing concentrations of nano-ZnO-SiO_2 composite 0.5, 1, 3, 5 and 10 g/L, total nitrogen removal efficiencies were obtained as 50%, 100 %, 98 %, 98 % and 93 % after 15 min irradiation time at room temperature and at original pH of OMW under 300 Watt (Figure 6.33). The maximum total nitrogen removal efficiency was obtained as 100 % at 1 g/L of nano-ZnO-SiO_2 composite. When the nano-ZnO-SiO_2 composite concentration was increased from 0.5 to 1 g/L the total nitrogen removal efficiency was obtained as 100 %. On the other hand, by using 3, 5 and 10 g/L concentration of nano-ZnO-SiO_2 composite; 98%, 98% and 93%, total

nitrogen yields were obtained, respectively. Although the removal efficiencies obtained for total nitrogen were high in this study high concentration of nano composite causes turbidity. The literature surveys showed that no data was found investigating the photo-removal of total nitrogen from OMW with UV lights by nano-ZnO-SiO_2 composite, yet.

A linear relationship between concentration of nano-ZnO-SiO_2 composite, effluent total nitrogen and total nitrogen removal efficiencies was not obtained (R=0.38) and this regression is not significant (ANOVA p=0.95 > α=0.05 and F=0.17).

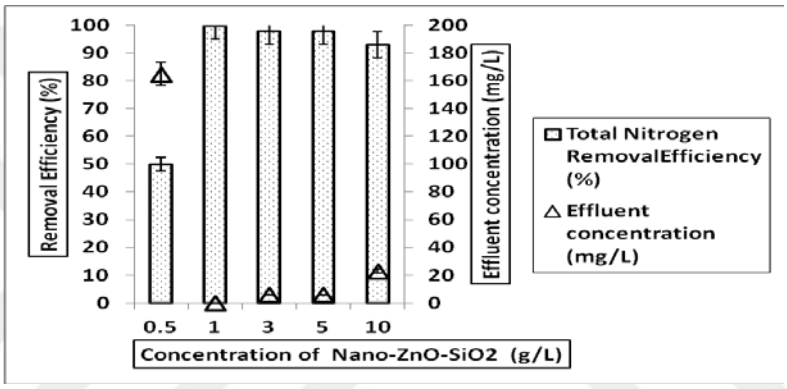

Figure 6.33 The effect of concentration of nano-ZnO-SiO_2 composite on the total nitrogen yield (T: room temperature, original pH of OMW, UV irradiation time: 15 min, UV power: 300 Watt, influent total nitrogen concentration: 330 mg/L)

0.5, 1, 3, 5 and 10 g/L concentrations of nano-ZnO-SiO_2 composite were chosen to investigate the optimum concentration for removal of total phosphorous from OMW. Total phosphorous removal efficiencies were obtained as 50 %, 52 %, 62 %, 84 % and 84 % after 15 min irradiation time at room temperature and at original pH of OMW under 300 Watt with increasing concentration of nano-ZnO-SiO_2 composite 0.5, 1, 3, 5 and 10 g/L, respectively(Figure 6.34). The maximum total phosphorous removal efficiency was obtained as 84 % at 5 g/L of nano-ZnO-SiO_2 composite. While the other pollutant parameters yield decreased with increasing concentration of nano composite, total phosphorous removal efficiencies increased with increasing concentration of nano-ZnO-SiO_2 composite from 1 to 10 g. As the concentration of nano-ZnO-SiO_2 composite was increased from 5 to 10 g, the total phosphorous yield remained same as 84 %. With increasing nano-ZnO-SiO_2 composite concentration,

more surface area of nano-ZnO-SiO_2 composite is generated and more OH^- radicals are formed, therefore the total phosphorus removal efficiency increased. The literature surveys showed that no data was found investigating the photo-removal of total phosphorous from OMW with UV lights by nano-ZnO-SiO_2 composite, yet.

A linear relationship between concentration of nano-ZnO-SiO_2 composite, effluent total phosphorous and total phosphorous removal efficiencies was not obtained (R=0.88) and this regression is not significant (ANOVA p=0.98 > α=0.05 and F=3.7).

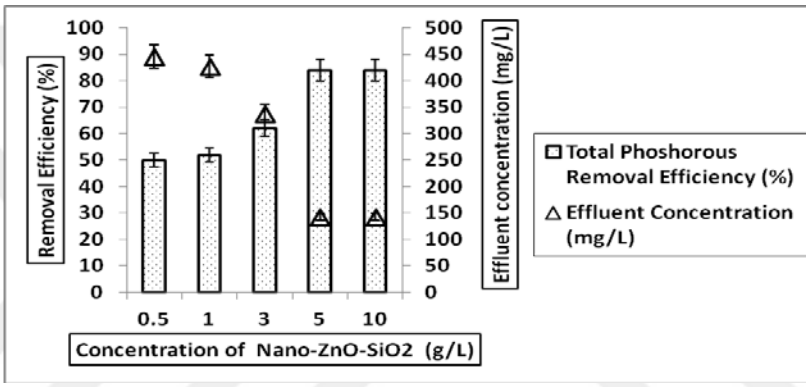

Figure 6.34 The effect of concentration of nano-ZnO-SiO_2 composite on the total phosphorous yield (T: room temperature, original pH of OMW, UV irradiation time: 15 min, UV power: 300 Watt, influent total phosphorous concentration: 890 mg/L)

6.4.2 Effects of Irradiation Time on the Treatment of OMW with UV

Effect of irradiation time on the removals of COD, total solids, phenol, total nitrogen and total phosphorous in the OMW for the nano-ZnO-SiO_2 composite concentration of 1 g/L, at original pH of OMW and 20 ^{0}C were illustrated in Figure 6.35, Figure 6.36, Figure 6.37, Figure 6.38 and Figure 6.39, respectively. 15, 30, 60, 90, 180 and 1440 min irradiation times were studied to obtain the optimum irradiation time. All experiments realized by using 1 g/L nano-ZnO-SiO_2 composite at original pH of OMW and room temperature under 300 Watt UV power.

With increasing irradiation times from 15 up to 1440 min, under 300 Watt UV power 78 %, 70 %, 60 %, 59 %, 58 % and 55 % COD removal efficiencies were

obtained after adding 1 g/L nano-ZnO-SiO_2 composite at room temperature and at original pH of OMW (Figure 6.35). The maximum COD removal efficiency was obtained as 78 % after 15 min irradiation time. Increasing the irradiation time from 15 to 1440 min decreased the COD yields Figure 6.35. The reason of this is the degradation of higher molecular weight organic compounds quickly as reported by Ruzmanova et al. 2013. On the other hand increasing the irradiation time from 15 min to 1440 min decreased the removal efficiencies, slightly. This situation can be explained as the formation of small colorless metabolite organic molecules which, at least temporarily, remain in the solution, for instance ethanol, glycerol and simple sugars which can be considered as degradation intermediates as reported by El Hajjouji et al., 2008. Metabolites of organic molecules that are formed after treatment with nano-ZnO-SiO_2 composite are only measured for polyphenols.

A linear relationship between concentration of nano-ZnO-SiO_2 composite, effluent total phosphorous and total phosphorous removal efficiencies was not obtained (R=0.53) and this regression is not significant (ANOVA p=0.40 > α=0.05 and F=1.58).

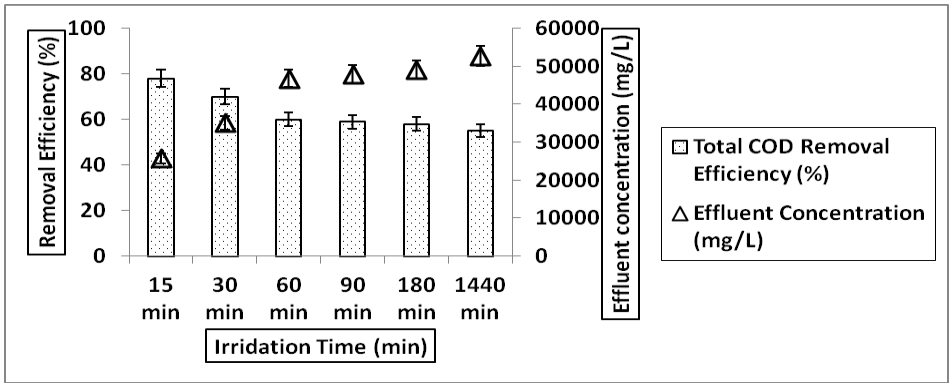

Figure 6.35 The effect of irradiation time under UV light on the COD yield (T: room temperature, original pH of OMW, concentration of nano-ZnO-SiO_2 composite: 1 g/L, UV power: 300 Watt, influent COD concentration: 117000 mg/L)

With increasing of irradiation times under UV from 15 up to 1440 min, total phenol removal efficiencies were obtained as 86 %, 74 %, 73 %, 72 %, 70 % and 70 % after adding 1 g/L nano-ZnO-SiO_2 composite at room temperature and at original pH of OMW under 300 Watt (Figure 6.36). The maximum total phenol removal

efficiency was obtained as 86 % after 15 min irradiation time. Decreasing the removal efficiencies while increasing the irradiation time can be associated with metabolite phenolic molecules such as para-coumaric acid and gallic acid can be formed during oxidation under the long irradiation time. These phenolic compounds measured and results were shown in this study further section.

Photo-degradation of phenol solution with ZnO at a dosage of 0.25 g/L could degrade 32% of phenol in 150 min reported by Sun et al. (2011). They also found that phenol removal from phenol solution with ZnO/SiO_2/UV was only 12 % after 90 min irradiation time. Feng et al. (2014) studied for treatment of phenol solution with Fe_3O_4, Fe_3O_4/ZnO and ZnO and obtained no degradation with Fe_3O_4, 65.5 % with Fe_3O_4/ZnO and 52 % with pure ZnO after 150 min irradiation time.

A linear relationship between irradiation time, effluent total phenol and total phenol removal efficiencies was not obtained (R=0.64) and this regression is not significant (ANOVA $p=0.33 > \alpha=0.05$ and F=1.09)

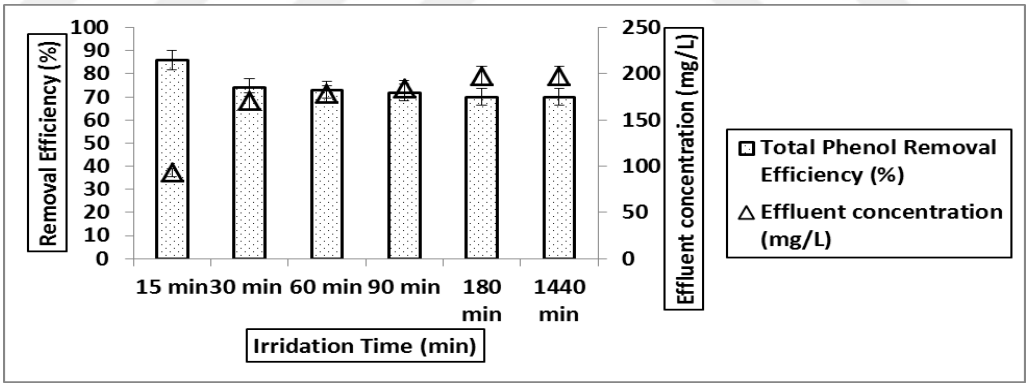

Figure 6.36 The effect of irradiation time under UV light on the total phenol yield (T: room temperature, original pH of OMW, concentration of nano-ZnO-SiO_2 composite: 1 g/L, UV power: 300 Watt, influent total phenol concentration: 660 mg/L)

With increasing irradiation times under UV from 15 up to 1440 min, TS removal efficiencies were obtained as 78 %, 77 %, 67 %, 66 %, 65 % and 63 % after adding 1 g/L nano-ZnO-SiO_2 at room temperature and at original pH of OMW under 300 Watt (Figure 6.37). The maximum TS removal efficiency was obtained as 78 % after 15 min irradiation time. Increasing the irradiation time from 15 min to 1440 min

decreased the yields of TS, slightly. These results imply the presence of solid compounds in the OMW that are resistant to further oxidation since TS are not completely removed even after 1440 min of irradiation time.

A linear relationship between irradiation time, effluent TS and TS removal efficiencies was not obtained (R=0.67) and this regression is not significant (ANOVA p=0.41 and F=1.28).

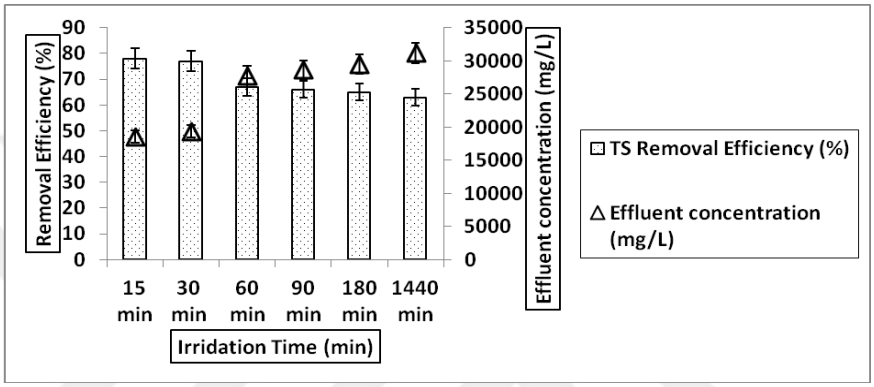

Figure 6.37 The effect of irradiation time under UV light on the TS yield (T: room temperature, original pH of OMW, concentration of nano-ZnO-SiO_2 composite: 1 g/L, UV power: 300 Watt, influent TS concentration: 84250 mg/L)

With increasing irradiation times under UV from 15 up to 1440 min, total nitrogen removal efficiencies were obtained as 100 %, 95 %, 87 %, 86 %, 85 % and 83 % after adding 1 g/L nano-ZnO-SiO_2 composite at room temperature and at original pH of OMW under 300 Watt (Figure 6.38). The maximum total nitrogen removal efficiency was obtained as 100 % after 15 min irradiation time. From these results, it is seen that nano-ZnO-SiO_2 composite improves the opportunity for contact between hydroxyl radicals and nitrogen compounds, resulting in greatly decreased whole of total nitrogen concentration under 15 min irradiation time. Increasing the irradiation time from 15 up to 1440 min decreased the yields of total nitrogen. This can be explained as follows: long irradiation times causes forming NH^{+4}, NO^{-3} ions reacting with other formed species after treatment under UV light. The literature surveys showed that no data was found investigating the photo-removal of total nitrogen from OMW with UV lights by nano-ZnO-SiO_2 composite, yet.

A linear relationship between irradiation time, effluent total nitrogen and total nitrogen removal efficiencies was not obtained (R=0.56) and this regression is not significant (ANOVA p=0.81 > α=0.05 and F=0.71).

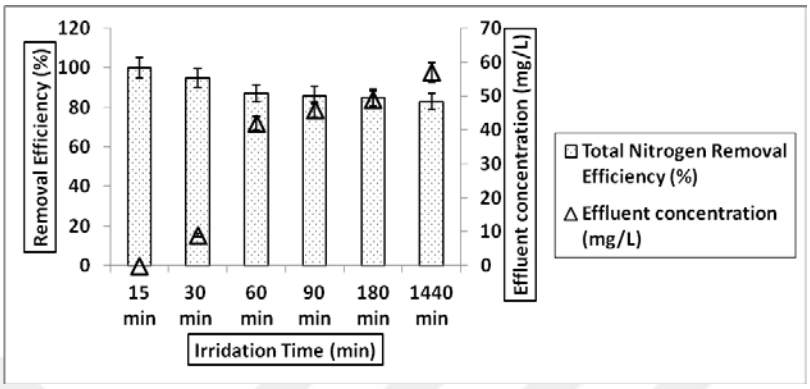

Figure 6.38 The effect of irradiation time under UV light on the total nitrogen yield (T: room temperature, original pH of OMW, concentration of nano-ZnO-SiO_2: 1 g/L, UV power: 300 Watt, influent total nitrogen concentration: 330 mg/L)

With increasing irradiation times under UV 15, 30, 60, 90, 180 and 1440 min, total phosphorous removal efficiencies were obtained as 84 %, 50 %, 43 %, 40 %, 38 % and 33 % after adding 5 g/L nano-ZnO-SiO_2 composite at room temperature and at original pH of OMW under 300 Watt (Figure 6.39). The maximum total phosphorous removal efficiency was obtained as 84 % after 15 min irradiation time. The optimum concentration of nano-ZnO-SiO_2 composite for the photo-treatment of phosphorous removal in the OMW under UV was chosen as 5g/L as mentioned in previous section. Total phosphorous includes polyphosphates and polyphosphates usually undergo hydrolysis and revert to the orthophosphate forms. Long irradiation times causes forming orthophosphate react with other formed species after treatment under UV light (Gray, 2005). The literature surveys showed that no data was found investigating the photo-removal of total phosphorous from OMW with UV lights by nano-ZnO-SiO_2 composite, yet.

A linear relationship between irradiation time, effluent total phosphorous and total phosphorous removal efficiencies was not obtained (R=0.46) and this regression is not significant (ANOVA p=0.89 > α=0.05 and F=0.41).

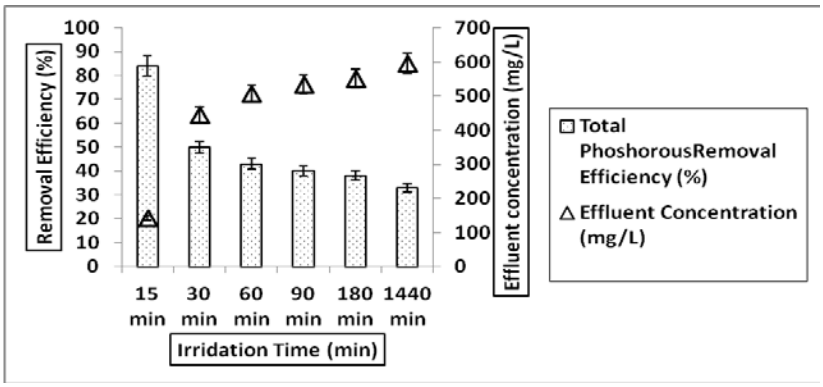

Figure 6.39 The effect of irradiation time under UV light on the total phosphorous yield (T: room temperature, original pH of OMW, concentration of nano-ZnO-SiO_2 composite: 1 g/L, UV power: 300 Watt, influent total phosphorous concentration: 890 mg/L)

6.4.3 Effects of pH of OMW on the Treatment of OMW with UV

The initial pH value of wastewater plays an important role in the photocatalytic degradation of organic compounds. Figure 6.40 demonstrates the effect of pH on the photocatalytic degradation of organic pollutants in OMW on the surface of nano-ZnO-SiO_2 composite. The obtained results showed that the COD removal efficiency decreased as the pH value of the OMW was increased from 4 to 7 and 10. Original pH of OMW (4.01), pH 7 and pH 10 were investigated for optimum pH level of the removal efficiency of COD with 1 g/L nano-ZnO-SiO_2 composite, under 15 min irradiation with 300 Watt UV light at room temperature. We obtained 78 %, 63 % and 59 % COD removal yields at original pH of OMW (4.01), pH 7 and pH 10, respectively. The maximum removal efficiency was obtained as 78 % at original pH of OMW (4.01).

An acidic pH value of 4.01 has been found to be favorable for the photocatalytic degradation of COD compounds in the OMW. The reason is that the point of zero charge of SiO_2 is in a pH range of 2 and 4.The surface of nano-ZnO-SiO_2 composite is positively charged in acidic medium. This favors the adsorption of organic pollutants in the first minutes of photooxidation on to the nano-ZnO-SiO_2 composite surface and facilitates the photo-degradation of COD.

The point of zero charge of ZnO is in a pH range of 8 and 9 (Fouad 2006). Zn^{2+} ions are formed by oxidation of ZnO with h^{+} when pH value is under 5 (Esen, 2011) Eq. (6.13).

$$ZnO+2h+VB \rightarrow Zn^{2+}+O^{*} \quad (6.13)$$

It can be considered; formed oxygen oxidizes the organic molecules in OMW. This reaction does not realize when pH values are up to 10 (Esen, 2011).

A linear relationship between pH of OMW and COD removal efficiencies was obtained (R=0.94) and this regression is significant (ANOVA $p=0.015 < \alpha=0.05$ and F=8.95).

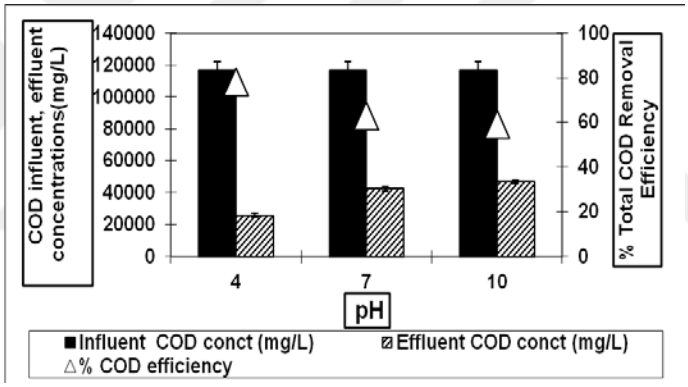

Figure 6.40 The effect of pH of OMW on COD yields under UV (T: room temperature, irradiation time: 15 min, concentration of nano-ZnO-SiO_2 composite: 1 g/L, 300 Watt UV light, influent COD concentration: 117000 mg/L)

Original pH of OMW (4.01), pH 7 and pH 10 were studied to investigate the optimum pH for removal of total phenol from OMW. All experiments realized with 1 g/L nano-ZnO-SiO_2 composite, under 300 Watt 15 min irradiation time at room temperature. The obtained phenol removal efficiencies were 86%, 79% and 75 % for original pH of OMW, pH 7 and pH 10, respectively, as illustrated in Figure 6.41. The maximum phenol yield (86%) was obtained at original pH of OMW among those pH values.

At higher pH, phenol exists as negatively charged phenolate species (Kashif & Ouyang, 2009). Low photo-degradation at higher pH is attributed to the fact that when the concentration of OH^- is higher in the solution, it prevents the penetration of UV light to reach the catalyst surface (Qamar et al., 2006). Moreover, high pH favors the formation of carbonate ions which are effective scavengers of OH^- ions and can reduce the degradation rate (Akbal & Onar, 2003).

A linear relationship between pH of OMW and total phenol removal efficiencies was obtained (R=0.98) and this regression is not significant (ANOVA p=0.085 > α=0.05 and F=40.33).

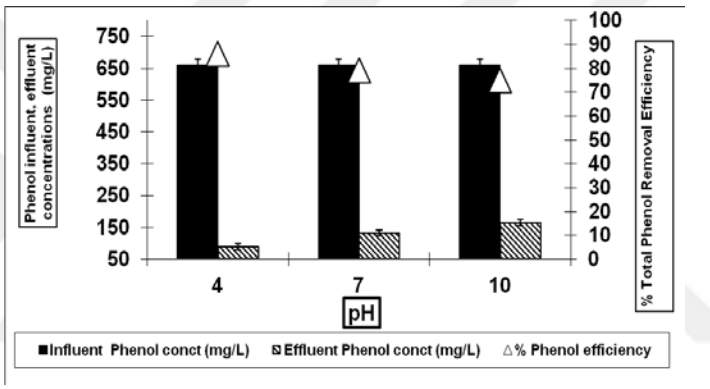

Figure 6.41 The effect of pH of OMW on total phenol yields under UV (T: room temperature, irradiation time: 15 min, concentration of nano-ZnO-SiO_2 composite: 1 g/L, 300 Watt UV light, influent total phenol concentration: 660 mg/L)

TS removal efficiencies decreased by increasing the pH of OMW from 4.01 to 7 and 10. The removal yields were obtained as 77 %, 48 % and 46 % at pH 4, pH 7 and pH 10, respectively (Figure 6.42). The maximum TS yield was found as 77 % at pH 4.01.

It appears that the effect of pH on the photo-degradation of the pollutants is related with the positive charged holes in the surface of nano-ZnO-SiO_2 composite are considered as the major oxidation species at low pH.

A pH dependence of the photocatalytic reactions has been reported for the treatment of several organic compounds with nano particles and nano composites.

Guettai & Amar (2005) also reported that, when pH<6 a strong adsorption of Methyl Orange on the TiO_2 particles is observed as a result of the electrostatic attraction of the positively charged TiO_2 with the dye and this lead to high photo-degradation rate. Badawy et al. (2011) studied effect of pH on the treatment of OMW with TiO_2 and reported that the COD removal increased with decreasing pH value of solution. Guo et al., (2014) studied removal of azo dyes and phenol with nano-TiO_2-SiO_2. On the other hand, the literature surveys showed that no data was found investigating the photocatalytic removal of total solids from OMW with UV lights by nano- ZnO-SiO_2 composite, yet.

A linear relationship between pH of OMW and total solids removal efficiencies was obtained (R=0.89) and this regression is not significant (ANOVA p=0.17 > α=0.05 and F=3.95).

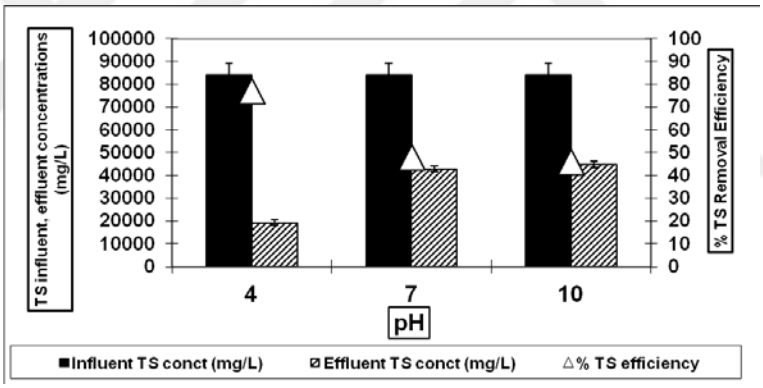

Figure 6.42 The effect of pH of OMW on TS yields under UV (T: room temperature, irradiation time: 15 min, concentration of nano-ZnO-SiO_2 composite: 1 g/L, 300 Watt UV light, influent TS concentration: 84250 mg/L)

Original pH of OMW (4.01), pH 7 and pH 10 were studied to detect the maximum total nitrogen yields with 1 g/L nano-ZnO-SiO_2 composite, under 15 min 300 Watt UV light at room temperature. We obtained 100 %, 100 % and 100 % total nitrogen yields at original pH of OMW (4.01), pH 7 and pH 10, respectively (Figure 6.43). Whole of total nitrogen were removed at all pH values in the OMW. Removal of total nitrogen at lower pH can be explained as follows; low pH values causes charging the nano-ZnO-SiO_2 composite positively. On the other hand, hydroxyl radicals are formed at alkaline pHs and this is resulting with high total nitrogen

removal efficiencies at higher pH values (Esen, 2011). These results showed that the photocatalysis of total nitrogen in the OMW was not dependent to pH.

Another way at the high pH level (10.0) some of the aqueous ammonia was removed through volatilization as ammonia is typically found in the gas form at high pH levels (Idelovitch & Michail, 1981).This mechanism succeeded the removal of total nitrogen at high pH values.

The literature surveys showed that no data was found investigating the photocatalytic removal of total nitrogen from OMW with UV lights by nano-ZnO-SiO_2 composite, yet.

A linear relationship between pH of OMW and total nitrogen removal efficiencies was not obtained (R=0.25) and this regression is not significant (ANOVA $p=0.20 > \alpha=0.05$ and F=0.07).

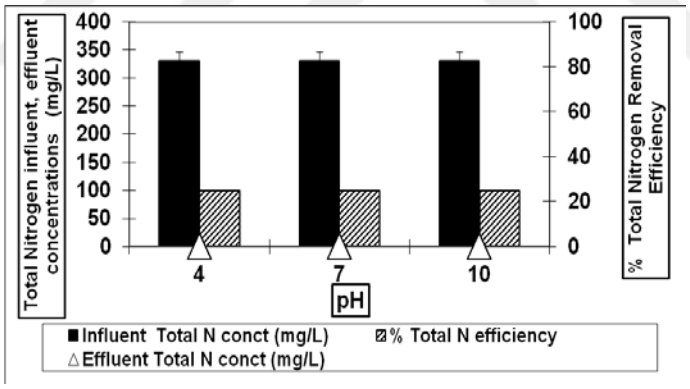

Figure 6.43 The effect of pH of OMW on total nitrogen yields under UV (T: room temperature, irradiation time: 15 min, concentration of nano-ZnO-SiO_2 composite: 1 g/L, 300 Watt UV light, influent total nitrogen concentration: 330 mg/L)

Original pH of OMW (4.01), pH 7 and pH 10 were studied to obtain maximum yield of total phosphorous removal. As seen from Figure 6.44 obtained removal efficiencies were 84 %, 55% and 86 % at original pH of OMW (4.01), pH 7 and pH 10 respectively. The maximum yield (86 %) was obtained at pH 10. Producing OH^- radicals were higher at alkaline pH (10) and this situation removed more total phosphorous compounds when compared with acidic pH (4.01).

The literature surveys showed that no data was found investigating the photocatalytic removal of total phosphorous from OMW with UV lights by nano-ZnO-SiO_2 composite, yet.

A linear relationship between pH of OMW and total phosphorous removal efficiencies was obtained (R=0.94) and this regression is not significant (ANOVA $p=0.32 > \alpha=0.05$ and F=7.68).

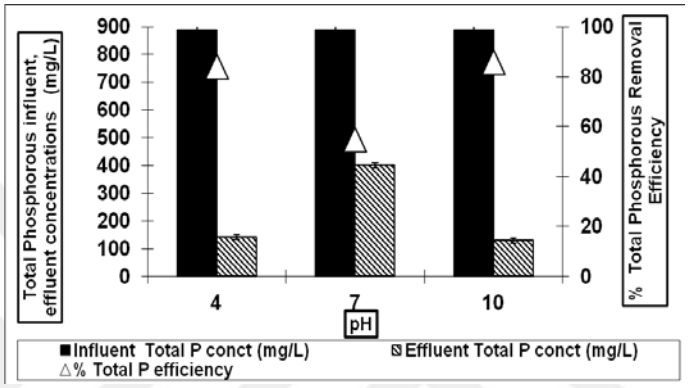

Figure 6.44 The effect of pH of OMW on total phosphorous yields under UV (T: room temperature, irradiation time: 15 min, concentration of nano-ZnO-SiO_2 composite: 1 g/L, 300 Watt UV light, influent total phosphorous concentration: 890 mg/L)

6.5 Treatment of OMW Under Sunlight

6.5.1 Effects of Concentration of Nano-ZnO-SiO_2 Composite on the Treatment of OMW under Sunlight

Effects of 0.5 g/L, 1g/L, 3 g/L, 5 g/L and 10 g/L nano-ZnO-SiO_2 composite concentrations on the removals of COD, phenol, total solids, total nitrogen and total phosphorous in the OMW with constant sunlight time (24 h was chosen due to preliminary studies results) at original pH of OMW (pH: 4.01) under sunlight irradiation with a power of 80 Watt at outdoor temperature (35°C ± 5°C). The results were given in Figures 6.45, 6.46, 6.47, 6.48 and 6.49 for COD, phenol, total solids, total nitrogen and total phosphorous, respectively.

As seen in Figure 6.45 when the concentration of nano-ZnO-SiO_2 composite were increased from 0.5 to 1, 3, 5 and to 10 g/L, the COD yields were obtained as 40 %, 60 %, 77 %, 68 % and 55 %, respectively, under 80 Watt sunlight power after 24 hours sunlight irradiation time at original pH of OMW (4.01) under 35°C ± 5°C outdoor temperature. The maximum COD yield (77 %) was obtained with 3 g/L nano-ZnO-SiO_2 composite. The increasing of the concentration of nano-ZnO-SiO_2 composite from 3 g/L up to 10 g/L decreased the removal efficiencies of COD. The optimum concentration of nano-ZnO-SiO_2 composite was determined as 3 g/L for maximum COD removal.

Heterogeneous photocatalytic reactions are known to show proportional increase in photodegradation with catalyst loading. Generally, in any given photocatalytic application, the optimum catalyst concentration must be determined in order to avoid excess usage of catalyst and to ensure the total absorption of efficient photons. Observation of decreasing the yields with increasing the concentration of nano composite is explained by the covering of pores in the excess nano-ZnO-SiO_2 composite concentrations. As a result the structural deformations of holes in the nano-composite and changes of pores in the nanocomposite surfaces during photocatalysis prevent the photooxidation of pollutant parameters (COD_{total}, COD_{dis}, total phenols, and TAAs) or other radical species (carbon based radicals, e.g., $CO^{3\cdot}$ radicals, etc.) as reported by Sponza & Oztekin (2015).

Above the optimum concentration of nano-ZnO-SiO_2 composite causes turbidity in samples of OMW under sunlight irradiation. The high nano-ZnO-SiO_2 composite concentrations decrease the removals of COD by preventing to reach of pollutants on the surface of nano-ZnO-SiO_2 composite due to turbidity resulting in low OH^{-} radical productions.

A linear relationship between concentration of nano-ZnO-SiO_2 composite, effluent COD and COD removal efficiencies was not obtained (R=0.81) and this regression is not significant (ANOVA $p=0.23 > \alpha=0.05$ and $F=1.95$).

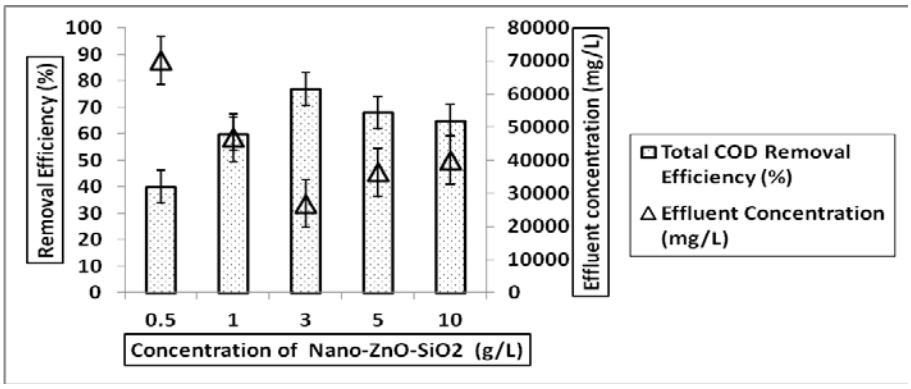

Figure 6.45 The effect of concentration of nano-ZnO-SiO_2 composite on the COD yield (outdoor temperature:35°C ± 5°C,original pH of OMW(4.01),Sunlight irradiation time:24 hour, Sunlight power: 80 Watt, influent concentration of COD: 117000 mg/L)

Semiconductors like ZnO and SiO_2 absorb photons taking a certain amount of energy and then are transferred from electron band to conductive band under sunlight. Meanwhile, an electron vacancy forms and joins the redox reaction with the absorbed substance, by transmigrating to the electron and vacancy catalyst surface (Ugurlu & Karaoglu, 2011). Mechanism in the photocatalyst realized through the usage of nano-ZnO-SiO_2 composite and reactions arising in this process are outlined as follows:

$$ZnO\text{-}SiO_2 + hv \rightarrow e^-_{cb} + h^+_{vb} \quad (6.14)$$

$$O_2 + e^-_{cb} \rightarrow O_2^{\bullet -} \quad (6.15)$$

$$O_2^{\bullet -} + H_2O \rightarrow O^{\bullet} + OH^- + O_2 + HO_2^- \quad (6.16)$$

$$H_2O + h^+_{vb} \rightarrow HO^{\bullet} + H^+ \quad (6.17)$$

Due to the high concentration of $HO^{\bullet}$ and $O_2^{\bullet -}$ absorbed in the particle surface, organic substances could be broken down through oxidative decomposition as indicated in Eq. (6.18):

$$\text{Organic composite} + O_2^{\bullet -} + HO^{\bullet} \rightarrow CO_2 + H_2O + \text{sub composite} \quad (6.18)$$

The total phenol removals were obtained as 50 %, 66 %, 73 %, 72 % and 70 % at 0.5, 1, 3, 5, and 10 g/L nano-ZnO-SiO_2 composite after 24 h irradiation time at a sunlight power of 80 Watt at outdoor temperature (35°C ± 5°C) and at original pH of

OMW, respectively (Figure 6.46). The maximum total phenol yield was obtained as 73 % at 3 g/L nano-ZnO-SiO_2 composite. Increasing the concentration of nano-ZnO-SiO_2 composite from 0.5 to 3 g/L nano-ZnO-SiO_2 composite increased the removal efficiencies, slightly, due to increase the number of photons absorbed and consequently the number of the phenolic compounds adsorbed. Conversely, when the nano-ZnO-SiO_2 composite concentration increased from 3 to 10 g/L the removal efficiencies decreased slightly. This result can be explained as follows: higher concentration of nano composite causes turbidity in the OMW samples and sunlight could not reach to the surface of nano composite effectively. Therefore photocatalytic yields slightly decreased and the phenolic compounds removed slightly lower.

Pardeshi & Patil (2008) studied the removal of phenol from phenol solution with ZnO under sunlight. The minimum amount of photo catalyst required for complete degradation of maximum amount of phenol was examined by varying the amount of photo catalyst from 50 to 350 mg ZnO/100 ml.75 mg/L phenol solution showed 100% degradation when 250 mg ZnO/100 ml was irradiated with sunlight for 8 h. As the amount of photo catalyst increases, the photo degradation efficiency increases up to an optimum loading of ZnO (250 mg/100 ml). This may be due to the fact that as the quantity of ZnO increased up to 250 mg/100 ML, the number of phenol molecules adsorbed was increased. Thus, the photo degradation efficiency was enhanced. Further increase in the amount of photo catalyst showed a negative effect on the phenol removal. The decrease in photo degradation efficiency above 250 mg of ZnO may be attributed to the screening effect of excess ZnO particles in the solution and scattering of light (Anandan et al., 2006).

A linear relationship between concentration of nano-ZnO-SiO_2 composite and total phenol removal efficiencies was not obtained ($R=0.73$) and this regression is not significant (ANOVA $p=0.41 > \alpha=0.05$ and $F=1.17$). There is only a linear relationship between 0.5 g and 3 g nano-ZnO-SiO_2 composite.

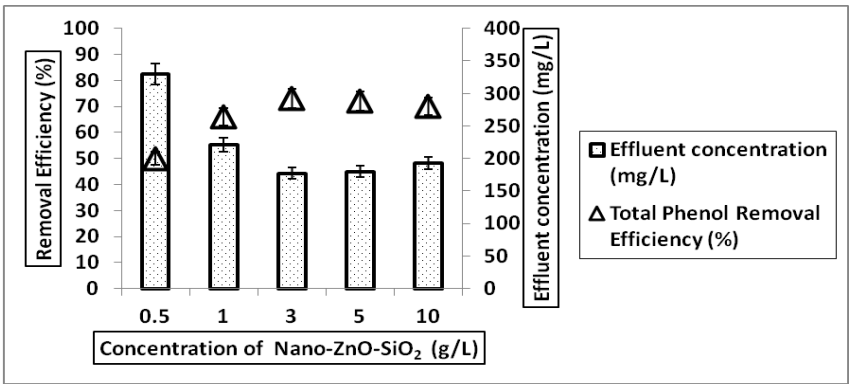

Figure 6.46 The effect of concentration of nano-ZnO-SiO_2 composite on the total phenol yield (outdoor temperature:35°C ± 5°C, original pH of OMW(4.01),Sunlight irradiation time:24 hour, Sunlight power: 80 Watt, influent total phenol concentration: 660 mg/L)

As seen Figure 6.47 when the nano-ZnO-SiO_2 composite concentrations were increased from 0.5 to 1, 3, 5 and 10 g/L TS yields were obtained as 45 %, 58 %, 64 %, 62 % and 60 %, respectively, under 80 Watt sunlight power after 24 hours sunlight irradiation at original pH of OMW (4.01) and 35°C ± 5°C outdoor temperature. The maximum TS yield (64 %) was obtained with 3 g/L nano-ZnO-SiO_2 composite. Firstly, the increasing of the concentration of nano-ZnO-SiO_2 composite from 0.5 up to 3 increased the removal efficiency from 45 % to 64%.More concentration of nano-ZnO-SiO_2 composite produces more hydroxide radicals to break solids bonds. The increasing of the concentration of nano-ZnO-SiO_2 composite from 3 g/L up to 10 g/L decreased slightly the removal efficiencies of TS from 64 % to 60 %. The optimum concentration of nano-ZnO-SiO_2 composite was determined as 3 g/L for maximum TS removal.

The slightly decrease of TS yields at high nano-ZnO-SiO_2 composite concentrations can be explained by the turbidity effect of high nano-ZnO-SiO_2 composite concentrations. High concentration of nano-ZnO-SiO_2 composite would affect the penetration of sunlight through the suspensions due to the light scattering effects.

A linear relationship between concentration of nano-ZnO-SiO_2 composite and TS removal efficiencies was not obtained (R=0.70) and this regression is not significant

(Anova p=0.37 > α=0.05 and F=0.99). There is a linear relationship between 0.5, 1 and 3 g nano-ZnO-SiO_2 composite.

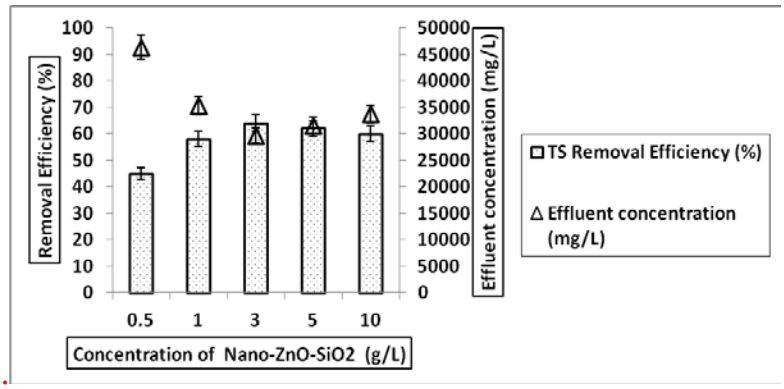

Figure 6.47 The effect of concentration of nano-ZnO-SiO_2 composite on the TS yield (outdoor temperature: 35°C ± 5°C, original pH of OMW (4.01), Sunlight irradiation time: 24 hour, Sunlight power: 80 Watt, influent TS concentration: 84250 mg/L)

The total nitrogen yields were obtained as 78 %, 81 %, 96 %, 87 % and 75 % at 0.5, 1, 3, 5, and 10 g/L nano-ZnO-SiO_2 composite after 24 h irradiation time under 80 Watt sunlight power at 35°C ± 5°C outdoor temperature and at original pH of OMW, respectively (Figure 6.48). The maximum total nitrogen yield was obtained as 96 % at 3 g/L nano-ZnO-SiO_2 composite. Increasing the concentration of nano-ZnO-SiO_2 composite from 0.5 to 3 g/L nano-ZnO-SiO_2 composite increased the removal efficiencies slightly, due to increase the number of photons absorbed and consequently the number of the total nitrogen adsorbed. On the other hand increasing the concentration of nano-ZnO-SiO_2 composite from 3 up to 10 g/L decreased the total nitrogen yields slightly due to turbidity of nano-ZnO-SiO_2 composite.

A linear relationship between concentration of nano-ZnO-SiO_2 composite and total nitrogen removal efficiencies was obtained (R=0.93) and this regression is not significant (ANOVA p=0.07 < α=0.05 and F=6.70).

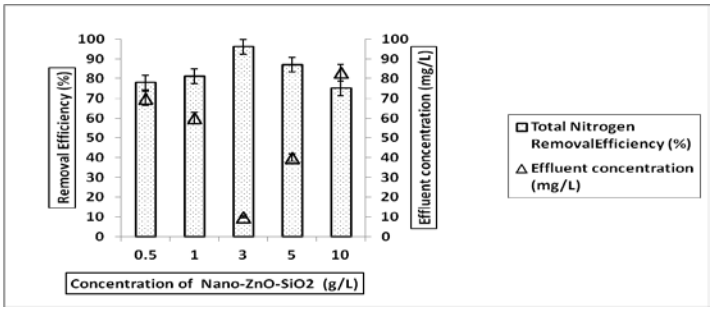

Figure 6.48 The effect of concentration of nano-ZnO-SiO_2 composite on the total nitrogen yield (outdoor temperature 35°C ± 5°C,original pH of OMW(4.01),Sunlight irradiation time:24 hour, Sunlight power: 80 Watt, influent total nitrogen concentration:330 mg/L)

As seen Figure 6.49 when the nano-ZnO-SiO_2 composite concentrations were increased from 0.5 to 1, 3, 5 and to 10 g/L; total phosphorous yields were obtained as 34 %, 42 %, 62 %, 80 % and 79 %, respectively, under 80 Watt 24 hours sunlight irradiation at original pH of OMW (4.01) and outdoor temperature of 35°C ± 5°C. The maximum total phosphorous yield (80 %) was obtained with 5 g/L nano-ZnO-SiO_2 composite. The increasing of the concentration of nano-ZnO-SiO_2 composite from 0.5 up to 5 g/L increased the total phosphorous yields from 34 % to 80 % effectively. On the other hand, the increasing the concentration of nano-ZnO-SiO_2 composite concentrations from 5 g/L up to 10 g/L did not increase the removal efficiencies of total phosphorous. Total phosphorous yields remained as 79 %.The optimum concentration of nano-ZnO-SiO_2 composite was determined as 3 g/L for maximum total phosphorous removal. High concentration of nano-ZnO-SiO_2 composite caused turbidity in the OMW samples and prevented producing OH^- radicals by reducing the decrease in the total phosphorous compounds.

A linear relationship between concentration of nano-ZnO-SiO_2 composite and total phosphorous removal efficiencies was obtained for 0.5, 1, 3 and 5 g/L nano-ZnO-SiO_2 composite (R=0.86) and this regression is not significant (ANOVA p=0.77 >α=0.05 and F=2.96).

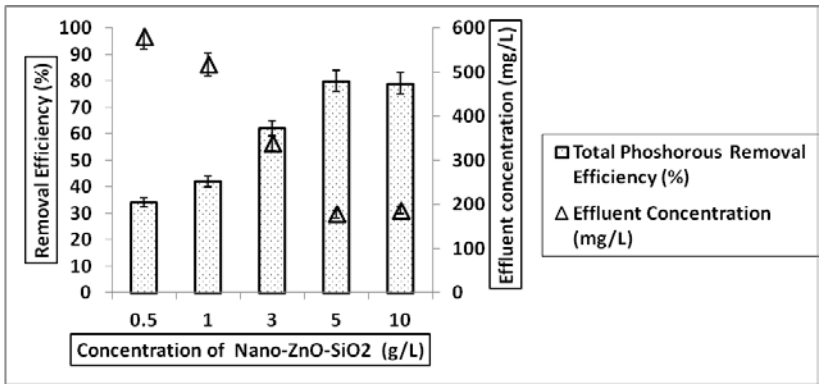

Figure 6.49 The effect of concentration of nano-ZnO-SiO_2 composite (outdoor temperature 35°C ± 5°C,original pH of OMW(4.01),Sunlight irradiation time:24 hour, Sunlight power: 80 Watt, influent total phosphorous concentration: 890 mg/L)

6.5.2 Effects of Irradiation Time on the Treatment of OMW under Sunlight

Effect of irradiation time on the removals of COD, total solids, phenol, total nitrogen and total phosphorous in the OMW for the nano-ZnO-SiO_2 composite concentration of 3 g/L, at original pH of OMW (4.01) at outdoor temperature (35°C ± 5°C) under 80 Watt sunlight irradiation were illustrated in Figure 6.50, Figure 6.51, Figure 6.52, Figure 6.53 and Figure 6.54, respectively. Concentration of nano-ZnO-SiO_2 composite was chosen as 3 g/L since the preliminary studies showed that the maximum COD yields was obtained at 3 g/l nano-composite concentration at original pH of OMW (4.01) at a temperature of 35 °C ± 5 °C. 8, 16, 24 and 36 h irradiation times were studied to obtain the optimum irradiation time. All experiments are realized by using 3 g/L nano-ZnO-SiO_2 composite at original pH of OMW at outdoor temperature (35°C ± 5°C) under 80 Watt sunlight power.

With increasing of sunlight irradiation times from 8, to 16, 24 and to 36 h, under 80 Watt sunlight power 65 %, 70 %, 77 % and 68 % COD removal efficiencies were obtained after adding 3 g/L nano-ZnO-SiO_2 composite at outdoor temperature (35°C ± 5°C) at original pH of OMW (4.01) (Figure 6.50). The maximum COD removal efficiency was obtained as 77 % after 24 h irradiation time. Firstly, the increasing the irradiation time from 8 h to 24 h increased the removal efficiencies of COD from 65 % to 77 %. On the other hand increasing the irradiation time from 24 to 36 h decreased the COD yields to 68 % (Figure 6.50).

Sun et al. (2011) studied the removal of methylene blue with nano-structured ZnO under sunlight irradiation. Their results showed that COD removal efficiencies decreased from 50 % to 48 % with the increase of reaction time from 4 h to 10 h similarly to our study. They obtained 48% COD removal for the pure ZnO after 10 h sunlight irradiation.

Low contact times cannot be enough for OH^- radical production throughout photooxidation process while high contact times could have changes the structure and the pores of nanocomposite, and the photocatalysts might have been covered completely with the particles of non-photodegraded pollutants (Sponza & Oztekin, 2015). In this study increasing the irradiation time from 8 h to 24 h increased the COD yields from 65 % to 77 % due to produced OH^- radicals. On the other hand increasing the irradiation time from 24 h to 36 h decreased the COD yields from 77 % to 68%.

The literature surveys showed that no data was found investigating the photo-removal of COD from OMW with sunlight by nano-ZnO-SiO_2 composite, yet.

A linear relationship between concentration of nano-ZnO-SiO_2 composite, and COD removal efficiencies was obtained for increasing irradiation time from 8 h to 24 h (R=0.73) and this regression is not significant (ANOVA $p=0.50 > \alpha=0.05$ and F=0.59).

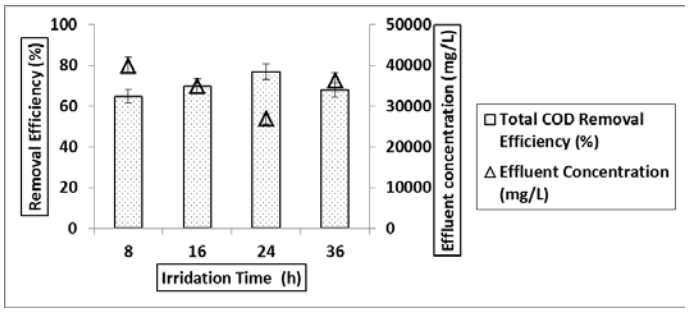

Figure 6.50 The effect of irradiation time under sunlight on the COD yield (outdoor temperature: 35°C ± 5°C, original pH of OMW (4.01), concentration of nano-ZnO-SiO_2 composite: 3 g/L, UV power: 80 Watt, influent COD concentration: 117000 mg/L)

8, 16, 24 and 36 h sunlight irradiation times were investigated to obtain the maximum removal efficiency of total phenol with 3 g/L nano-ZnO-SiO_2 composite at original pH of OMW (4.01) at outdoor temperature (35°C ± 5°C), 80 Watt sunlight irradiation. 50 %, 62 %, 73 % and 68 % total phenol removal efficiencies were obtained as the irradiation time were increased from 8 to 16, 24 and 36 h, respectively (Figure 6.51). As the irradiation time was increased from 8 to 24 h, the total phenol yields increased from 50 % to 73 %. On the other hand, the increasing of irradiation time from 24 h to 36 h decreased the total phenol yield from 73 % to 68 %, slightly.

Guo et al. (2014) studied removal of phenol (initial concentration of phenol is 80 mg/L) with TiO_2–SiO_2 (concentration of TiO_2–SiO_2 is 50 mg/L) from phenol solution under different sunlight irradiation times (20, 40, 60, 80, 100, 120 and 140 min). They obtained maximum yield (90 %) within 120 min. When the irradiation time was increased from 120 min to 140 min the total phenol not increased. Increasing the irradiation time did not increase the phenol yield as aforementioned in our study. Optimum irradiation times were required for total phenol removal to break the bonds of phenolic molecules.

A linear relationship between concentration of nano-ZnO-SiO_2 composite, and total phenol removal efficiencies was obtained as the irradiation time was increased from 8 to 24 h (R=0.94) and this regression is not significant (ANOVA p=0.33 > α=0.05 and F=4.51).

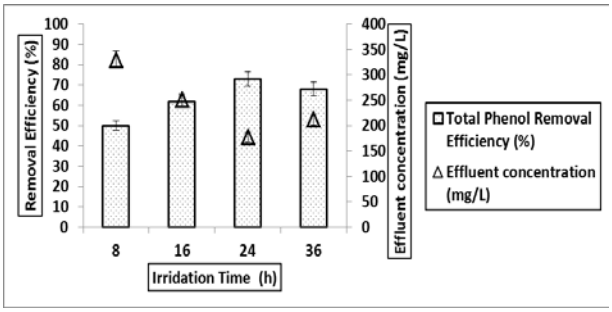

Figure 6.51 The effect of irradiation time under sunlight on the total phenol yield (outdoor temperature: 35°C ± 5°C, original pH of OMW (4.01), concentration of nano-ZnO-SiO_2 composite: 3 g/L, UV power: 80 Watt, influent total phenol concentration: 660 mg/L)

With increasing of irradiation times from 8 up to 36 h, 48 %, 50 %, 67 % and 64 % TS removal efficiencies were obtained after adding 3 g/L nano-ZnO-SiO_2 composite at outdoor temperature (35°C ± 5°C), at original pH of OMW (4.01) under 80 Watt sunlight power (Figure 6.52). The maximum TS removal efficiency was obtained as 67 % after 24 h irradiation time. Firstly, increasing the irradiation time from 8 h to 24 h increased the removal efficiencies of TS from 48 % to 67 %. On the other hand increasing the irradiation time from 24 to 36 h decreased the TS yields to 64 % (Figure 6.52). Total solids decrease the amount of sunlight in the OMW sample able to penetrate on the surface of nano-ZnO-SiO_2 composite at long irradiation times. Therefore, the TS yields were slightly high for 24 h (67 %) compared to 36 h (64 %) sunlight irradiation times.

A linear relationship between concentration of nano-ZnO-SiO_2 composite, and TS removal efficiencies was obtained as the sunlight irradiation time was increased from 8 to 24 hours (R=0.84) and this regression is not significant (ANOVA p=0.81> α=0.05 and F=1.28).

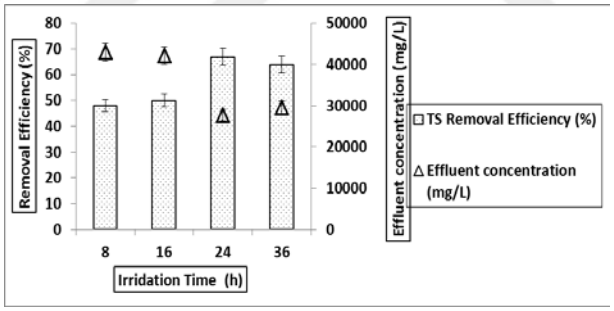

Figure 6.52 The effect of irradiation time under sunlight on the TS yield (outdoor temperature: 35°C ± 5°C, original pH of OMW (4.01), concentration of nano-ZnO-SiO_2 composite: 3 g/L, UV power: 80 Watt, influent TS concentration: 84250 mg/L)

8, 16, 24 and 36 h sunlight irradiation times were studied to obtain optimum irradiation time for total nitrogen removal. All experiments were realized with 3 g/L nano-ZnO-SiO_2 composite at original pH of OMW (4.01), 80 Watt sunlight irradiation at outdoor temperature (35°C ± 5°C). The removal efficiencies were 33 %, 69 %, 96 % and 86 % as increasing the irradiation time from 8, 16, and 24 and to 36 h, respectively (Figure 6.53). The maximum total nitrogen yield (96 %) was

obtained after 24 h sunlight irradiation time. As the irradiation time was increasing from 8 to 24 h, the photooxidized total nitrogen yields increased from 33 % to 96 %. On the other hand increasing of irradiation time from 24 h to 36 h decreased the total nitrogen yields slightly to 86 %. The photogenerated reactive oxygen species were formed maximum after 24 h sunlight irradiation time to break the total nitrogen compounds with a maximum yield of 96 %.

A linear relationship between concentration of nano-ZnO-SiO_2 composite and total nitrogen removal efficiencies was obtained as the sunlight irradiation time was increased from 8 to 24 hours (R=0.99) and this regression is significant (ANOVA $p=0.04 < \alpha=0.05$ and F=246.93).

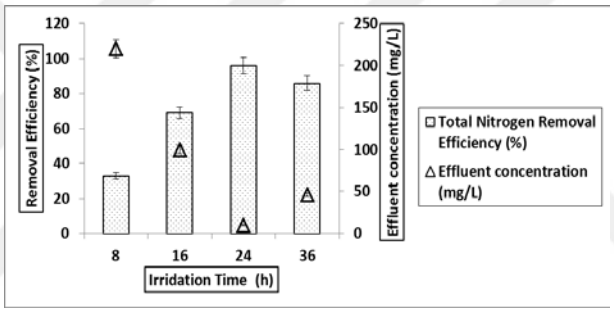

Figure 6.53 The effect of irradiation time under sunlight on the total nitrogen yield (outdoor temperature: 35°C ± 5°C, original pH of OMW (4.01), concentration of nano-ZnO-SiO_2 composite: 3 g/L, UV power: 80 Watt, influent total nitrogen concentration: 330 mg/L)

With increasing of irradiation times from 8, 16, 24 and to 36 h; 48 %, 50 %, 62 % and 40 % total phosphorus removals was observed under 80 Watt sunlight power after adding 3 g/L nano-ZnO-SiO_2 composite at outdoor temperature (35°C ± 5°C) at original pH of OMW (4.01) (Figure 6.54). The maximum total phosphorous removal efficiency was obtained as 62 % after 24 h irradiation time. Firstly, increasing the irradiation time from 8 h to 24 h increased the removal efficiencies of total phosphorous from 48 % to 62 %. On the other hand increasing the irradiation time from 24 to 36 h decreased the total phosphorous yields to 40 % (Figure 6.54). The producing OH^- radicals were optimum at 24 h to obtain maximum yield of total phosphorous (62 %). Above 24 h irradiation time, the structure of nano-ZnO-SiO_2

composite can be changed under long irradiation time or the surface of the nano-ZnO-SiO_2 composite can be deteriorated.

A linear relationship between concentration of nano-ZnO-SiO_2 composite and total phosphorous removal efficiencies was obtained only for increasing the irradiation time from 8 to 24 h (R=0.56) and this regression is not significant (ANOVA p=0.65> α=0.05 and F=0.23).

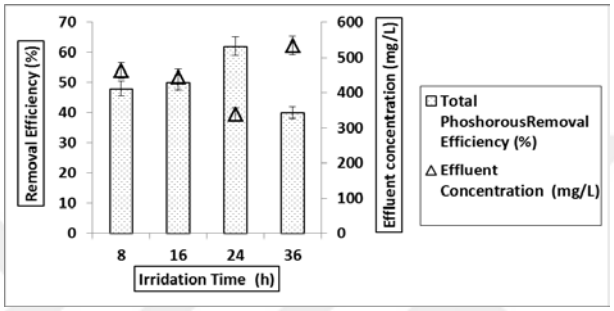

Figure 6.54 The effect of irradiation time under sunlight on the total phosphorous yield (outdoor temperature: 35°C ± 5°C, original pH of OMW (4.01), concentration of nano-ZnO-SiO_2 composite: 3 g/L, UV power: 80 Watt, influent total phosphorous concentration: 890 mg/L)

6.5.3 Effect of pH on the Treatment of OMW under Sunlight

The effect of pH on photocatalysis efficiency was tested at three different pH values (original pH of OMW (4.01), 7 and 10) in the OMW samples with 3 g/L nano-ZnO-SiO_2 composite under 24 h sunlight irradiation at an UV power of 80 Watt at 35 °C ± 5 °C outdoor temperature.

The obtained results showed that the COD removal efficiency decreased as the pH value of the OMW was increased from 4 to 7 and to 10. Original pH of OMW (4.01), pH 7 and pH 10 were investigated for optimum pH level of the maximum removal efficiency of COD with 3 g/L nano-ZnO-SiO_2 composite , under 24 h irradiation with 80 Watt sunlight power at an outdoor temperature of 35 °C ± 5 °C. We obtained 77 %, 67 % and 66 % COD removal yields at original pH of OMW (4.01), at pH 7 and at pH 10, respectively **(**Figure 6.55). The maximum removal efficiency was obtained as 77 % at original pH of OMW (4.01) (Figure 6.55).

The reason of low COD removal yields at high pH levels is the presence of carbonate ions, which could scavenge the hydroxyl radicals, or holes produced on the activated nano composite surface, comprising a less reactive carbonate radical with low OH^- radical production and degradation/ mineralization process (Feitz & Waite, 2003; Mazellier et al., 2002).

A linear relationship between pH of OMW and COD removal efficiencies was obtained (R=0.90) and this regression is not significant (ANOVA $p=0.23 > \alpha=0.05$ and F=4.48).

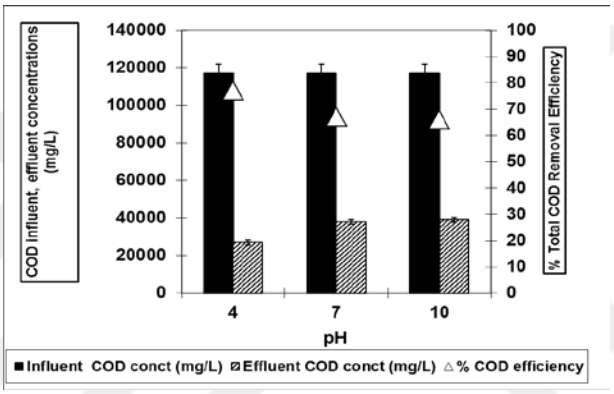

Figure 6.55 The effect of pH on COD yields under sunlight in OMW (outdoor temperature: 35°C ± 5°C, irradiation time: 24 h, concentration of nano-ZnO-SiO_2 composite: 3 g/L, 80 Watt sunlight power, influent concentration of COD: 117000 mg/L)

Original pH of OMW (4.01), pH 7 and pH 10 were studied to investigate the optimum pH for removal of total phenol from OMW. All experiments realized with 3 g/L nano-ZnO-SiO_2 composite, under 80 Watt 24 h irradiation time at 35 °C ± 5 °C outdoor temperature. The obtained phenol removal efficiencies were 75 %, 73 % and 70 % for original pH of OMW, pH 7 and pH 10, respectively as illustrated in Figure 6.56. The maximum phenol yield (75 %) was obtained at original pH of OMW among those pH values.

The favorable adsorption of total phenol onto SiO_2 in the nano-ZnO-SiO_2 composite at acidic regions enhances the electron hole separation, allowing more positive holes to oxidize. In fact, at low pH values, the degradation takes place mainly through the reaction of adsorbed compounds with the photo-generated holes

(Bayarri et al., 2005; Tunesi & Anderson, 1991). Tang & Huang (1995) studied the intermediates of 2, 4-dichlorophenol photooxidation by CdS (Cadmium Sulfide) and found that the predominant mechanism may be direct oxidation of organic compounds by photo-generated holes. At high pH values, surface of SiO_2 is not charged positively to oxidize effectively the total phenol.

A linear relationship between pH of OMW and total phenol removal efficiencies was obtained (R=0.99) and this regression is not significant (ANOVA p=0.04 > α=0.05 and F=75).

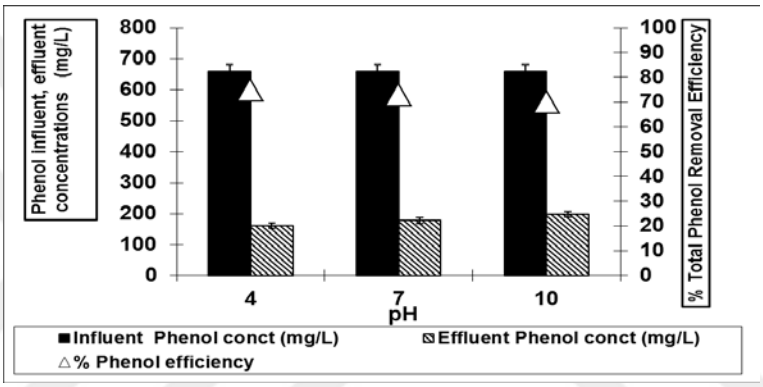

Figure 6.56 The effect of pH of OMW on total phenol yields under sunlight (outdoor temperature: 35°C ± 5°C, irradiation time: 24 h, concentration of nano-ZnO-SiO_2 composite: 3 g/L, 80 Watt sunlight power, influent concentration of total phenol: 660 mg/L)

TS removal efficiencies decreased by increasing the pH of OMW from 4.01 to 7 and 10. The removal yields were obtained as 64 %, 55 % and 53 % at pH 4, pH 7 and pH 10, respectively (Figure 6.57). The maximum TS yield was found as 64 % at pH 4.01. It is noted that the reported pHzpc (zero point of charge) of SiO_2 are 2–4, (Sverjensky, 2005) indicating the positively charged holes on its surface, which are in good agreement with the results obtained in this study. This explain why the effect of pH on the photo-degradation of the pollutants is related with the positive charged holes in the surface of nano-ZnO-SiO_2 composite and they are considered as the major oxidation species at low pH. Under acidic conditions the total solids were splitted by OH^- that was produced by positive charged surface of nano-ZnO-SiO_2 composite. As results the spilled total solids were settled in the bottom.

A linear relationship between pH of OMW and total solids removal efficiencies was obtained (R=0.93) and this regression is not significant (ANOVA p=0.18 > α=0.05 and F=7.40).

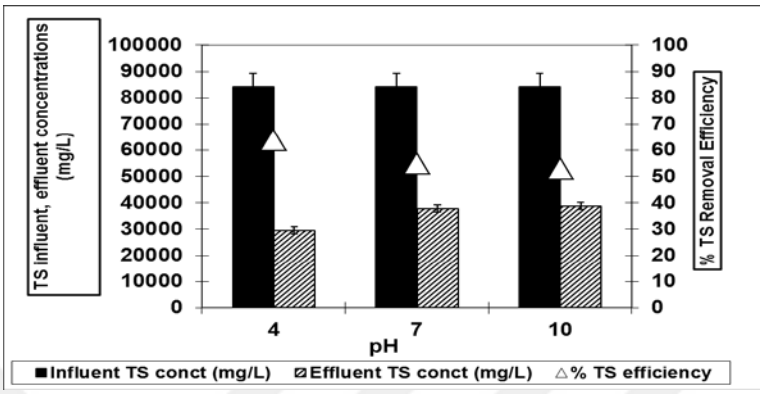

Figure 6.57 The effect of pH of OMW on TS yields under sunlight (outdoor temperature: 35°C ± 5°C, irradiation time: 24 h, concentration of nano-ZnO-SiO_2 composite: 3 g/L, 80 Watt sunlight power, influent concentration of TS: 84250 mg/L)

Original pH of OMW (4.01), pH 7 and pH 10 were studied to detect the maximum total nitrogen yields with 3 g/L nano-ZnO-SiO_2 composite, under 24 h photooxidation time, under 80 Watt sunlight power at outdoor temperature of 35°C ± 5°C . We obtained 96 %, 95 % and 95 % total nitrogen yields at original pH of OMW (4.01), pH 7 and pH 10, respectively (Figure 6.58). High total nitrogen removals were obtained at all pH values in the OMW samples. Removal of total nitrogen at lower pH can be explained as follows; low pH values causes charging the nano-ZnO-SiO_2 composite positively. On the other hand, hydroxyl radicals formed at alkaline pHs can be enough to photooxidize the total nitrogen effectively at higher pH values (Esen, 2011). These results showed that the photocatalysis of total nitrogen in the OMW was not dependent to pH.

A linear relationship between pH of OMW and total nitrogen removal efficiencies was obtained (R=0.86) and this regression is not significant (ANOVA p=0.32 > α=0.05 and F=3).

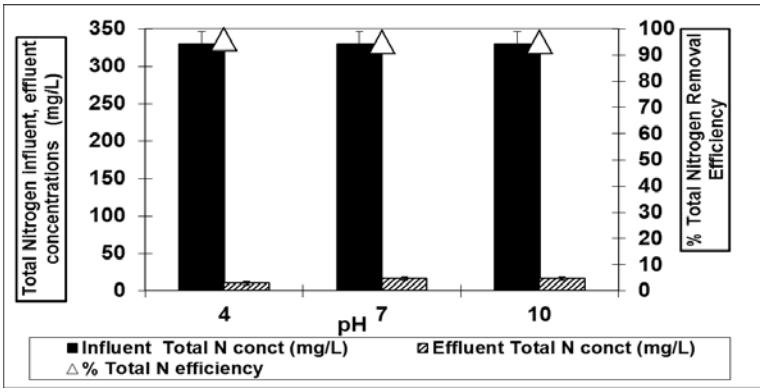

Figure 6.58 The effect of pH of OMW on total nitrogen yields under sunlight (outdoor temperature: 35°C ± 5°C, irradiation time: 24 h, concentration of nano-ZnO-SiO_2 composite: 3 g/L, 80 Watt sunlight power, influent concentration of total nitrogen: 330 mg/L)

Original pH of OMW (4.01), pH 7 and pH 10 were studied to obtain maximum yield of total phosphorous removal. As seen from Figure 6.59 obtained removal efficiencies were 62 %, 65% and 67 % at original pH of OMW (4.01), pH 7 and pH 10, respectively. The maximum phosphorus yield (67 %) was obtained at pH 10. The produced OH^- radicals were higher at alkaline pH (10) and this situation removed more total phosphorous compounds when compared with acidic pH (4.01).

A linear relationship between pH of OMW and total phosphorous removal efficiencies was obtained (R=0.99) and this regression is not significant (ANOVA $p=0.03 > \alpha=0.05$ and F=75).

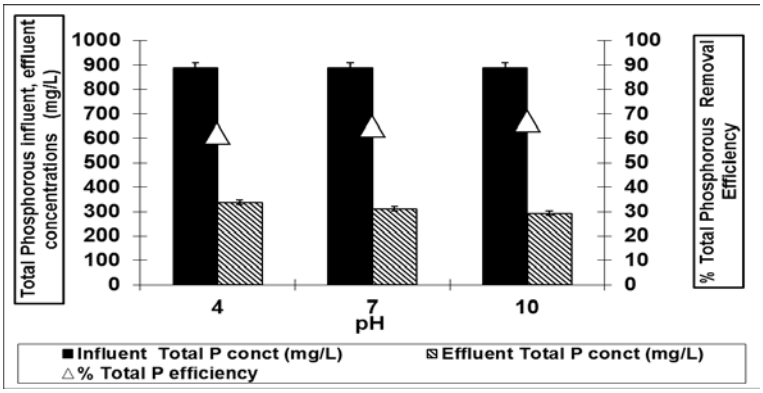

Figure 6.59 The effect of pH of OMW on total phosphorous yields under sunlight (outdoor temperature: 35°C ± 5°C, irradiation time: 24 h, concentration of nano-ZnO-SiO_2 composite: 3 g/L, 80 Watt sunlight power, influent concentration of total phosphorous: 890 mg/L)

6.6 Investigation of Photocatalytic Degradation Kinetic of COD and Total Phenol Using Nano-ZnO-SiO_2 Composite in the OMW

In this section, zero-order kinetic, first-order kinetic and second-order kinetic models were discussed to indicate the removal kinetics of COD and phenol on the surface of nano-ZnO-SiO_2 composite throughout photodegradation under UV.

6.6.1 Zero-Order Kinetics

A Zero order reaction has a rate that is independent of the concentration of the reactants. Increasing the concentration of the reacting species will not speed up the rate of the reaction i.e. the amount of substance reacted is proportional to the time. Zero order reactions are typically found when a material that is required for the reaction to proceed, such as a surface or a catalyst, is saturated by the reactants. The rate law for a zero order reaction is:

$$r=k \tag{6.19}$$

where r is the reaction rate and k is the reaction rate coefficient with units of concentration or time. If, and only if, this zeroth order reaction 1) occurs in a closed system, 2) there is no net build-up of intermediates, and 3) there are no other reactions occurring, it can be shown by solving a mass balance equation for the system that:

where r is the reaction rate and k is the reaction rate coefficient with units of concentration or time. If, and only if, this zeroth order reaction 1) occurs in a closed system, 2) there is no net build-up of intermediates, and 3) there are no other reactions occurring, it can be shown by solving a mass balance equation for the system that:

$$r = -\frac{d[A]}{dt} = k \tag{6.20}$$

If this differential equation is integrated it gives an equation often called the integrated zero order rate law.

$$[A]t = -kt + [A]_0 \tag{6.21}$$

Where $[A]_t$ represents the concentration of the chemical of interest at a particular time, and $[A]_0$ represents the initial concentration (Rushton et al., 2007). Eq.21 is in the form y = mx+b where slope = m = -k and the y-intercept = b =$[A]_0$.

Where A_0 is the influent concentration of OMW (mg/L) and A is the effluent concentration of OMW (mg/L) at any time t (min), respectively and k_0 is the constant of pseudo-zero-order reaction (min^{-1}).

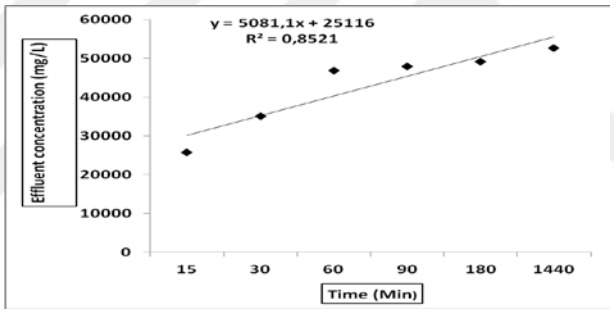

Figure 6.60 Pseudo-zero-order reaction of COD (T: room temperature, irradiation time: 15 min, concentration of nano-ZnO-SiO_2 composite: 1 g/L, 300 Watt UV light)

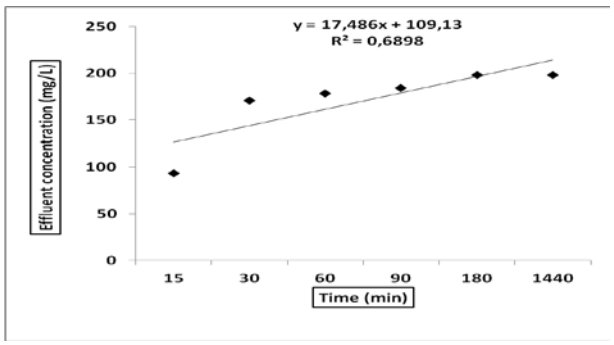

Figure 6.61 Pseudo-zero-order reaction of total phenol (T: room temperature, irradiation time: 15 min, concentration of nano-ZnO-SiO_2 composite: 1 g/L, 300 Watt UV light

The R^2 values for pseudo-zero-order reaction were found as 0.8521 for COD and 0.6898 for total phenol, respectively, in the photocatalytic studies performed with nano-ZnO-SiO_2 composite (Figure 6.60 and Figure 6.61). Pseudo-zero-order reaction's the zero order rate kinetic constant is k_0. The k_0 values evaluated from Pseudo-zero-order reaction plots were found as 5081 min^{-1} for COD and 17.48 min^{-1} for total phenol, respectively (Figure 6.60 and Figure 6.61). The k_0 values found from the pseudo first order reactions are not acceptable due to excessively high k_0 values for COD and total phenol removals.

6.6.2 First-Order Kinetics

A first order reaction depends on the concentration of only one reactant (a unimolecular reaction). Other reactants can be present, but each will be zero order. The rate law for a reaction that is first order with respect to a reactant A is;

$$\frac{-d[A]}{dt} \equiv r = k[A] \tag{6.22}$$

k is the first order rate constant, which has units of 1/s. The integrated first order rate law is:

$$ln[A] = -kt + ln[A]_0 \tag{6.23}$$

A plot of ln [A] vs. time *t* gives a straight line with a slope of -k (Rushton et al., 2007).

Where A^0 is the influent concentration of OMW (mg/L) and A is the effluent concentration of OMW (mg/L) at any time t (min), respectively and k_1 is the constant of pseudo-firs-order reaction (min^{-1}).

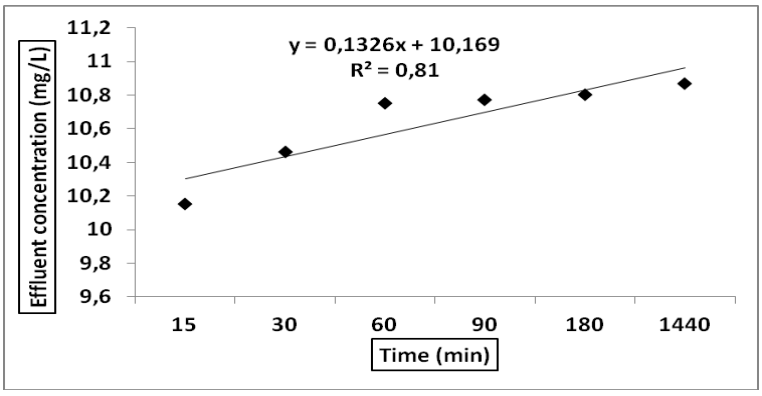

Figure 6.62 First-order reaction of COD (T: room temperature, irradiation time: 15 min, concentration of nano-ZnO-SiO_2 composite: 1 g/L, 300 Watt UV light)

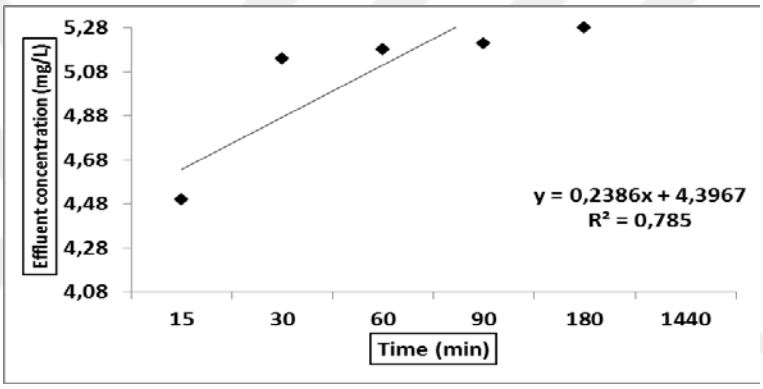

Figure 6.63 First-order reaction of total phenol (T: room temperature, irradiation time: 15 min, concentration of nano-ZnO-SiO_2 composite: 1 g/L, 300 Watt UV light)

The R^2 values for first-order reaction were obtained as 0.81 for COD and 0.78 for total phenol, respectively, in the photocatalytic studies performed with nano-ZnO-SiO_2 composite (Figure 6.62 and Figure 6.63). First-order reaction's in the first order rate kinetic constant is k_1. The k_1 values evaluated from first -order reaction plots were found to be 0.13 min^{-1} for COD and 0.23 min^{-1} for total phenol, respectively (Figure 6.62 and Figure 6.63). The k_1 values of COD and total phenol were found meaningful for the photodegradation of both COD and phenol from OMW with suitable linear correlation (R^2 = 0.78 and 0.81) between photooxidation time and treated pollution parameters.

6.6.3 Second-Order Kinetics

A second order reaction depends on the concentrations of one second order reactant, or two first order reactants (Rushton et al., 2007).
Its reaction rate is given by:

$$\frac{1}{[A]} = \frac{1}{[A]_0} + kt \qquad (6.24)$$

Where A_0 is the influent concentration of OMW (mg/L) and A is the effluent concentration of OMW (mg/L) at any time t (min), respectively and k_2 is the constant of pseudo-second-order reaction (min^{-1}).

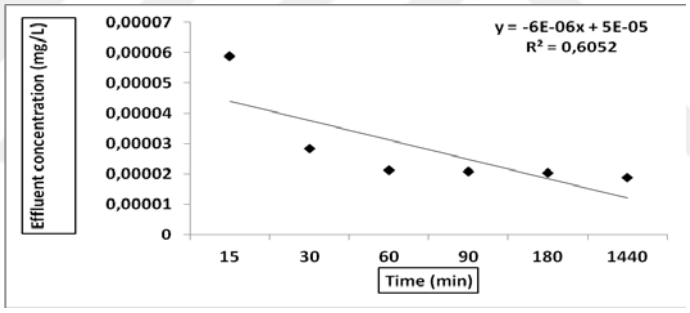

Figure 6.64 Second-order reaction of COD (T: room temperature, irradiation time: 15 min, concentration of nano-ZnO-SiO_2 composite: 1 g/L, 300 Watt UV light)

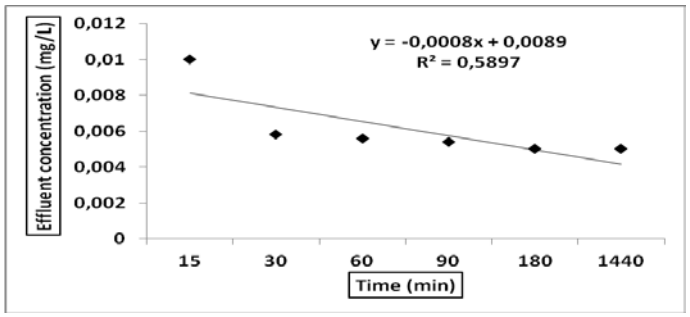

Figure 6.65 Second-order reaction of total phenol (T: room temperature, irradiation time: 15 min, concentration of nano-ZnO-SiO_2 composite: 1 g/L, 300 Watt UV light)

The R^2 values for second-order reaction were found as 0.60 for COD and 0.58 for total phenol, respectively, in the photocatalytic studies performed with nano-ZnO-SiO_2 composite (Figure 6.64 and Figure 6.65). Second-order reaction's the second order rate kinetic constant is k_2. The k_2 values evaluated from second-order reaction plots were found as -6E-06 min^{-1} for COD and -0.0008 min^{-1} for total phenol, respectively (Figure 6.64 and Figure 6.65). The k_2 values of COD and total phenol were found to be not acceptable for photodegradation from the OMW since are very low with low R^2 values.

As results of kinetic studies it was found that the COD and phenol from the OMW were photodegraded according to first order reaction kinetic since the k_1 values calculated are meaningful. From the first- order reaction plots k_1 values for COD and phenol photodegradation were found to be 0.13 min^{-1} and 0.23 min^{-1}. In the other words, COD and total phenol were removed from OMW under 300 Watt UV irradiation according to first-order reaction kinetics.

6.7 Measurement of the Concentration of Phenolic Compounds by HPLC in Raw and Treated OMW with Nano-ZnO-SiO_2 Composite under UV Irradiation

Raw OMW and treated OMW with 1 g/L nano-ZnO-SiO_2 composite under 15 min UV irradiation (300 Watt) at original pH of OMW (pH 4.01) and a temperature of ±20 ^{0}C with an UV power of 300 W, gallic acid, p-coumaric acid and trans p-coumaric acid polyphenols measured with HPLC. Three polyphenols can be seen Figure 6.66 in raw OMW. Gallic acid, p-coumaric acid and trans-p-coumaric acid amounts were measured as 65.51821 mg/L, 43.85360 and 43.85381 mg/L, respectively, in raw OMW (Figure 6.66).

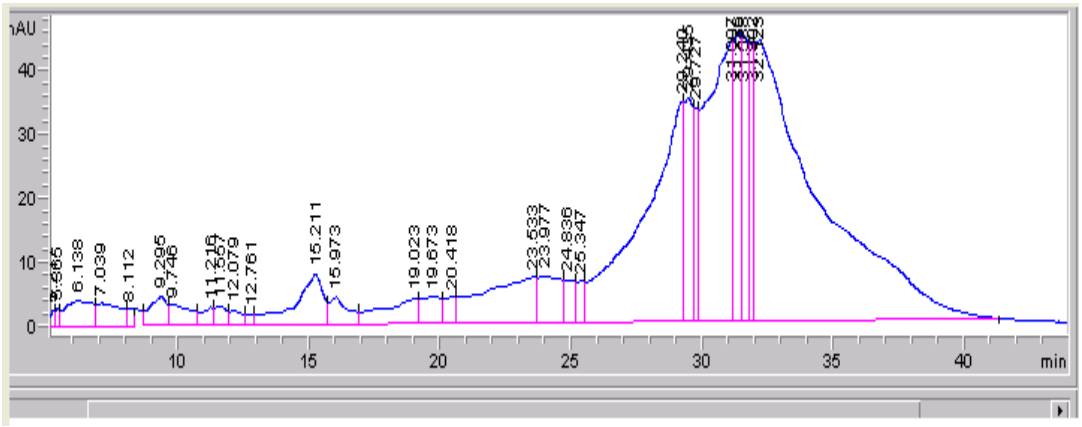

RetTime [min]	Type	Area [mAU*s]	Amt/Area	Amount [ng/ul]	Grp	Name
9.295	BV	207.19920	3.16209e-1	65.51821		gallic
31.097	VV	2943.03613	1.49008e-2	43.85360		PARA
31.0995	VV	2943.03619	1.49009e-2	43.85381		PARA T
Totals :				153.22562		

Figure 6.66 The concentration of gallic acid, p-coumaric acid and trans p- coumaric acid found in raw OMW

Three polyphenols can be seen from Figure 6.67 in the treated OMW. Gallic acid amount was found as 65.51821 mg/L in raw OMW but after treatment with UV, whole of gallic acid in OMW treated. The yield was %100 after photooxidation. P-coumaric acid and trans p- coumaric acid measured as 43.85360 and 43.85381 mg/L, respectively, in raw OMW. On the other hand after treatment under UV, p-coumaric acid and trans p-coumaric acid measured as 39.16515 and 39.16585 mg/L, respectively. Removal efficiencies of, p-coumaric acid and trans p- coumaric acid was % 10 and % 10, respectively.

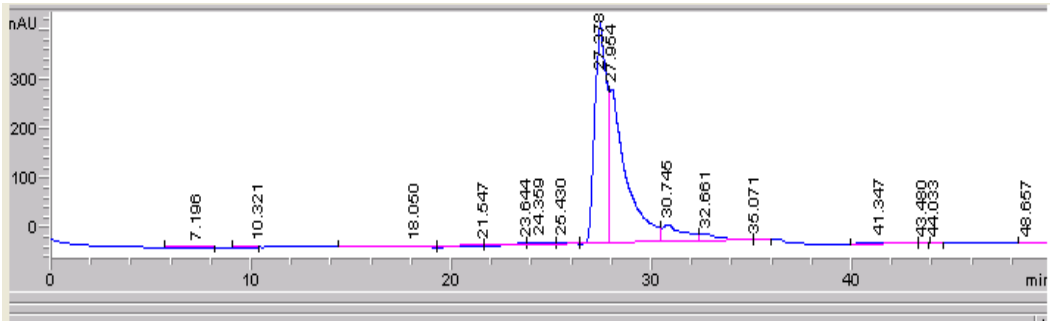

RetTime [min]	Type	Area [mAU*s]	Amt/Area	Amount [nq/ul]	Grp	Name
8.858		-	-	-		qallic
30.745	VV	2628.39185	1.49008e-2	39.16515		PARA
30.745	VV	2628.39188	1.49009e-2	39.16585		PARA T
Totals :				78.331		

Figure 6.67 The concentration of gallic acid, p-coumaric acid and trans p- coumaric acid found in treated OMW with UV photooxidation (nano-ZnO-SiO_2 composite concentration: 1 g/L, T: ±20 ^{0}C, pH: 4.01, UV irradiation time: 15 min, UV power: 300 Watt).

Table 6.4 Removal efficiencies of polyphenols (gallic acid, p-coumaric acid and trans p- coumaric acid) in OMW.

Polyphenols	Raw OMW (mg/L)	Treated OMW	Removal Efficiency (%)
Gallic acid	65.51821	0	100
p-coumaric acid	43.85360	39.16515	10
Trans p- coumaric	43.85381	39.16585	10

6.8 UV Absorption Spectra of OMW

The UV–visible spectra of the OMW were measured with a spectro-photometer in the wave lengths range varying between 190 nm, 400 nm, 600 nm, 800 nm, 1000 nm and 1100 nm. UV absorption spectra of raw OMW and treated OMW under UV irradiation can be seen in Figure 6.68 and Figure 6.69, respectively. The maximum absorbance peaks were seen at between 245 and 270 nm at wavelengths between 190 nm and 400 nm as 3.784 A and 3.527 A in raw OMW. After the OMW was treated under UV light with 1 g/L nano-ZnO-SiO_2 composite, the measured absorbance values were illustrated in Figure 6.69. The maximum absorbance peaks decreased close to zero after UV treatment. The reason of this situation can explained as follows; organic pollutants (polyphenols, carbonaceous compounds, nitrogenous

compounds) were photodegraded to CO_2 and H_2O and unconvertible pollutants remained inert in the treated OMW.

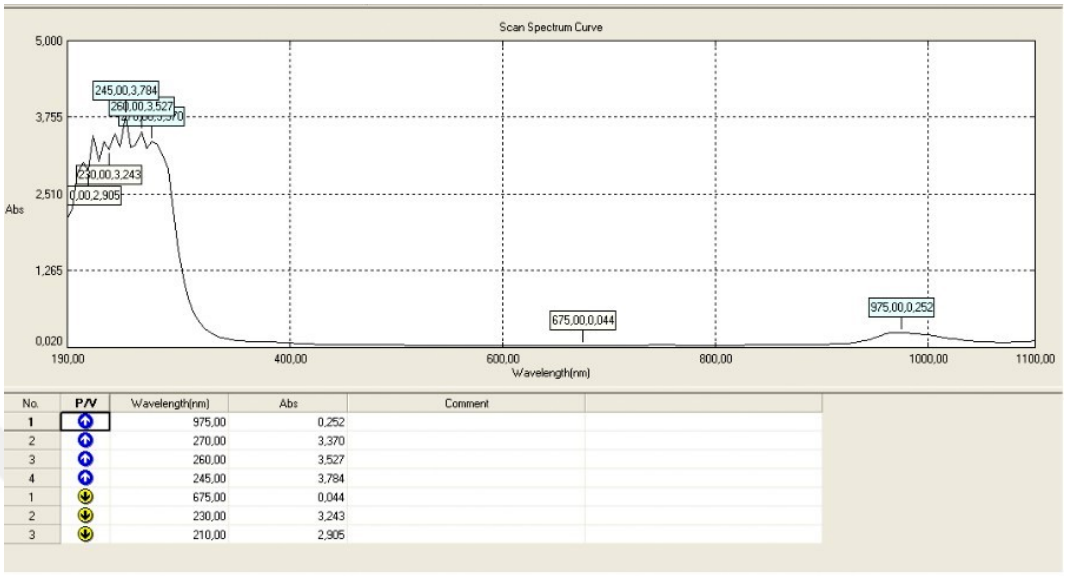

No.	P/V	Wavelength(nm)	Abs	Comment
1	↑	975,00	0,252	
2	↑	270,00	3,370	
3	↑	260,00	3,527	
4	↑	245,00	3,784	
1	↓	675,00	0,044	
2	↓	230,00	3,243	
3	↓	210,00	2,905	

Figure 6.68 UV absorption spectra in the raw OMW.

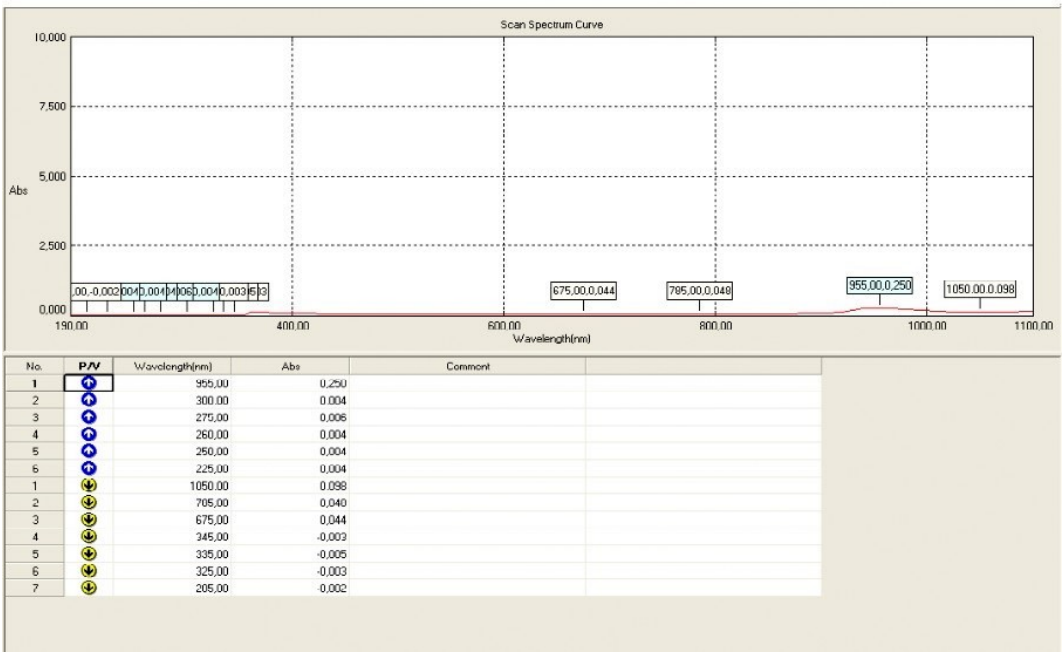

No.	P/V	Wavelength(nm)	Abs	Comment
1	↑	955,00	0,250	
2	↑	300,00	0,004	
3	↑	275,00	0,006	
4	↑	260,00	0,004	
5	↑	250,00	0,004	
6	↑	225,00	0,004	
1	↓	1050,00	0,098	
2	↓	795,00	0,040	
3	↓	675,00	0,044	
4	↓	345,00	-0,003	
5	↓	335,00	-0,005	
6	↓	325,00	-0,003	
7	↓	205,00	0,002	

Figure 6.69 UV absorption spectra in the treated OMW under UV irradiation (T: room temperature, irradiation time: 15 min, concentration of nano-ZnO-SiO_2 composite: 1 g/L, 300 Watt UV light)

6.9 Measurement of Inert Chemical Oxygen Demand Fractions of Olive Mill Wastewater

The total COD of a raw wastewater is usually made up of biodegradable and non-biodegradable fractions (Ekama et al., 1986). On the whole, the biodegradable fraction consists of soluble, readily biodegradable organics and particulate, slowly biodegradable organics, while the non- biodegradable fraction consists of soluble and particulate inert organics. Four batch reactors were operated in parallel and started with the almost a similar initial COD of 5000 mg/L both for glucose and OMW. OMW was diluted with pure water the ratio of 1:1 (V: V) for four times to decrease the COD concentration from 117000 mg/L to 5000 mg/L. The COD and glucose levels were stabilized and a plateau value was observed with unchanged COD concentrations during consecutive 10 days.

Figure 6.70 shows the total inert COD, soluble inert COD fractions of raw OMW, total inert COD of glucose solution and soluble inert COD of glucose solution. Total inert COD and dissolved inert COD of OMW and glucose solutions tests were performed. The experiments took 35 days to reach plateau values. As a result after the inert COD of glucose solution and dissolved glucose solution reached close to zero, the total inert COD of raw OMW was found as 8765 mg/L with calculation dilution ratio. The soluble inert COD of raw OMW was found as 3674 mg/L with calculation the dilution ratio.

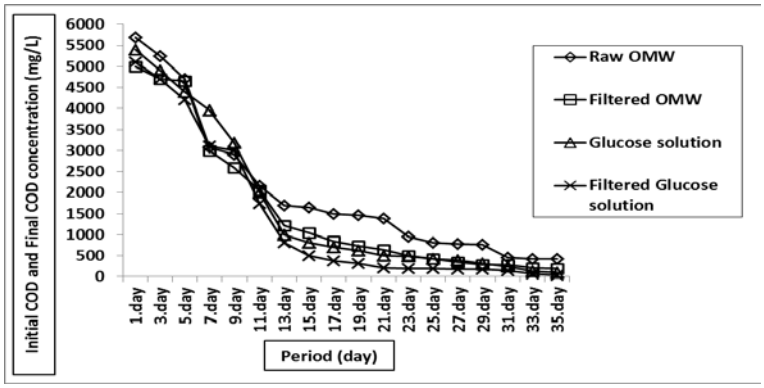

Figure 6.70 Total inert COD, soluble inert COD of raw OMW, total inert COD of glucose solution and soluble inert COD of glucose solution (T: ±20 ^{0}C, original pH of OMW: 4.01)

Figure 6.71 shows the total inert COD, soluble inert COD fractions after treatment of OMW (at original pH of OMW, temperature of 20 ^{0}C, after 15 min irradiation time under UV light, concentration of nano-ZnO-SiO_2 composite: 1 g/L, UV power: 300 Watt), total inert COD of glucose solution and soluble inert COD of glucose solution. When compared the mineralization times of total inert and soluble inert COD of raw OMW experiments. It was observed that the degradation period was shorter after photooxidation and took approximately 31 days to reach a standard plateau. After treatment of OMW with photodegradation under UV, the total inert COD and soluble inert COD concentrations of OMW obtained as 420 mg/L and 225 mg/L, respectively with calculation dilution ratio.

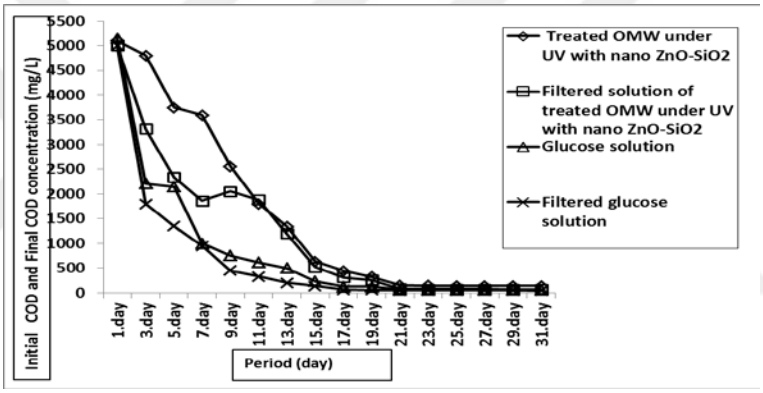

Figure 6.71 Total inert COD and dissolved inert COD of treatment of OMW with UV irradiation (T: ±20 ^{0}C, nano-ZnO-SiO_2 composite concentration: 1g/L, Irradiation time: 15 min, UV power: 300 Watt, original pH of OMW: 4.01)

The resulting total inert COD and soluble inert COD of OMW removal efficiency after photocatalytic treatment was found to be 92 % and 89 %, respectively as shown in Table 6.5.

Table 6.5 Removal efficiencies of total inert COD and soluble inert COD of OMW

Parameter	Raw OMW (mg/L)	Treatment of OMW with UV (mg/L)	Removal Efficiency (%)
Total Inert COD	8765	420	95
Soluble Inert COD	3674	225	93

6.10 Recovery of Nano-ZnO-SiO_2 Composite

Recovery of nano-ZnO-SiO_2 composite is a key of decreasing the cost of treatment of OMW and a friendly treatment approach. In this study, six sequential treatment steps were investigated for determination of reusability of nano-ZnO-SiO_2 composite. 1g/L nano-ZnO-SiO_2 composite were used for six times under 15 min UV irradiation (300 Watt), with 1 g/L nano-ZnO-SiO_2 composite for 1 liter OMW at original pH of OMW (4.01), at room temperature. COD, total phenol and TS parameters measured to determine the removal of OMW wastewater after six sequential with the same nano-ZnO-SiO_2 composite. All results were shown in tables 6.6, 6.7 and 6.8 for COD, total phenol and TS, respectively.

After the utilization of 1 g/L of nano-ZnO-SiO_2 composite in the first, second, third, fourth, fifth and sixth times the removal yields of the COD, total phenol and TS parameters were shown in Figure 6.72 (Table 6.6), Figure 6.73 (Table 6.7), and Figure 6.74 (Table 6.8), respectively. The yield of COD decreased from 78 %, to 60 %, 51 %, 48 %, and 30 % and to 5 %, respectively, after six sequential treatment steps with the same nano-ZnO-SiO_2 composite as illustrated in Figure 6.72 and Table 6.6. The removal efficiencies of total phenol decreased from 86 %, to 50 %, 42 %, 20 %, and 15 % and to 7 % as shown in Figure 6.73 and Table 6.7. At last, the TS removal efficiency also decreased from 77 %, 55 %, 41 %, 33 %, and 30 % to 9 %, respectively (Figure 6.74 and Table 6.8). Final concentrations after sixth treatment were obtained as 1312 mg/L for COD, 19 mg/L for total phenol and 2142 mg/L for TS After sixth times utilization of the same nano-ZnO-SiO_2 composite. This showed that aged nano-ZnO-SiO_2 composite can be used several times for treatment of the OMW wastewater for removal the pollutant parameters and decrease the cost spent for treatment.

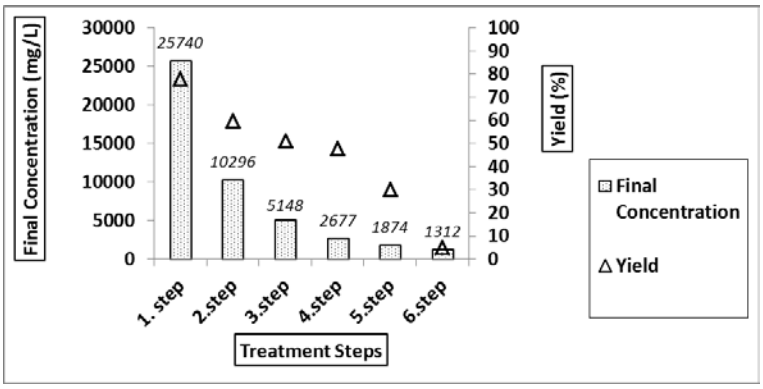

Figure 6.72 Effluent COD concentrations after sixth utilization of the same nano-ZnO-SiO_2 composite (T: room temperature, nano-ZnO-SiO_2 composite concentration: 1 g/L, UV irradiation time: 15 min, UV power: 300 Watt, pH: 4.01 (original pH of OMW), initial concentration of COD: 117000 mg/L).

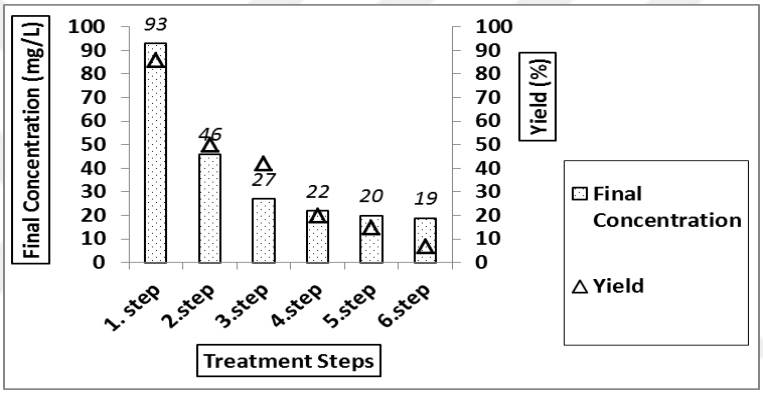

Figure 6.73 Effluent total phenol concentrations after sixth utilization of the same nano-ZnO-SiO_2 composite (T: room temperature, nano-ZnO-SiO_2 composite concentration: 1 g/L, UV irradiation time: 15 min, UV power: 300 Watt, pH: 4.01 (original pH of OMW), initial concentration of total phenol: 660 mg/L).

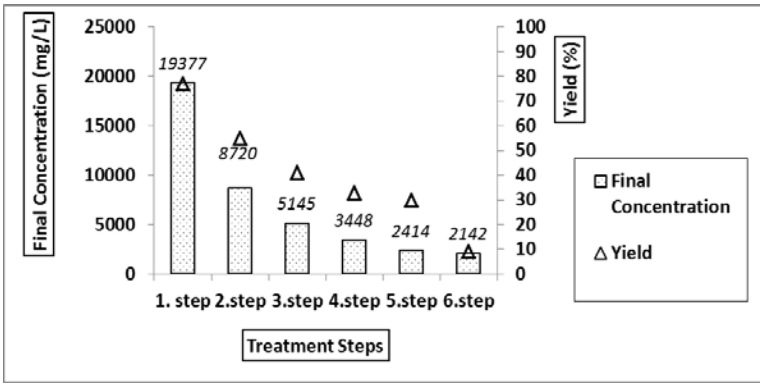

Figure 6.74 Effluent TS concentrations after sixth utilization of the same nano-ZnO-SiO_2 composite (T: room temperature, nano-ZnO-SiO_2 composite concentration: 1 g/L, UV irradiation time: 15 min, UV power: 300 Watt, pH: 4.01 (original pH of OMW), initial concentration of TS: 84250 mg/L).

Table 6.6 Calculation of COD yields by recovery of nano-ZnO-SiO_2 composite (T: room temperature, nano-ZnO-SiO_2 composite concentration: 1 g/L, UV irradiation time: 15 min, UV power: 300 Watt, pH: 4.01 (original pH of OMW), initial concentration of COD: 117000 mg/L).

Steps	Initial Concentration of COD (mg/L)	Final Concentration of COD (mg/L)	Yield (%)
First step	117000	25740	78
Second step	25740	10296	60
Third Step	10296	5148	51
Fourth Step	5148	2677	48
Fifth Step	2677	1874	30
Sixth Step	1874	1312	5
Total	117.000	1312	98

Table 6.7 Calculation of total phenol yields by recovery of nano-ZnO-SiO_2 composite (T: room temperature, Nano-ZnO-SiO_2 composite concentration: 1 g/L, UV irradiation time: 15 min, UV power: 300 Watt, pH: 4.01 (original pH of OMW), initial concentration of total phenol: 660 mg/L).

Steps	Initial Concentration of Total Phenol (mg/L)	Final Concentration of Total Phenol (mg/L)	Yield (%)
First step	660	93	86
Second step	93	46	50
Third Step	46	27	42
Fourth Step	27	22	20
Fifth Step	22	20	15
Sixth Step	20	19	7
Total	660	19	97

Table 6.8 Calculation of TS yields by recovery of nano-ZnO-SiO_2 composite (T: room temperature, nano-ZnO-SiO_2 composite concentration: 1 g/L, UV irradiation time: 15 min, UV power: 300 Watt, pH: 4.01 (original pH of OMW), initial concentration of TS: 84250 mg/L).

Steps	Initial Concentration of TS (mg/L)	Final Concentration of TS (mg/L)	Yield (%)
First step	84250	19377	77
Second step	19377	8720	55
Third Step	8720	5145	41
Fourth Step	5145	3448	33
Fifth Step	3448	2414	30
Sixth Step	2414	2142	9
Total	84250	2142	97

Considering the final concentrations of COD, total phenol and TS, in the treated OMW after six times, this treated wastewater can be discharged to the sewage systems according to discharge limits illustrated in Regulation of Water Pollution Control, The Official Newspaper dated 31.12.2004' 'The Official Newspaper

Numbered 25687 (2004), (discharge limits of COD and total phenol; 4000 mg/L and 20 mg/L SKKY, Table 25, respectively) (Table 6.9).

Table 6.9 Discharge limits according to Regulation of Control of Water Pollution (Table 25) (2004) a; not considering this parameters for wastewater assessment

Parameter	Sewer systems, in the infrastructure systems ending with ultimate treatment
Temperature (°C)	40
pH	6.5-10.0
COD (mg/L)	4000
Total Phenol (mg/L)	20
Total Nitrogen (mg/L)	- [(a)]
Total Phosphorous (mg/L)	- [(a)]

Treated OMW can be used for irrigation water, (according to COD and total phenol parameters) however pH, salt, conductivity, ions (Ca^{+2} and Mg^{+2}), oil and grease, pathogen microorganism, heavy metal concentration in OMW must be measured before using for irrigation water 'Regulation of Wastewater Treatment Plant Technical Methods,' Table E7.2, (2010) for irrigation of treated wastewater (Table 6.10), pH of OMW must be 6-9.

Table 6.10 Limits for irrigation of treated wastewater according to Wastewater Treatment Plant Technical Methods Notification' Table E7.2., (2010)

Parameters		Units	The degree of damage in use		
			None (I. class water)	Less-Middle (II. class water)	Dangerous (III. class water)
Salinity					
Conductivity		µS/cm	< 700	700-3000	>3000
Total Dissolved Solids		mg/L	< 500	500-2000	>2000
Permeability					
SAR_{Tad}	0-3		EC ≥ 0.7	0.7-0.2	< 0.2
	3-6		≥ 1.2	1.2-0.3	< 0.3
	6-12		≥ 1.9	1.9-0.5	< 0.5
	12-20		≥ 2.9	2.9-1.3	< 1.3
	20-40		≥ 5.0	5.0-2.9	< 2.9
Specific ion toxicity					
Sodium (Na)					
Surface Irrigation		mg/L	< 3	3-9	> 9
Trickling Irrigation		mg/L	< 70	> 70	
Chloride (Cl)					
Surface Irrigation		mg/L	< 140	140 –350	> 350
Trickling Irrigation		mg/L	< 100	> 100	
Boron (B)		mg/L	< 0.7	0.7-3.0	> 3.0

6.11 Cost Analysis

Cost analysis investigated for treatment of 1 liter OMW with 1 g/L nano-ZnO-SiO_2 composite under 300 Watt UV light, at original pH of OMW (4.01) at room temperature. Firstly, 20 UV lamps require for the setup of UV reactor also electricity consumption and nano-ZnO-SiO_2 composite synthesis costs are considered. All the consumptions were calculated and are given in Table 6.11. Total cost of treatment OMW was found as 500.75 TL for treat 1 liter of OMW. 500 TL was spent for 20 UV lamps, while the chemical cost, electricity consumption and nanocomposite cost were only 0.75 TL for 1 liter OMW treatment.

Table 6.11 Cost analysis for photocatalytic treatment of OMW under UV light

Cost Analysis	Treatment of OMW under UV light
UV	**1 UV lamp:** 25 TL **20 UV lamp:** 20 * 25 = 500 TL
Electricity consumption	**15 min UV irradiation:** 0.11 TL
Chemicals	**Nano-ZnO particles (500 g):** 20 € (66.66 TL) **Nano-SiO_2 particles (100 g):** 35 € (116.55 TL)
Cost analysis for treatment of 1 liter OMW: 1 g nano-ZnO-SiO_2 was used for treatment of 1 liter OMW under UV light.	**For 1 g nano-ZnO- SiO_2 composite:** **0.5 g nano-ZnO particles:**0.02 € (0.06 TL) **0.5 g nano-SiO_2 particles:**0.17 € (0.58 TL)
Total cost for treatment of 1 liter OMW	500 TL (investment cost) + 0.11 TL + 0.06 TL + 0.58 TL = **500. 75 TL** (that price includes investment cost)
The cost of chemicals is calculated according to market prices. Electricity costs are calculated according to the consumer price in industrial units. Recent euro exchange rate was used to convert the Euro currency to Turkish Liras (1€ = 3.33 TL).	

6.12 A Summary for Statistical ANOVA Test Results

The one-way analysis of variance (ANOVA) is used to determine whether there are some significant differences between the dependent and independent parameters (Lund & Lund, 2013). In this section the relationships between pollutant removals and operating parameters of three treatment methods were investigated according to regressions based on linearity and non-linearity purposes , and alfa (α) values to detect the significance of the linear regressions .

For adsorption process; significant linear regressions between COD, TS, total nitrogen and total phosphorous removals and increasing nano-ZnO-SiO_2 composite levels were not observed (Table 6.12) and these regressions are not significant. On the other hand significant linear regression between total phenol and increasing the nano- ZnO-SiO_2 composite levels were obtained but this regression is not significant.

Significant linear regressions between COD, total phenol, TS and total phosphorous removals and increasing adsorption times were observed (Table 6.12) and regressions of total phenol and TS are significant. On the other hand significant linear regression between total phenol and increasing the nano- ZnO-SiO_2 composite

levels was not obtained and regressions of COD, total nitrogen and total phosphorous are not significant.

Significant linear regressions between COD, total phenol, TS, total nitrogen and total phosphorous removals and decreasing pH values were observed (Table 6.12) and regressions of COD, total nitrogen and total phosphorous are significant. On the other hand regressions of total phenol and TS are no significant.

For photooxidation with UV process; significant linear regressions between TS and total phosphorous removals and increasing nano-ZnO-SiO_2 composite levels were observed (Table 6.12). On the other hand significant linear regression between COD, total phenol and total nitrogen and increasing the nano- ZnO-SiO_2 composite levels were not obtained and regressions of COD, total phenol, TS, total nitrogen and total phosphorous are not significant.

Significant linear regressions between COD, total phenol, TS, total nitrogen and total phosphorous removals and increasing irradiation times under UV light were not observed (Table 6.12) and these regressions are not significant.

Significant linear regressions between COD, total phenol, TS and total phosphorous removals and decreasing pH values were observed (Table 6.12) and regressions of total phenol, TS, total nitrogen and total phosphorous are not significant. On the other hand significant linear regression between total nitrogen and decreasing pH values was not observed. Regression of COD was obtained as significant.

For photooxidation with sunlight treatment process; significant linear regressions between COD, total nitrogen and total phosphorous removals and increasing nano-ZnO-SiO_2 composite levels were observed (Table 6.12) and regressions of total nitrogen and total phosphorous are significant. On the other hand significant linear regressions between TS and total nitrogen and decreasing pH

values were not observed. Regressions of COD, total phenol and TS are not significant.

Significant linear regressions between total phenol, TS and total nitrogen removals and increasing irradiation times under sunlight were not observed (Table 6.12) and regressions of COD, total phenol, TS and total phosphorous are not significant. On the other hand significant linear regressions between COD and total phosphorous and increasing irradiation times under sunlight were not observed. Regression of total nitrogen is significant.

Significant linear regressions between COD, total phenol, TS, total nitrogen and total phosphorous removals and decreasing pH values were observed (Table 6.12) and regressions of total phenol and total phosphorous are significant. On the other hand regressions of COD, TS and total nitrogen are not significant.

Table 6.12 Anova summary of treatment process

	Adsorption Process		**UV process**		**Sunlight Process**	
Concentration of nano-ZnO-SiO_2 composite	Linear	α values (Significant)	Linear	α values (Significant)	Linear	α values (Significant)
	-Total Phenol	----	-TS -Total Phosphorous	----	-COD -Total Nitrogen -Total Phosphorous	-Total Nitrogen -Total Phosphorous
Adsorption/ Irradiation Time	-COD -Total Phenol -TS -Total Phosphorous	-Total Phenol -TS	----	----	-Total Phenol -TS -Total Nitrogen	-Total Nitrogen
pH	-COD -Total Phenol -TS -Total Nitrogen -Total Phosphorous	-COD -Total Nitrogen -Total Phosphorous	-COD -Total Phenol -TS -Total Phosphorous	-COD	-COD -Total Phenol -TS -Total Nitrogen -Total Phosphorous	-Total Phenol -Total Phosphorous

CHAPTER SEVEN
CONCLUSION

OMW treatment was studied with two treatment mechanism (adsorption, photooxidation under UV and sunlight) using nano-ZnO-SiO_2 composite in this study. Treatment of OMW was studied under different operational conditions to obtain the optimum treatment conditions. Effect of concentration of nano-ZnO-SiO_2 composite, adsorption/irradiation time and pH of OMW were investigated and two power sources were used for photooxidation to compare the removal efficiencies of pollutant parameters and the cost.

COD, total phenol, TS, total nitrogen, total phosphorous, polyphenols (gallic acid, p-coumaric acid and trans p-coumaric acid) and inert COD were investigated in raw OMW and treated OMW. Table 7.1 shows the maximum removal efficiencies obtained for adsorption and photocatalytic studies under UV oxidation and sunlight oxidation.

According to results in Table 7.1; adsorption with nano-ZnO-SiO_2 composite is not suitable when compared with photooxidation under UV or sunlight. Maximum removal efficiencies of COD, total phenol, TS, total nitrogen and total phosphorus were 28 %, 39 %, 33 %, 16 % and 21 %, respectively, for adsorption process. Maximum yields of COD (28 %) and total phenol (39 %) were obtained with 3 g/L nano-ZnO-SiO_2 composite, after 180 min contact time at original pH of OMW (4.01). Maximum yield of TS was obtained as 33 % with 3 g/L nano-ZnO-SiO_2 composite, after 90 min contact time at original pH of OMW (4.01). For maximum removal efficiency of total nitrogen (16 %) 5 g/L nano-ZnO-SiO_2 composite was required, after 60 min contact time at pH 7. Finally, maximum yield of total phosphorous (21 %) was obtained with 5 g/L nano-ZnO-SiO_2 composite, after 90 min contact time at original pH of OMW (4.01). Required adsorption times changes between 60-180 min for maximum yields of pollutant parameters. Study of isotherms shows us the Langmuir isotherm is suitable both for COD and phenol adsorption since R^2 values were 0.93 and 0.94, respectively with suitable kinetic constants.

Table 7.1 The comparison of removal efficiencies.

Treatment Processes	Maximum Removal Efficiencies (%)				
	COD	Total Phenol	TS	Total Nitrogen	Total Phosphorous
Adsorption Treatment conditions	pH: 4.01 3 g/L nano-ZnO-SiO_2 composite 180 min contact time	pH:4.01 3 g/L nano-ZnO-SiO_2 composite 180 min contact time	pH:4.01 3 g/L nano-ZnO-SiO_2 composite 90 min contact time	pH:7 5 g/L nano-ZnO-SiO_2 composite 60 min contact time	pH:4.01 5 g/L nano-ZnO-SiO_2 composite 90 min contact time
Yields (%)	28 %	39 %	33 %	16 %	21 %
Photocatalytic treatment conditions under UV light	pH:4.01 1 g/L nano-ZnO-SiO_2 composite 15 min irradiation time	pH:4.01 1 g/L nano-ZnO-SiO_2 composite 90 min irradiation time	pH:4.01 1 g/L nano-ZnO-SiO_2 composite 15 min irradiation time	pH:7 1 g/L nano-ZnO-SiO_2 composite 60 min irradiation time	pH:10 5 g/L nano-ZnO-SiO_2 composite 15 min irradiation time
Yields (%)	78 %	86 %	77 %	100 %	86 %
Photocatalytic treatment under sun light	pH:4.01 3 g/L nano-ZnO-SiO_2 composite 24 hours irradiation time	pH:4.01 3 g/L nano-ZnO-SiO_2 composite 24 hours irradiation time	pH:4.01 3 g/L nano-ZnO-SiO_2 composite 24 hours irradiation time	pH:7 3 g/L nano-ZnO-SiO_2 composite 24 hours irradiation time	pH:10 5 g/L nano-ZnO-SiO_2 composite 24 hours irradiation time
Yields (%)	77%	73 %	64 %	96 %	80 %

Photooxidation with UV of OMW is suitable for treatment of OMW. COD, total nitrogen and total phosphorous yields are slightly higher than sunlight irradiation. Total phenol and TS yields of under UV irradiation are strongly higher than the yields with using sunlight irradiation. 1 g/L nano-ZnO-SiO_2 composite is enough for maximum removal of all pollutant parameters excluding total phosphorous since maximum yield of total phosphorous was obtained at 5 g/L nano-ZnO-SiO_2 composite. The maximum yields of COD (78 %) and TS (77 %) were obtained with 1 g/L nano-ZnO-SiO_2 composite, after 15 min irradiation time at original pH of OMW (4.01). The maximum removal efficiency of total phenol (86 %) needs long irradiation time (90 min) while the optimum nano-ZnO-SiO_2 composite concentration was 1 g/L at original pH of OMW (4.01). The whole total nitrogen was

removed with 1 g/L nano-ZnO-SiO_2 composite, after 60 min irradiation time at pH 7. The maximum yield of total phosphorous (86 %) was obtained with 5 g/L nano-ZnO-SiO_2 composite, after 15 min contact time at pH 10.

On the other hand for treatment of OMW with sunlight 3 g/L nano-ZnO-SiO_2 composite is required for maximum yields of COD (77 %), total phenol (73 %), TS (64 %) and total nitrogen (96 %) after 24 h sunlight irradiation excluding total phosphorous since the maximum yield of total phosphorous (80 %) was obtained with 5 g/L nano-ZnO-SiO_2 composite after 24 h sunlight irradiation time. The maximum yields of COD (77 %), total phenol (73 %), TS (64 %) were obtained at original pH of OMW (4.01). The maximum yields of total nitrogen (96 %) and total phosphorous (80 %) were obtained at pH 7 and pH 10, respectively. For maximum removal efficiencies long irradiation times (24 hours) requires for photooxidation with sunlight. On the other hand very short UV irradiation time (15 min) is adequate for high photooxidation yields excluding total phenol (90 min) and total nitrogen (60 min).

For maximum removals of COD, total phenol and TS the optimum pH was found at pH: 4.01 is original pH of OMW. This decrease the cost of the chemical utilized in both photocatalytic studies, (under UV light and sunlight). pH 7 is suitable for treatment of total nitrogen on the other hand this case is valid for pH 10 for total phosphorous removal.

Nano-ZnO-SiO_2 core/shell nanocomposites are successfully fabricated by a simple physical method in this study under laboratory conditions to obtain synergetic effects of nano particles.

Reuse of nano-ZnO-SiO_2 composite was investigated in this study. According to results, nano-ZnO-SiO_2 composite can be used after six times for removals of COD, total phenol and TS. The yield of COD decreased from 78 %, to 60 %, 51 %, 48 %, and 30 % and to 5 %, respectively, after six sequential treatment steps. The removal efficiencies of total phenol decreased from 86 %, to 50 %, 42 %, 20 %, 15 % and to 7

% and additionally the TS removal efficiency also decreased from 77 %, 55 %, 41 %, 33 %, 30 % to 9 %, respectively, after 1st, 2nd, 3rd, 4th, 5th and 6th usage of the same nano-ZnO-SiO_2 composite. After six times treatment the effluent concentrations of COD, total phenol and TS were obtained as 1312 mg/L, 19 mg/L and 2142 mg/L, respectively. These effluent concentrations show that treated OMW can be discharged to the sewage systems according to discharge limits illustrated in Regulation of Water Pollution Control (2004) published in the Official Newspaper. Total removal efficiencies of COD, total phenol and TS were obtained as 98 %, 97 % and 97 %, respectively. The recovery and reuse of nano-ZnO-SiO_2 composite minimizes the operating costs of the UV process.

Cost analysis was made for the removal of OMW under UV light. Total cost of OMW treatment was 500.75 TL for 1 liter OMW, while 500 TL was spent for 20 UV lamps. Only 0.75 TL was spent for treatment of 1 liter OMW. Sunlight is natural source and can be used for the treatment of other wastewater types with optimum concentration of nano-ZnO-SiO_2 composite, irradiation times and pH values.

Recommendations for future studies; some of the recommendations for future studies are listed below:

- Nano-ZnO-SiO_2 composite have been recommended to be an efficient nano-composite for the removal of various toxic, organic pollutants such as COD, total phenol, TS, total nitrogen and total phosphorous in OMW because the removal yields obtained in this study were high for photooxidation process both of UV and sunlight.

- Various operating parameters such as irradiation time of UV light, pH values of the wastewater**,** concentration of catalyst nano-ZnO-SiO_2 composite and type of catalysts are important in the photo-degradation efficiency of pollutants in OMW. The optimum nano-ZnO-SiO_2 composite concentration, pH of OMW, irradiation time should be taken into consideration during photocatalytic treatment of other toxic industrial wastewater.

- Reusability of nanocomposite decreases the cost of treatment; nano-ZnO-SiO_2 composite can be used for removal different types of pollutants for different wastewater types such as saline, piggery and brine industries.

REFERENCES

Abd Aziz, R. & Sopyan, I. (2009). Synthesis of TiO_2–SiO_2 powder and thin film photocatalysts by sol-gel method. *Indian Journal of Chemistry, 48,* 951–957.

Abdel Aal, A., Barakat, M. & Mohamed, R. (2008). Electrophoreted Zn– TiO_2–ZnO nanocomposite coating films for photocatalytic degradation of 2-chlorophenol. *Applied Surface Science, 254*, 4577–4583.

Abdel-Ghani, N.T., Hefray M. & El-Chaghaby, G.A.F. (2007). Removal of lead from aqueous solution using low cost abundantly available adsorbent. *International Journal of Environmental Science and Technology, 4(1),* 67-73.

Achak, M., Hafidi, A., Mandi, L. & Ouazzani, N. (2014). Removal of phenolic compounds from olive mill wastewater by adsorption onto wheat bran, *Desalination and Water Treatment, 52*, 13-15, 2875-2885.

Achak, M., Hafidi, A., Ouazzani, N., Sayadi, S. & Mandi, L. (2009). Low cost biosorbent "banana peel" for the removal of phenolic compounds from olive mill wastewater: Kinetic and equilibrium study. *Journal of Hazardous Materials, 166,* 117–125.

Achak, M., Hafidi, A., Ouazzani, N., Sayadi, S. & Mandi, L. (2009). Low cost biosorbent "banana peel" for the removal of phenolic compounds from olive mill wastewater: kinetic and equilibrium studies. *Journal of Hazardous Materials, 166,* 117-125.

Achak, M., Mandi, L. & Ouazzani, N. (2009a). Removal of organic pollutants and nutrients from olive mill wastewater by a sand filter. *Journal of Environmental Management, 90,* 2771–2779.

Achak, M., Ouazzani, N. & Mandi, L. (2009b). Treatment of modern olive mill effluent by infiltration-percolation on a sand filter. Traitement des margines d'une huilerie moderne par infiltration-percolation sur un filtre à sable. *Revue des Sciences de l'Eau, 22,* 421–433.

Achak, M., Ouazzani, N., Yaacoubi, A. & Mandi, L. (2008). Modern olive mill effluent characterization and their treatment by coagulation–flocculation using lime and aluminium sulphate. Caractérisation des margines issues d'une huilerie mod-erne et essais de leur traitement par coagulation-floculation par la chaux et lesulfate d'aluminium. *Revue des Sciences de l'Eau, 21,* 53–67.

Adhoum, N. & Monser, L. (2004). Decolourisation and removal of phenolic compounds from olive mill wastewater by electrocoagulation. *Chemical Engineering and Processing, 43,* 1281–1287.

Ahmadi, M., Vahabzadeh, F., Bonakdarpour, B., Mofarrah, E. & Mehranian, M. (2005). Application of the central composite design and response surface methodology to the advanced treatment of olive oil processing wastewater using Fenton's peroxidation. *Journal of Hazardous Materials, 123,* 187–195.

Akbal, F. & Onar, A.N. (2003). Photocatalytic degradation of phenol. *Environmental Monitoring and Assessment, 83,* 295–302.

Akdemir, E.O. & Ozer, A. (2009). Investigation of two ultrafiltration membranes for treatment of olive oil mill wastewater. *Desalination, 249,* 660–666.

Aktas, E.S., Imre, S. & Ersoy, L. (2001). Characterization and lime treatment of olive mill wastewater. *Water Research, 35,* 2336–2340.

Al Malah, K., Azzam, M.O.J. & Abulail, N.I. (2000). Olive mills effluent (OME) wastewater post-treatment using activated clay. *Separation and Purification Technology, 20,* 225–234.

Al Mallah, K., Asma, O.J. & Abu Lail, N.I. (2000). Olive mills effluent (OME) wastewater post-treatment using activated clay. *Separation and Purification Technology, 20,* 225–234.

Ali, M.A., İsmail, A.A., Najmy, R. & Al-Hajry,A. (2014). Preparation and characterization of ZnO–SiO2 thin films as highly efficient photocatalyst. *Journal of Photochemistry and Photobiology A: Chemistry, 275,* 37– 46.

Allen, N. S., Edge, M., Verran, J., Stratton, J., Maltby J. & Bygott, C. (2008). Photocatalytic titania based surfaces: environmental benefits. *Polymer Degradation and Stability, 93 (9),* 1632–1646.

Alok, M. (2006). Removal of the dye, Amaranth From waste water using hen feathers as potential adsorbent. *Electronic Journal of Environmental, Agricultural and Food Chemistry, 5(2),* 1296-1305.

Ammary, B.Y, (2005).Treatment of olive mill wastewater using an anaerobic sequencing batch reactor. *Desalination, 177,* 157–165.

Anandan, S., Vinu, A., Venkatachalam, N., Arabindoo, B. & Murugesan, V. (2006). Photo catalytic activity of ZnO impregnated Hb and mechanical mix of ZnO/Hb in the degradation of monocrotophos in aqueous solution. *Journal of Molecular Catalysis A: Chemical, 256,* 312–320.

Azbar, N., Keskin, T., Catalkaya, E.C. (2008a). Improvement in anaerobic degradation of olive mill effluent (OME) by chemical pretreatment using batch systems. *Biochemical Engineering Journal, 38,* 379–383.

Azbar, N., Keskin, T., Yuruyen, A. (2008b). Enhancement of biogas production from olive mill effluent (OME) by co-digestion. *Biomass Bioenergy, 32,* 1195–1201.

Azzam, M.O.J., Al-Malah, K.I. & Abu-Lail, N.I. (2004). Dynamic post treatment response of olive mill effluent wastewater using activated carbon. *Journal of Environmental Science and Health A, 39,* 269–280.

Badawy, M.I., Ghaly, M.Y. & Ali, M.E.M. (2011). Photocatalytic hydrogen production over nanostructured mesoporous titania from olive mill wastewater. *Desalination, 267,* 250–25.

Bala, H., Zhang, Y., Ynag, H., Wang, C., Li, M., Lv, X. & Wang, Z. (2007). Preparation and characteristics of calcium carbonate/silica nanoparticles with core–shell structure. *Colloids and Surfaces A: Physicochemical and Engineering Aspects, 294,* 8–13.

Bayarri, B., Gimenez, J., Curco, D. & Esplugas, S. (2005). Photocatalytic degradation of 2,4-dichlorophenol by TiO_2/UV: kinetics, actinometries and models. *Catalysis Today, 101,* 227-236.

Beltran, F.J., Garcia-Araya, J.F., Frades, J., Alvarez, P. & Gimeno, O. (1999). Effects of single and combined ozonation with H_2O_2 or UV radiation the chemical degradation and biodegradability of debittering table olive industrial wastewaters. *Water Research, 33,* 723-732.

Benitez, F.J., Beltran-Heredia, J., Torregrosa, J. & Acero J.L. (1999). Treatment of olive mill wastewaters by ozonation, aerobic degradation and the combination of both treatments. *Journal of Chemical Technology and Biotechnology, 74,* 639–646.

Benitez, F.J., Beltran-Heredia, J., Torregrosa, J., Acero J.L. & Cercas, V. (1997). Aerobic degradation of olive mill wastewaters. *Applied Microbiology and Biotechnology, 47,* 185–188.

Bessa, E., Sant'Anna, Jr. G.L. & Dezotti, M. (2001). Photocatalytic/H_2O_2 treatment of oil field/produced waters. *Applied Catalysis B: Environmental, 29*, 125–134.

Bingham, S. & Daoud, W.A. (2011). Recent advances in making nano-sized TiO_2 visible-light active through rare-earth metal doping. *Journal of Materials Chemistry, 21*, 2041–2050.

Boubaker, F. & Ridha, B.C. (2008). Modelling of the mesophilic anaerobic co-digestion of olive mill wastewater with olive mill solid waste using anaerobic digestion model No. 1 (ADM1). *Bioresource Technology, 99*, 6565–6577.

Boukhoubza, F., Ait Boughrous, A., Yacoubi-Khebiza, M., Jail, A., Hassani, L., LoukiliIdrissi, L. & Nejmeddine, A. (2008). Impact of olive oil wastewater on the physi-cochemical and biological quality of groundwater in the Haouz plain, south of Marrakesh (Morocco). *Environmental Technology, 29*, 959–974.

Brunetti, G., Senesi, N. & Plaza, C. (2007). Effects of amendment with treated and untreated olive oil mill wastewaters on soil properties, soil humic substances and wheat yield. *Geoderma, 138*, 144–152.

Byrappa, K., Subramani, A.K., Ananda, A., Rai, K.M.L., Dinesh, R. & Yoshimura, M. (2006). Photocatalytic degradation of Rhodamine B dye using hydrothermally synthesized ZnO. *Bulletin of Material Science, 29*, 433–438.

Caputo, A.C., Scacchia, F. & Pelagagge, P.M. (2003). Disposal of byproducts in olive oil industry: waste-to-energy solutions. *Applied Thermal Engineering, 23*, 197–214.

Centi, G., Perathoner, S., Torre, T. & Verduna, M.G. (2000). Catalytic wet oxidation with H_2O_2 of carboxylic acids on homogeneous and heterogeneous Fenton type catalysts. *Catalysis Today, 55*, 61–69.

Chakrabarti, S. & Dutta, B.K. (2004). Photocatalytic degradation of model textile dyes in wastewater using ZnO as semiconductor catalyst. *Journal of Hazardous Materials, 112(3),* 269–78.

Chamkha, M., Patel, B.K.C., Garcia, J.L., Labat, M. (2001). Isolation of Clostridium biofermentants from oil mill wastewater converting cinnamic acid to 3-phenylpropionic acid and emendation of species. *Anaerobe, 7,* 189–197.

Chatzisymeon, E., Foteinis, S., Mantzavinos, D. & Tsoutsos, T. (2013). Life cycle assessment of advanced oxidation processes for olive mill wastewater treatment. *Journal of Cleaner Production, 54,* 229–234.

Chedeville, O., Debacq, M. & Porte, C. (2009). Removal of phenolic compounds presenting olive mill wastewaters by ozonation. *Desalination, 249,* 865–869.

Chen, C.C., Lu, C.S., Chung, Y.C. & Jan, J.L. (2007). UV light induced photodegradation of malachite green on TiO_2 nanoparticles. *Journal of Hazardous Materials, 141,* 520–528.

Cheng, X., Yua, X. & Xing, Z. (2012). Characterization and mechanism analysis of N doped TiO_2 with visible light response and its enhanced visible activity. *Applied Surface Science, 258,* 3244–3248.

Chou, K.S. & Chen, C.C. (2007). Fabrication and characterization of silver core and porous silica shell nanocomposite particles. *Microporous and Mesoporous Materials, 98,* 208–213.

Chu, D., Masuda, Y., Ohji, T. & Kato, K. (2010). Formation and photocatalytic application of ZnO nanotubes using aqueous solution. *Langmuir, 26,* 2811–2815.

Clifford, A.B. & Luis, S. (1979). Hydrophobic and coulombic interactions in the micellar binding of phenols and phenoxide ions. *The Journal of Chemical Physics*, 680–683.

Colon G., Belver C. & Fernandez-Garcıa M. (2007). *Synthesis, properties and application of oxide nanoparticles.* USA: John Wiley & Sons Publication.

Crittenden, J.C. (2005). *Water treatment: principles and design.* USA: Wiley.

Daneshvar, N., Aber, S., Dorraji, M.S.S., Khataee, A.R. & Rasoulifard, M.H. (2007). Photocatalytic degradation of the insecticide diazinon in the presence of prepared nanocrystalline ZnO powders under irradiation of UV-C light. *Separation and Purification Technology, 58(1),* 91–8.

Daskalaki, V.M. & Kondarides, D.I. (2009) Efficient production of hydrogen by photo-induced reforming of glycerol at ambient conditions. *Catalysis Today, 144,* 75–80.

Dermeche, S., Nadour, M., Larroche, C., Moulti-Mati, F. & Michaud, P. (2013). Olive mill wastes: biochemical characterizations and valorization strategies. *Process Biochemistry, 48,* 1532–1552.

Detlef, B. (2004). Photocatalytic water treatment: solar energy applications. *Solar Energy, 77,* 445-459.

Devarenne, A., K. (2015). O*live oil commission of California holds informational meeting.* October, 23, 2015. Retrieved from http://www.oliveoiltimes.com.

Dhaouadi, H. & Marrot, B. (2008). Olive mill wastewater treatment in a membrane bioreactor: process feasibility and performances. *Chemical Engineering Journal, 145,* 225–231.

Dobkin, D.M. (2003). *Silane/Oxygen Thermal CVD.* September, 11, 2015. Retrieved from http://www.enigmaticconsulting.com/semiconductor_processing/CVD_Fundamentals/films/SiO2_properties.html.

Drouiche, M., Le Mignot, V., Lounici, H., Belhocine, D., Grib, H. & Pausse, A. (2004). A compact process for the treatment of olive mill wastewater by combining UF and UV/H_2O_2 techniques. *Desalination, 169,* 81–88.

El Hajjouji, H., Barje, F., Pinelli, E., Bailly, J.R., Richard, C., Winterton, P., Revel, J.C. & Hafidi, M. (2008). Photochemical UV/TiO_2 treatment of olive mill wastewater (OMW). *Bioresource Technology, 99,* 7264–7269.

El Saliby, I., Shon, H., Kandasamy, J. & Vigneswaran, S. (2009). Nanotechnology forwater and wastewater treatment: in brief. In: Vigneswaran, S.V. (Ed.), Water and Wastewater Treatment Technologies. *Encyclopedia of Life Support Systems (EOLSS).*

El-Abbassi, A., Hafidi, A., Khayet, M. & Garcia-Payo, M.C. (2013). Integrated direct contact membrane distillation for olive mill wastewater treatment. *Desalination, 323,* 31-38.

Esen, B. (2011). *Hidrotermal yöntemle sentezlenen nano metal oksitlerin fotokatalitik özelliklerinin incelenmesi.* Master Thesis, Ankara University, Ankara.

Faust, S.D. & Aly, O.M. (1987). *Adsorption processes for water treatment.* UK: Butterworth Scientific Ltd. 509 S., 204 Abb., 107 Tab., ISBN 0-409-90000-1.

Feitz, A.J. & Waite, T.D. (2003). Kinetic modeling of TiO_2-catalyzed photodegradation of trace levels of microcystin-LR. *Environmental Science & Technology, 37 (3),* 561-568.

Feng, X., Guo, H., Patel, K., Zhou, H. & Lou, X. (2014). High performance, recoverable Fe_3O_4/ ZnO nanoparticles for enhanced photocatalytic degradation of phenol. *Chemical Engineering Journal, 244,* 327–334.

Fouad, O.A., Ismail, A.A., Zaki, Z.I. & Mohamed, R.M. (2006). Zinc oxide thin films prepared by thermal evaporation deposition and its photocatalytic activity. *Applied Catalysis B: Environmental, 62,* 144–149.

Franco, C.A., Cortés, F.B. & Nassar, N.N. (2014). Adsorptive removal of oil spill from oil-in-fresh water emulsions by hydrophobic alumina nanoparticles functionalizedwith petroleum vacuum residue. *Journal* of *Colloid* and *Interface Science*, 425, 168–177.

Frascari, D., Bacca, A.E.M., Zama, F., Bertin, L., Fava, F. & Pinelli, D. (2016). Olive mill wastewater valorisation through phenolic compounds adsorption in a continuous flow column. *Chemical Engineering Journal, 283,* 293–303.

Galanakis, C., Dimou, D., Pasadakis, N., Papanicolaou, K. & Gekas, V. (2006). *Adsorption of olive mill wastewater on raw and activated Greek lignites*. Conference: Protection and Restoration of the Environment VIII, At Chania, July, Greece.

Gaya, U. I. & Abdullah, A. H. (2008). Heterogeneous photocatalytic degradation of organic contaminants over titanium dioxide: a review of fundamentals, progress and problems. *Journal of Photochemistry and Photobiology C, 9 (1),* 1–12.

Gernjak, W., Krutzler, T., Glaser, A., Malato, S., Caceres, J. & Bauer, R. (2003). Photo-Fenton treatment of water containing natural phenolic compounds. *Chemosphere, 50,* 71–78.

Gernjak, W., Maldonado, M.I., Malato, S., Caceres, J., Krutzler, T. & Glaser, A. (2004). Pilot plant treatment of olive mill wastewater (OMW) by solar TiO_2 photocatalysis and solar photo-Fenton. *Solar Energy, 77,* 567–572.

Giannes, A., Diamadopoulos, E. & Ninolakis, M. (2003). Electrochemical treatment of olive oil mill wastewater using a Ti/Ta/Pt/Ir electrode. *Proceeding 3rd International Conference on Oxidation Technologies for Water and Wastewater Treatment,* 147–152.

Gizgis, N., Georgiou, M. & Diamadopoulos, E. (2005). Sequential anaerobic/aerobic biological treatment of olivemill wastewater and municipal wastewater. *Proceeding 3rd Eur Bioremediation Conference Chania*.

Gomec, C.Y., Erdim, E., Turan, I., Aydin, A.F. & Ozturk, I. (2007). Advanced oxidationtreatment of physico-chemically pre-treated olive mill industry effluent. *Journal* of *Environmental Science and Health, 42,* 741–747.

Gotsi, M., Kalogerakis, N., Psillakis, E., Samaras, P. & Mantzavinos, D. (2005). Electrochemical oxidation of olive oil mill wastewaters. *Water Research, 39,* 4177–4187.

Gray, N.F. (2005).*Water technology.* USA: Elsevier.

Gu, T., Tsai, G. & Tsao, G.T. (1991). Multicomponent adsorption and chromatography with uneven saturation capacities. *AIChE Journal, 37,* 1333–1340.

Guettaı, N. & Amar, H. A. (2005). Photocatalytic oxidation of methyl orange in presence of titanium dioxide in aqueous suspension Part I: Parametric study. *Desalination, 185,* 427–437.

Guo, N., Liang, Y., Lan, S., Liu, L., Jia, G., Gan, S., Zou, H. & Xu, X. (2014). Uniform TiO_2–SiO_2 hollow nanospheres: Synthesis, characterizationand enhanced adsorption–photodegradation of azo dyes and phenol. *Applied Surface Science, 305,* 562–574.

Hamdi, M., Garcia, J.L. & Ellouz, R. (1992). Integrated biological proces for olive mill wastewater treatment. *Bioprocess Engineering, 8,* 79–84.

Hanifi, S. & El Hadrami, I. (2009). Olive mill wastewaters: diversity of the fatal productin olive oil industry and its valorisation as agronomical amendment of poor soils: a review. *Journal of Agronomy, 8*, 1–13.

Hao, O.J., Kim, H. & Chiang, P.C. (2000). Decolorization of wastewater. *Critical Reviews in Environmental Science and Technology, 30(4),* 449–505.

Hariharan, C. (2006). Photocatalytic degradation of organic contaminants in water by ZnO nanoparticles: revisited. *Applied Cataysis A: General, 304*, 55–61.

Herrmann J.M., Duchamp C. & Karkmaz M. (2007). Environmental green chemistry as defined by photocatalysis. *Journal of Hazardous Materials, 146 (3),* 624–629.

Herrmann J.M., Matos J., Disdier J., Guillard C., Laine J., Malato S. & Blanco J. (1999). Solar photocatalytic degradation of 4-chlorophenol using the synergistic effect between titania and activated carbon in aqueous suspension. *Catalysis Today, 54,* 255.

Hoffmann, M.R., Martin, S.T., Choi, W. & Bahnemann, D.W. (1995). Environmental applications of semiconductor photocatalysis. *Chemical Reviews, 95,* 69–96.

Ibhadon, A., O. & Fitzpatrick, P. (2013). Heterogeneous Photocatalysis: Recent Advances and Applications. *Catalysts, 3,* 189-218.

Idelovitch, E. & Michail, M. (1981). Nitrogen removal by free ammonia stripping from high pH ponds. *Journal (Water Pollution Control Federation), 53(9),* 1391-1401.

Inan, H., Dimoglo, A., Simsek, H. & Karpuzku, M. (2003). Olive oil mill wastewater treatment by means of electrocoagulation. *Separation and Purification Technology*, *36*, 23–31.

Ismail, A., Ibrahim, I. & Mohamed, R. (2003). Sol–gel synthesis of vanadia–silica for photocatalytic degradation of cyanide. *Applied Catalysis B: Environmental, 45*,161–166.

Jarboui, R., Sellami, F., Kharroubi, A., Gharsallah, N. & Ammar, E. (2008). Olive millwastewater stabilization in open-air ponds: impact on clay-sandy soil. *Bioresource Technology, 99*, 7699–7708.

Jin, Y., Wang, J., Sun, B., Blakesley, J.C. & Greenham, N.C. (2008). Solutionprocessed ultraviolet photodetectors based on colloidal ZnO nanoparticles. *Nano Letters, 8(6),* 1649-53.

Kallel, M., Belaid, C., Boussahel, R., Ksibi, M., Montiel, A. & Elleuch, B. (2009). Olivemill wastewater degradation by Fenton oxidation with zero-valent iron andhydrogen peroxide. *Journal of Hazardous Materials, 163*, 550–554.

Kamat, P., V. (2002). Photophysical, photochemical and photocatalytic aspects of metal nanoparticles. *Journal of Physical Chemistry B, 106*, 7729-7744.

Karageorgos, P., Coz, A., Charalabaki, M., Xekoukoulotakis, N., Kalogerakis, N. & Mantzavinos, D. (2006). Ozonation of weathered olive mill wastewaters. *Journal of Chemical Technology & Biotechnology, 81(9),* 1570-1576.

Kashıf, N. & Ouyang, F. (2009). Parameters effect on heterogeneous photocatalyse degradation of phenol in aqueous dispersion of TiO_2. *Journal of Environmental Sciences, 21,* 527–533.

Kaur, A. & Gupta, U. (2009). A review on applications of nanoparticles for the precon-centration of environmental pollutants. *Journal of Materials Chemistry, 19,* 8279–8289.

Kestioglu, K., Yonar, T. & Azbar, N. (2005). Feasibility of physico-chemical treatment and advanced oxidation processes (AOPs) as a means of pretreatment of olive mill effluent (OME). *Process Biochemistry, 40,* 2409–2416.

Khatamian, M. & Alaji, Z. (2012). Efficient adsorption-photodegradation of4-nitrophenol in aqueous solution by using ZnO/HZSM-5 nanocomposites. *Desalination, 286,* 248–253.

Khoufi, S., Aloui, F. & Sayadi, S. (2006). Treatment of olive oil mill wastewater by combined process electro-Fenton reaction and anaerobic digestion. *Water Research, 40,* 2007–2016.

Kiril-Mert, B., Yonar, T., Yalili-Kilic, M. & Kestioglu, K. (2010). Pre-treatment studies on olive mill effluent using physicochemical, Fenton and Fenton-like oxidations processes. *Journal of Hazardous Materials, 174,* 122–128.

Kumar, H. & Rani, R. (2013). Structural and Optical Characterization of ZnO Nanoparticles Synthesized by Microemulsion Route, *International Letters of Chemistry, Physics and Astronomy, 14,* 26-36.

Lafi, W.K., Al-Anber, M., Al-Anber, Z.A., Al-Shannag, M. & Halil, A. (2010). Coagulation and advanced oxidation processes in the treatment of olive mill wastewater (OMW). *Desalination* and *Water Treatment, 24,* 251–256.

Lafi, W.K., Shannak, B., Al-Shannag, M., Al-Anber, Z. & Al-Hasan, M. (2009). Treatment of olive mill wastewater by combined advanced oxidation and biodegradation. *Separation and Purification Technology, 70,* 141–146.

Lakshmanan, R. (2013). *Application of magnetic nanoparticles and reactive filter materials for wastewater treatment*. PhD Thesis, Royal Institute of Technology School of Biotechnology Stockholm.

Lea, J. & Adesina, A.A. (1998). The photo-oxidation of sodium dodecyl sulfate in aerated aqueous TiO_2 suspension. *Journal of Photochemistry and Photobiology A: Chemistry, 118,* 111–122.

Lee, H.B., Yoo, Y.M. & Han, Y.H. (2006). Characteristic optical properties and synthesis of gold–silica core–shell colloids. *Scripta Materialia, 55,* 1127–1129.

Lewis, J.A. (2000). Colloidal processing of ceramics. Journal of the American *Ceramic Society, 83(10),* 2341–2359.

Li, F., Huang, X., Jiang, Y., Liu, L. & Li, Z. (2009). Synthesis and characterization of ZnO/SiO_2 core/shell nanocomposites and hollow SiO_2 nanostructures. *Materials Research Bulletin, 44,* 437–441.

Li, Z., Shi, T. & Guo, L. (2010). Preparation and morphology of porous SiO2 ceramics derived from fir flour templates, *Journal of Serbian Chemical Society. 75 (3),* 385–394.

Liu, R. & Liang, P. (2008). Determination of trace lead in water samples by graphite furnace atomic absorption spectrometry after preconcentration with nanometer titanium dioxide immobilized on silica gel. *Journal of Hazardous Materials, 152,* 166–171.

Lucas, M.S. & Peres, J.A. (2009). Removal of COD from olive mill wastewater by Fenton'sreagent: kinetic study. *Journal of Hazardous Materials 168*, 1253–1259.

Lund, A & Lund, M. (2013), *One-way ANOVA*, 10 September 2015, https://statistics.laerd.com/statistical-guides/one-way-anova-statistical-guide.php

Malato, S., Blanco, J., Vidal, A. & Richter, C. (2002). Photocatalysis with solar energy: at a pilot-plant scale: an overview. *Applied Catalysis B: Environmental, 37 (1)*, 1-15.

Mantzavinos, D. & Kalogerakis, N. (2005). Treatment of olive mill effluents. Part I. Organic matter degradation by chemical and biological processes-an overview. *Environmental International, 31*, 289–295.

Mathur, N., Bhatnagar, P., Mohan, K., Bakre, P., Nagar, P., Bijarnia, M. (2007) Mutagenicity evaluation of industrial sludge from common effluent treatment plant. *Chemosphere, 67(6)*, 1229–35.

Maurice, V., Georgelin, T., Siaugue, J.M. & Cabuil, V. (2009). Synthesis and characterization of functionalized core–shell-Fe_2O_3–SiO_2 nanoparticles. *Journal of Magnetism and Magnetic Materials, 321*, 1408–1413.

Mazellier, P., Leroy, E., De Laat, J., Legube, B., (2002). Transformation of carbendazim induced by the H_2O_2/UV system in the presence of hydrogenocarbonate ions: involvement of the carbonate radical. *New Journal of Chemistry, 26*, 1784-1790.

Mills, A. & McFarlane, M. (2007). Current and possible future methods of assessing the activities of photocatalyst films. *Catalysis Today, 129(1-2)*, 22–28.

Minne, S.C., Manalis, S.R. & Quate, C.F. (1995). Parallel atomic force microscopy using cantilevers with integrated piezoresistive sensors and intergrated piezoelectric actuators. *Applied Physics Letters, 67,* 3918.

Mohamed, E.F. (2011). *Removal of organic compounds from water by adsorption and photocatalytic oxidation.* PhD Thesis, Institute National Polytechnique of Toulouse, Toulouse.

Mohamed, R.M., Baeissa, E.S., Mkhalid, I.A. & Al-Rayyani, M.A. (2013). Optimization of preparation conditions of $ZnO–SiO_2$ xerogel by sol–gel technique for photodegradation of methylene blue dye. *Applied Nanoscience, 3,* 57–63.

Moraetis, D., Stamati, F.E., Nikolaidis, N.P. & Kalogerakis, N. (2011). Olive mill wastewater irrigation of maize: impacts on soil and groundwater. *Agricultural Water Management, 98,* 1125–1132.

Narayan, R. (2010). Use of nanomaterials in water purification. *Materials Today, 13,* 44–46.

Nassar, N.N. & Ringsred, A. (2012). Rapid adsorption of methylene blue from aqueous solutions by goethite nanoadsorbents. *Environmental Engineering Science,* 790–797.

Nassar, N.N., Ararb, A.L., Mareia, N.N., Abu Ghanimb, M.M., Dwekatb, M.S. & Sawalhab, S.H. (2014). Treatment of olive mill based wastewater by means of magnetic nanoparticles: Decolourization, dephenolization and COD removal. *Environmental Nanotechnology, Monitoring & Management 1–2,* 14–23.

Niaounakis, M. & Halvadakis, C.P. (2004). *Olive-mill waste management– literature review and patent survey.* Typothito – George Dardanos Publications, Athens, Greece.

Niaounakis, M. & Halvadakis, C.P. (2006). *Characterization of olive processing waste olive processing waste management: literature review and patent survey* Italy: Elsevier, (second ed.).

Ntougias, S., Gaitis, F., Katsaris, P., Skoulika, S., Iliopoulos, N. & Zervakis, G.I. (2013). The effects of olives harvest period and production year on olive mill wastewater properties – evaluation of pleurotus strains as bioindicators of the effluent's toxicity. *Chemosphere, 92*, 399–405.

Ntwaeaborwa, O.M., Swart, H.C., Kroon, R.E. & Terblans, J.J. (2009). Synthesis, characterization, and luminescent properties of ZnO–SiO_2:PbS. *American Vacuum Society A, 27*, 767.

Paraskeva, C.A., Papadakis, V.G., Tsarouchi, E., Kanellopoulou, D.G. & Koutsoukos, P.G. (2007). Membrane processing for olive mill wastewater fractionation. *Desalination, 213*, 218–229.

Paraskeva, P. & Diamadopoulos, E. (2006). Review Technologies for olive mill wastewater (OMW) treatment: a review. *Journal of Chemical Technology* and *Biotechnology, 81*, 1475–1485.

Pardeshi, S.K. & Patil, A.B. (2008). A simple route for photocatalytic degradation of phenol in aqueous zinc oxide suspension using solar energy. *Solar Energy, 82*, 700–705.

Pescod, M.B. (1992). *Food and Agriculture Organization of the United Nations,* 29 October 2015, http://www.fao.org/docrep/t0551e/t0551e05.htm

Pirbazari, M. (1980). *Performance Predictions for Removal of Toxic and Carcinogenic Compounds from Water Supplies by Adsorption, Ph. D. Dissertation,* The University of Michigan, USD.

Polyanskiy, M. (2015). Optical constants of SiO2 (Silicon dioxide, Silica, Quartz), 2 November 2015, http://refractiveindex.info/?shelf=main&book=SiO2&page=Malitson.

Qamar, M., Muneer, M. & Bahneman, D. (2006). Heterogeneous photocatalysed degradation of two selected pesticide derivatives, triclopyr and daminozid in aqueous suspensions of titanium dioxide. *Journal of Environmental Management, 80,* 99–106.

Qu, X., Alvarez, P.J.J. & Li, Q. (2013). Applications of nanotechnology in water and wastewater treatment. *Water Research, 47,* 3931-3946.

Regulation of Wastewater Treatment Plant Technical Methods, (2010). Table E7.2.

Regulation of Water Pollution Control, (2004). The Official Newspaper dated 31.12.2004, The Official Newspaper Numbered 25687.

Rivas, J.F., Beltran, F.J., Gimeno, O. & Acedo, B. (2001a). Wet air oxidation of wastewater from olive oil mills. *Chemical Engineering* & *Technology, 24*, 415–421.

Rivas, J.F., Beltran, F.J., Gimeno, O. & Frades, J. (2001b). Treatment of olive oil mills wastewater by Fenton's reagent. *Journal of Agricultural and Food Chemistry, 49*, 1873–1880.

Rozzi, A. & Malpei, F. (1996). Treatment and disposal of olive mill effluents. *International Biodeterioration and Biodegradation, 47,* 135–144.

Rushton G.T., Burns, W.G., Lavin, J.M., Chong, Y.S., Pellechia, P. & Scimizu, K.D. (2007). Determination of the Rotational Barrier for Kinetically Stable Conformational Isomers via NMR and 2D TLC An Introductory Organic Chemistry Experiment. *Journal of Chemical Education, 84,* 1499.

Ruzmanova, Y., Ustundas, M., Stoller, M. & Chianese, A. (2013). Photocatalytic Treatment of Olive Mill Wastewater by N-doped Titanium Dioxide Nanoparticles under Visible Light. *Chemical Engıneerıng Transactions, 32,* 2233-2238.

Salem, I. (2003). Recent studies on the catalytic activity of titanium, zirconium, and hafnium oxides. *Catalysis Reviews, 45,* 205–296.

Sanghi, R. & Verma, P. (2013). Decolorisation of aqueous dye solutions by low-cost adsorbents: a review. *Coloration Technology, 129*, 85-108.

Sarika, R., Kalogerakis, N. & Mantzavinos, D. (2005). Treatment of olive mill effluents. Part II. Complete removal of solids by direct flocculation with polyelectrolytes. *Environment International, 31*, 297–304.

Savage, N. & Diallo, M.S. (2005). Nanomaterials and water purification: opportunitiesand challenges. *The Journal of Nanoparticle Research, 7,* 331–342.

Scheffé, H. (1959). *The Analysis of variance.* USA: Wiley.

Selli, E., Baglio, D., Montanarella, L. & Bidoglio, G. (1999). Role of humic acids in the TiO_2-photocatalyzed degradation of tetrachloroethene in water. *Water Research, 33,* 1827–1836.

Shaheen, H. & Karim, R.A., (2007). Management of Olive–Mills Wastewater in Palestine. *An-Najah University Journal for Research – A (Natural Sciences*), 63–83.

Singhal, A., Achary, S., Tyagi, A., Manna, P. & Yusuf, S. (2008). Colloidal Fe-doped ZnO nanocrystals: facile low temperature synthesis, characterization and properties. *Materials Science and Engineering: B, 153*, 47–52.

Sowmya, A. & Meenakshi, S. (2013). An efficient and regenerable quaternary amine modified chitosan beads for the removal of nitrate and phosphate anions. *Journal of Environmental Chemical Engineering, 1*, 906–915.

Sponza, D. & Oztekin, R. (2015). Photodegradation of Polyphenols and Aromatic Amines in Olive Mill Effluents with Ni Doped C/TiO_2. *Journal of Chemistry Volume 2015*, 12 pages.

State, S. (2008). *Crystal structure of ZnS (wurtzite) with coordination polyhedra.* September, 11, 2015. Retrieved from https://en.wikipedia.org/wiki/Zinc_oxide.

Stumm, W. (1992). Chemistry of the solid-water interface. USA: John Wiley & Sons.

Sun, H., Feng, X., Wang, S., Ang, H.M. & Tade, M.O. (2011). Combination of adsorption, photochemical and photocatalytic degradation of phenol solution over supported zinc oxide: Effects of support and sulphate oxidant. *Chemical Engineering Journal, 170*, 270–277

Sun, J., Dong, S., Feng, J., Yin, X. & Zhao, X. (2011). Enhanced sunlight photocatalytic performance of Sn-doped ZnO for Methylene Blue degradation. *Journal of Molecular Catalysis A: Chemical, 335*, 145–150

Sverjensky, D.A. (2005). Prediction of surface charge on oxides in salt solutions: revisions for 1:1 (MþL2) electrolytes. *Geochimica et Cosmochimica Acta,69(2)*, 225–257.

Tanada, S., Kabayama, M., Kawasaki, N., Sakiyama, T., Nakamura, T., Araki, M. & Tamura, T. (2002). Removal of phosphate by aluminum oxide hydroxide. *Journal of Colloid and Interface Science, 257*, 135–140.

Tang, W.Z. & Huang, C.P. (1995). Photocatalyzed oxidation pathways of 2,4 dichlorophenol by CdS in basic and acidic aqueous solutions. *Water Research, 29 (2),* 745-756.

Tchobanoglous, G., Burton, F.L., Stenset, H.D. (2003). *Wastewater engineering treatment and reuse*. USA: McGraw-Hill Edition, 4th Edition.

Teker, M., Imamoglo, M. & Saltabas, O. (1999). Adsorption of Copper and Cadmium ions by activated carbon from rice Hulls. *Turkish Journal of Chemistry, 23*, 185-191.

Tunesi, S. & Anderson, M. (1991). Influence of chemisorption on the photodecomposition of salicylic acid and related compounds using suspended titania ceramic membranes. *Journal of Physical Chemistry, 95*, 3399-3405.

Turano, E., Curcio, S., De Paola, M.G., Calabro, V.& Iorio, G. (2002). An integrated centrifugation–ultrafiltration system in the treatment of olive mill wastewater. *Journal of Membrane Science, 209*, 519–531.

Ubay, G. & Ozturk, I. (1997). Anaerobic treatment of olive mill effluents. *Water Science and Technology, 26,* 287–294 .

Ugurlu, M. & Karaoglu, M.H. (2011). TiO_2 supported on sepiolite: Preparation, structural and thermal characterization and catalytic behaviour in photocatalytic treatment of phenol and lignin from olive mill wastewater. *Chemical Engineering Journal, 166,* 859–867.

Vlyssides, A.G., Loukakis, H., Karlis, P.K., Barampouti, E.M.P. & Mai, S.T. (2004). Olive mill wastewater detoxification by applying pH related Fenton's oxidation process. *Fresenius Environmental Bulletin, 13,* 501–504.

Vlyssides, A.G., Loukakis, H.N., Israilides, C., Barampouti, E.M. & Mai, S. (2003). Detoxification of olive mill wastewater using a Fenton process. *Proceedings 2nd Euro Bioremediation Conference,* (531–534).

Wu, J. (2004). *Modeling adsorption of organic compounds on activated carbon*. Academical Thesis. Printed in Sweden by Solfjädern Offset AB, Umeå University, Umeå.

Xu, P., Zeng, G.M., Huang, D.L., Feng, C.L., Hu, S., Zhao, M.H., Lai, C., Wei, Z., Huang, C., Xie, G.X. & Liu, Z.F. (2012). Use of iron oxide nanomaterials in wastewater treat-ment: a review. *Science of The Total Environment, 424,* 1–10.

Yalili Kilic, M. & Akal Solmaz, S.K. (2013). *Treatment Alternatives of Olive Mill Wastewater (OMW)*. A Review, ICOEST.

Yalili Kilic, M., Yonar, T. & Kestioglu, K. (2013) Pilot-scale treatment of olive oil mill wastewater by physicochemical and advanced oxidation processes. *Environmental Technology, 34,* 1521–1531.

Yu, D., Cai, R. & Liu, Z. (2004). Studies on the photodegradation of Rhodamine dyes on nanometer-sized zinc oxide. *Spectrochimica Acta, Part A, 60,* 1617–1624.

Zhai, J., Tao, X., Pu, Y., Zeng, X. & Chen, J. (2010). Core/shell structured ZnO/SiO_2 nanoparticles: Preparation, characterization and photocatalytic property. *Applied Surface Science, 257,* 393–397.

Zhang, J., Liu, Z., Han, B., Li, Z., Yang, G., Li, J. & Chen, J. (2006). Preparation of silica and TiO_2–SiO_2 core–shell nanoparticles in water-in-oil microemulsion using compressed CO_2 as reactant and antisolvent. *The Journal of Supercritical Fluids, 36,* 194–201

Zhang, Q., Dandeneau, C.S., Zhou, X. & Cao, G. (2009). ZnO nanostructures for dye-Sensitized solar cells. *Advanced Materials*, *21*(41), 4087-108.

Zorpas, A.A. & Costa, C.N. (2010). Combination of Fenton oxidation and composting for the treatment of the olive solid residue and the olive mile wastewater from the olive oil industry in Cyprus. *Bioresource Technology*, *101*, 7984–7987.

Zouari, N. & Ellouz, R. (1996). Toxic effect of coloured olive compounds on the anaerobic digestion of olive oil mill effluent in UASB-like reactors. *Journal of Chemical Technology and Biotechnology*, *66*, 414–420.